CHAPTER 3

Basins due to lithospheric stretching

When Earth breaks up and heaven expands
How will the change strike me and you
In the house not made with hands?

(ROBERT BROWNING, *BY THE FIRE SIDE* (1855))

SUMMARY

Intracontinental sags, rifts, failed rifts, and passive continental margins fall within an evolutionary suite of basins unified by the process of lithospheric stretching. Rifts are areas of crustal thinning, demonstrated by the shallow depth to the Moho, high surface heat flows, volcanic activity, seismic activity with predominantly extensional focal mechanism solutions, negative Bouguer gravity anomalies, and commonly elevated rift margin topography.

The nature of the fault systems and associated sedimentary basins within extending continental lithosphere depends on the initial crustal structure and geotherm, strain rate and total amount of strain. Discrete, localized continental rifts appear to form on normal thickness crust and extend slowly over long periods of time. At higher strain rates, localized rifts may evolve into passive margins. Wide extended domains with supradetachment basins occur on previously thickened crust that extends quickly over a short period of time. Local anomalies in the ductile lower crust may be amplified to produce core complexes within these wide extended terranes.

Passive continental margins are in general seismically inactive, and tectonics are dominated by gravity-driven collapse, halokinesis, and growth faulting. Heat flows are near-normal in mature examples. Passive continental margins can be divided into two types: (i) volcanic margins are characterized by extensive extrusive basalts and igneous underplating and significant surface uplift at the time of break-up, and (ii) nonvolcanic margins lack evidence for strong thermal activity, and consist of extensive sediment drapes overlying a strongly rifted basement. On conjugate margins, the extended continental lithosphere may lie at considerable oceanic depths beneath a very thin drape of sediment, or may be covered by sediment prisms over 10 km thick. There may be considerable asymmetry between conjugate margins, especially in the ductile lower crust.

Early investigations suggested that rifting fell into two end-member classes. Active rifting involves the stretching of the continental lithosphere in response to an active thermal process in the asthenosphere, such as the impingement of a hot mantle plume on the base of the lithosphere. Passive rifting, however, involves the mechanical stretching of the continental lithosphere from distant extensional forces, with passive upwelling of asthenosphere. Subsidence in rifts is an isostatic response to the stretching of the continental lithosphere. The postrift stage of failed rifts and the postrift or drift stage of passive continental margins is due to thermal contraction during cooling of the stretched lithosphere. The sediment loads are supported flexurally during this long phase of cooling. Dynamical models of the lithosphere incorporate a rheological understanding of a layered lithosphere undergoing extension. These numerical models make predictions of strain rate evolution as a function of the changing temperature field and viscosity within this layered lithosphere.

The simplest formulation of continental extension is the uniform stretching model of McKenzie (1978a) and its derivatives. The prototype uniform stretching model involves uniform stretching with depth, instantaneous extension, 1-D heat transport by conduction, no magmatic activity, no internal radiogenic heat sources, and the operation of Airy isostasy throughout. The uniform stretching model makes important first-order predictions. Initial fault-controlled subsidence is dependent on the initial crustal to lithospheric thickness ratio and on the stretch factor β. The subsequent thermal subsidence has

the form of a negative exponential, and depends on the stretch factor β alone. The uniform stretching model serves as a useful approximation for subsidence and paleotemperature in rifted basins such as the North Sea, and in sediment-starved passive margins, such as the Bay of Biscay and the Galicia margin of the eastern central Atlantic. However, sediment-nourished passive margins require the postrift subsidence to be modeled with flexural rather than Airy isostatic support. Volcanic margins require the effects of melt segregation, igneous underplating, and transient dynamic uplift to be accounted for.

Subsequent modifications to the prototype uniform stretching model have investigated the effects of depth-dependent stretching, extension by simple shear along transcrustal detachments, protracted rifting periods, elevated asthenospheric temperatures, magmatic activity, induced mantle convection within the upwelled asthenosphere, radiogenic heat sources, greater depths of lithospheric necking, and flexural support. These modifications affect the predictions of synrift and postrift subsidence, and in particular predict elevated synrift topography in the form of topographic swells or rift margin uplifts.

Dynamical approaches to lithospheric extension involve plane-stress or plane-strain models with various boundary conditions, and initial conditions. Dynamic models are especially instructive in explaining why rifts remain narrow, with small bulk extensional strains, or develop into oceanic spreading centres. One set of dynamic models indicates that at moderate to low initial strain rates, extension is limited by an increase in viscosity in the mantle lithosphere below the Moho. In contrast, at high initial strain rates, complete rifting results from the concentration of the extensional force on a progressively thinner high-strength layer within the lithosphere. Analogue models are able to replicate the narrow, localized rifts and extensive, tilted fault block terranes observed at passive margins as a function of strain rate. Analogue models also show that gravity spreading of weak, previously thickened crust leads to wide extended terrains and exhumed ductile lower crust in core complexes.

Igneous activity is a common feature of some continental rifts and passive margins at the point of break-up. Igneous activity is caused by adiabatic decompression due to one or a combination of lithospheric stretching, elevated asthenospheric temperatures, and presence of volatiles. Hot plumes derived from the core–mantle boundary have a profound effect on asthenospheric temperatures, melt generation by adiabatic decompression and surface uplift. Plume heads occupy areas of the asthenosphere generally 1000–2000 km across with temperature anomalies of 100–200 °C, and in the oceans are responsible for bathymetric swells 1–2 km above the surrounding seafloor. The elevation of sublithospheric temperatures over a mantle plume may generate large amounts of melting and the upward migration of melts to form igneous underplates and extrusive basalts. Transient surface uplift is caused by the dynamic effects of hot asthenospheric flow, whereas permanent uplift results from igneous underplating of the crust. Consequently, volcanically active passive margins and continental rifts stand elevated topographically compared to nonvolcanic equivalents. The amount of melt generated and its composition is related to the plate thickness, excess temperature, stretch factor, and percentage of volatiles.

The amount of extension (stretch factor β) and the strain rate history can be estimated by a number of techniques. The thermal subsidence history of boreholes allows the amount of lithospheric stretching and strain rate history to be estimated. Crustal stretching can be calculated from imagery of the depth to the Moho using gravity and seismic data. Stretch factors can also be estimated from forward sequential tectonostratigraphic modeling using well-constrained crustal and basin profiles derived from deep seismic reflection and refraction data.

3.1 INTRODUCTION TO RIFTS, FAILED RIFTS, AND PASSIVE CONTINENTAL MARGINS

Rifts, failed rifts, intracratonic sags, and passive margins form part of an evolutionary sequence of basins unified by the processes of lithospheric extension (Dietz 1963; Dewey and Bird 1970; Falvey 1974; Kinsman 1975; Veevers 1981). Two linked mechanisms explain the majority of observations in these basins: (i) brittle extension of the crust, causing extensional fault arrays and fault-controlled subsidence, and (ii) thermal relaxation following ductile extension of the lithosphere, leading to regional postrift subsidence.

The main difference between rift basins and basins experiencing regional subsidence but lacking major extensional faulting (sags) can be simply explained as follows (Fig. 3.1). In true rifts, tensile deviatoric stresses due to uplift, thinning, or regional stress fields are sufficient to overcome rock strength, and therefore cause

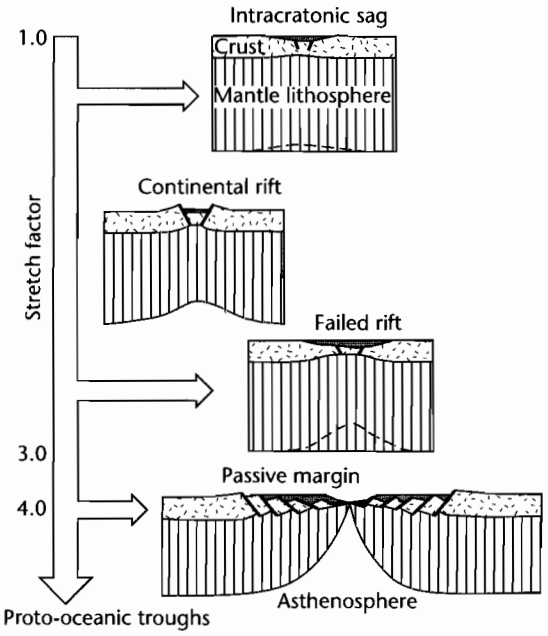

Fig. 3.1 Basins in the rift–drift suite as a function of increasing amounts of continental stretching.

faulting. If the deviatoric stresses are insufficient to cause brittle fracture, then uplift or subsidence may occur without fracturing. If the thermal "supply" is switched off and not renewed, the thermal contraction effect causes subsidence, so that sags can be regarded as immature continental basins that have failed to develop into either rifts or spreading centres, whilst rift basins that have experienced a subsequent sag phase can likewise be regarded as having failed to develop fully into oceanic spreading centres. The evolution of a rift system into a passive continental margin takes place when new oceanic lithosphere is created at a spreading centre, the rift–drift transition. In terms of mechanisms for basin formation, continental margin wedges record the response of the lithosphere to its continued cooling and to the considerable loading of the sediment itself.

In this chapter, the mechanisms of lithospheric extension are focused upon as a means of explaining the rift–drift suite of sedimentary basins. This suite of sedimentary basins is characterized by a distinctive set of geological, geophysical, and geomorphological observations that are strongly suggestive of elevated heat flows, volcanicity, extensional faulting, and thinned crust. Embedded within the overarching theme of lithospheric extension are complexities caused by the total amount of stretching, strain rate, and thermal and mechanical properties of the continental lithosphere undergoing extension.

3.2 GEOLOGICAL AND GEOPHYSICAL OBSERVATIONS IN REGIONS OF CONTINENTAL EXTENSION

3.2.1 Rifts

Rifts are areas of crustal extension and seismic studies show them to overlie thinned crust. Regions of rifting at the present day are characterized by negative Bouguer gravity anomalies, high heat flow, and volcanic activity, all of which suggest that in addition to crustal extension, a thermal anomaly exists at depth. The essential observations in zones of continental extension are summarized below.

Heat flow: The presence of active volcanoes and elevated heat flows in rift zones demonstrates active thermal processes. However, the measured values of heat flow are often difficult to interpret, because of complications due to convective heat transport, shallow magmatic intrusions, groundwater convection, and variability of conductive sediments and rocks. In general, rift zones have heat flows of 90–110 $mW m^{-2}$. This is up to a factor of 2 higher than in surrounding unstretched terranes (Fig. 3.2). Values are higher in volcanic rifts such as the Eastern Rift, Kenya, and lower in nonvolcanic rifts such as those of Malawi, Tanganyika, and the Jordan–Dead Sea Rift zone of the Middle East. In areas devoid of active tectonics and volcanicity, continental heat flow values appear to be strongly correlated with the type of underlying crust. In NE North America, for example, the higher heat flows over the Appalachians (average 58 $mW m^{-2}$) than over the North American Shield (average 29 $mW m^{-2}$) may be explained by the different thicknesses of underlying tonalitic crust (Pinet et al. 1991) containing the radiogenic heat producing elements uranium, thorium, and potassium (§2.2). In general, granitic terranes have high surface heat flows, whereas basic and ultrabasic igneous rocks and many sedimentary rocks are associated with low surface heat flows. The large variations caused by this internal radiogenic heat production makes the interpretation of surface heat flows in terms of continental stretching problematical.

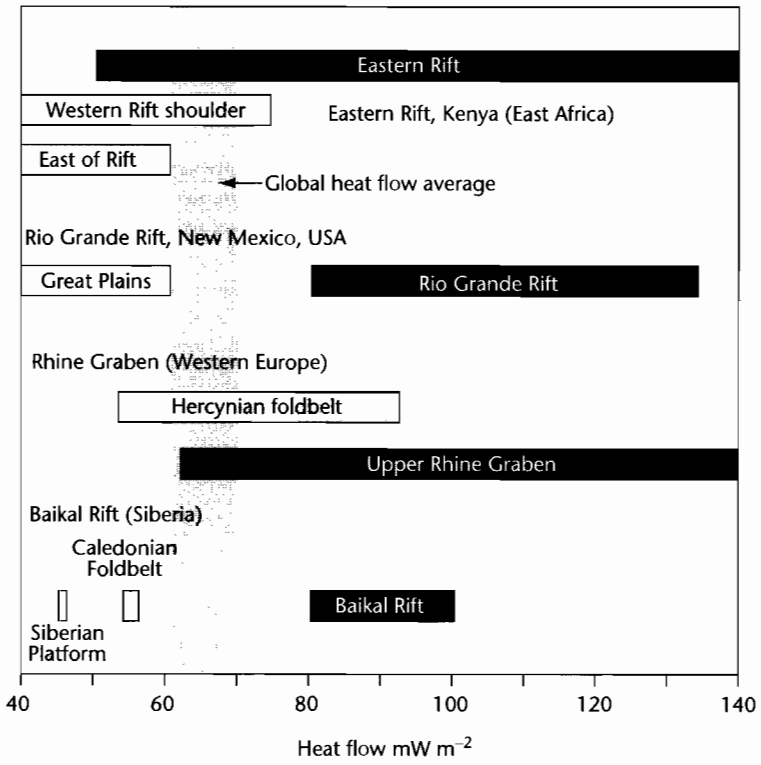

Fig. 3.2 Heat flows in some continental rifts and surrounding regions, compared to the global heat flow average. Dark boxes are rift zones; light boxes are rift flanks or adjacent unstretched regions.

Seismicity: Rift zones are characterized by high levels of earthquake activity. On the continental lithosphere, earthquake epicenters commonly delineate active rift zones or reactivated orogenic belts, as in southern Africa. Focal mechanism solutions in general indicate normal dip–slip faulting with orientations roughly parallel to the long-axis orientation of the rift. In some continental rifts, such as the Rhine Graben, strike–slip focal mechanisms dominate dip–slip solutions by 3:1. Although earthquakes are common in regions of continental rifting, they typically have moment magnitudes of up to 5.0 (Rhine Graben) or 6.0 (East African Rift), with shallow focal depths of < 30 km, indicating that the earthquakes are located in the brittle mid-upper crust.

Crustal thickness: Scismic studies show that the Moho is elevated beneath rift zones. The southern Rhine Graben is an example (Fig. 3.3). The Moho reaches a depth of 24 km near the Kaiserstuhl volcano due west of Freiburg, Germany directly beneath the centre of the graben. The Moho is dome-shaped, deepening to the north, NW and NE to about 30 km. Approximately 3 km of synrift sedimentary rocks are found in the graben, so the continental crust has been thinned from 30 km to 21 km, that is, by a factor of *c.* 1.4. In the North Sea failed rift, the crust (pre-Triassic) is > 31 km thick beneath the Shetland Platform and Scandinavian Shield, but is < 16 km thick beneath the Viking Graben (Klemperer 1988). The continental crust has therefore been thinned by a factor of approximately 2 immediately beneath the deepest part of the Viking Graben (Fig 3.4). An important observation, however, is that some regions of extensive, diffuse extension such as the Basin and Range, SW USA, are located on previously thickened crust. The Moho was therefore anomalously deep at the onset of extension, and extension/thinning has brought the Moho back to "normal" depth. This is also the case for the Tibetan Plateau, which is undergoing

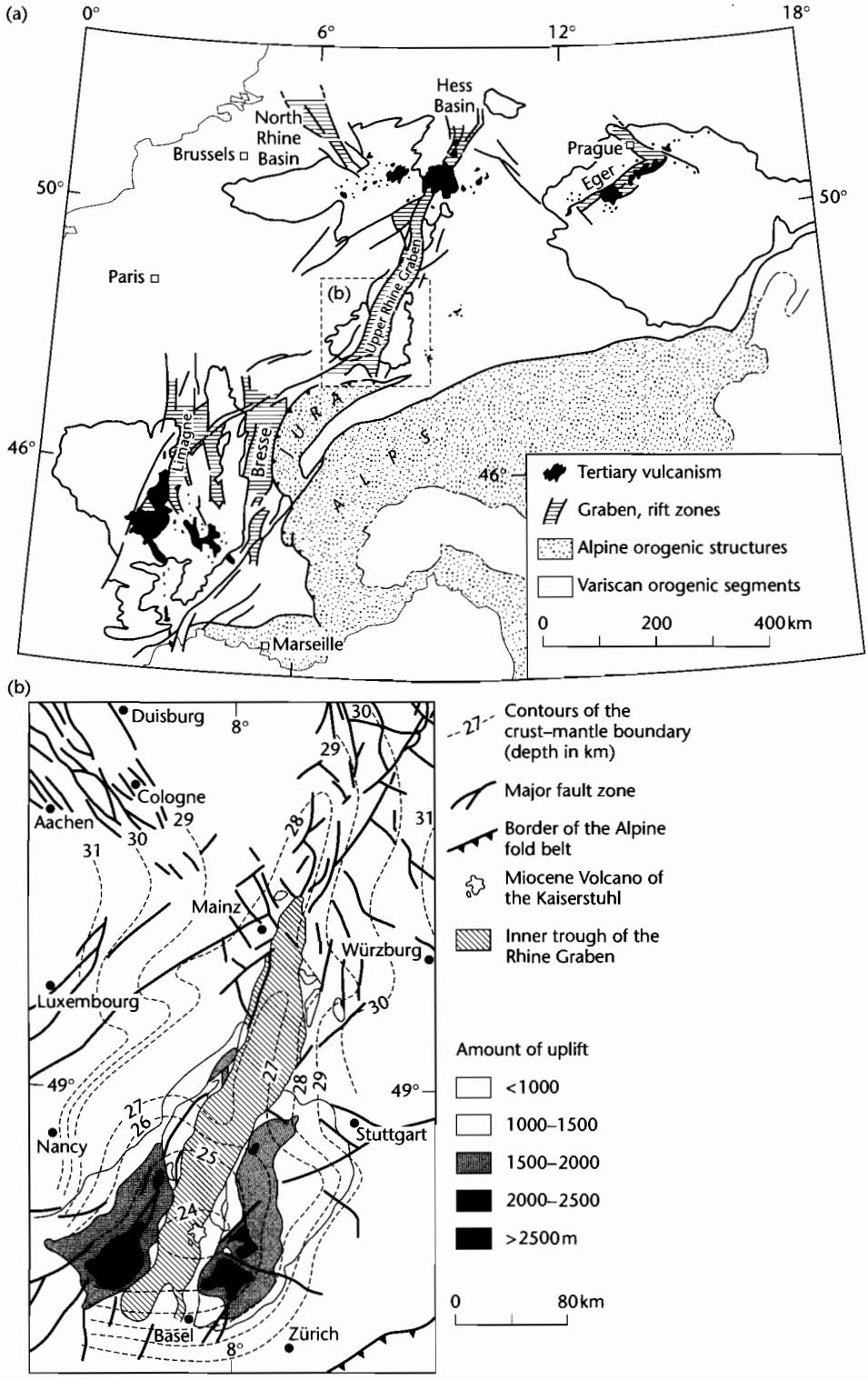

Fig. 3.3 (a) Location of main elements of the late Eocene–Recent Western European Rift System, with sites of Tertiary volcanicity; (b) Depth to the Moho below sea-level (in km), showing a mantle bulge in the southern Rhine Graben centred on the Kaiserstuhl volcano (Illies 1977). The largest amounts of denudation are found on the rift flanks above the shallow mantle. Reproduced courtesy of the Board of the Stichting Netherlands Journal of Geosciences.

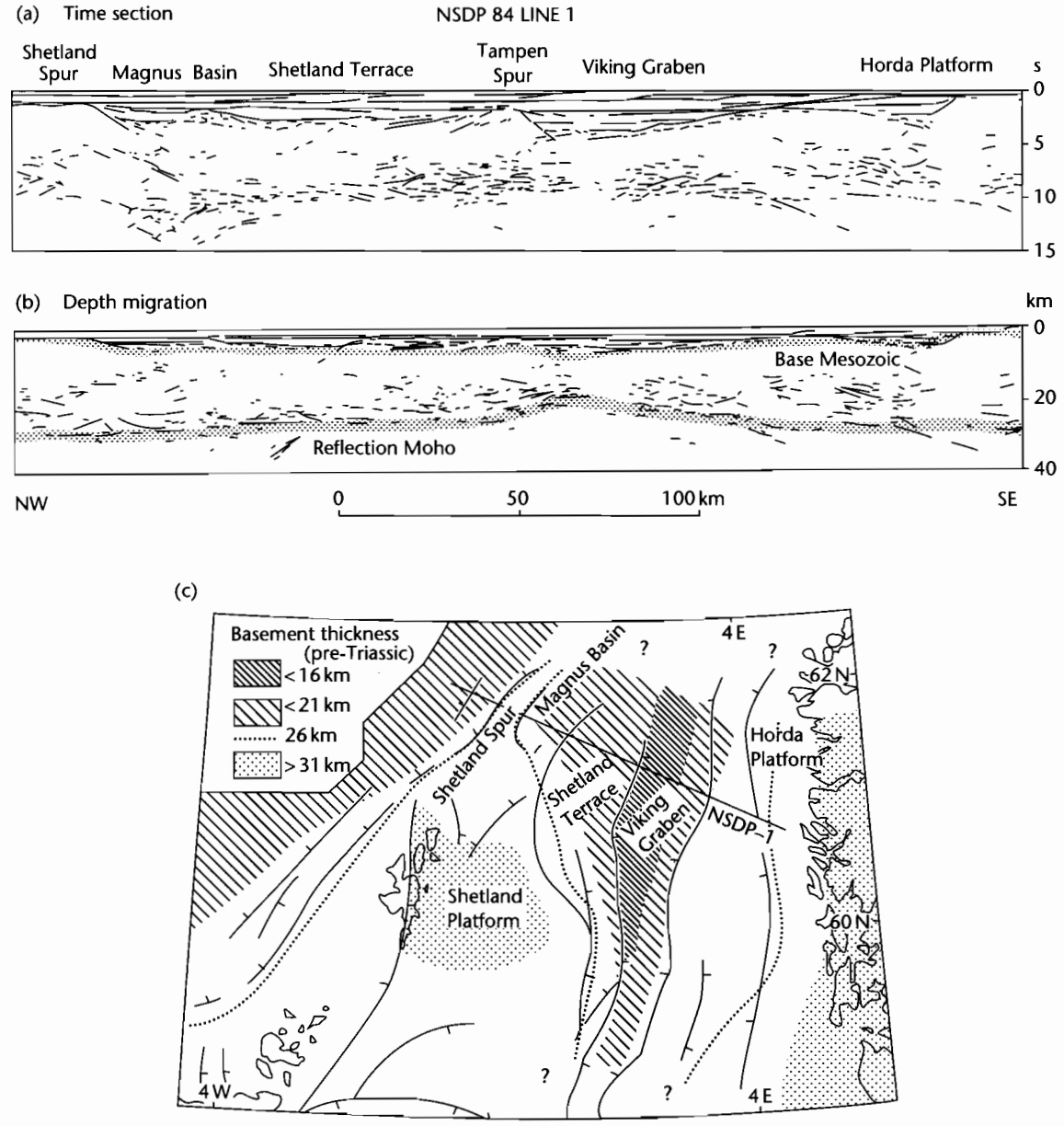

Fig. 3.4 Crustal thickness changes in the North Sea area as a result of Mesozoic rifting (after Klemperer 1988). (a) Unmigrated line drawing in two-way travel time of NSDP line 1 from the Shetland Spur to the Norwegian coast (location in (c)); (b) Depth-migrated version showing the depth of the reflection Moho; (c) Contour map of the interpreted thickness of the prerifting basement (pre-Triassic) showing that the Viking Graben has been stretched by a factor of 2 compared to the Shetland Platform.

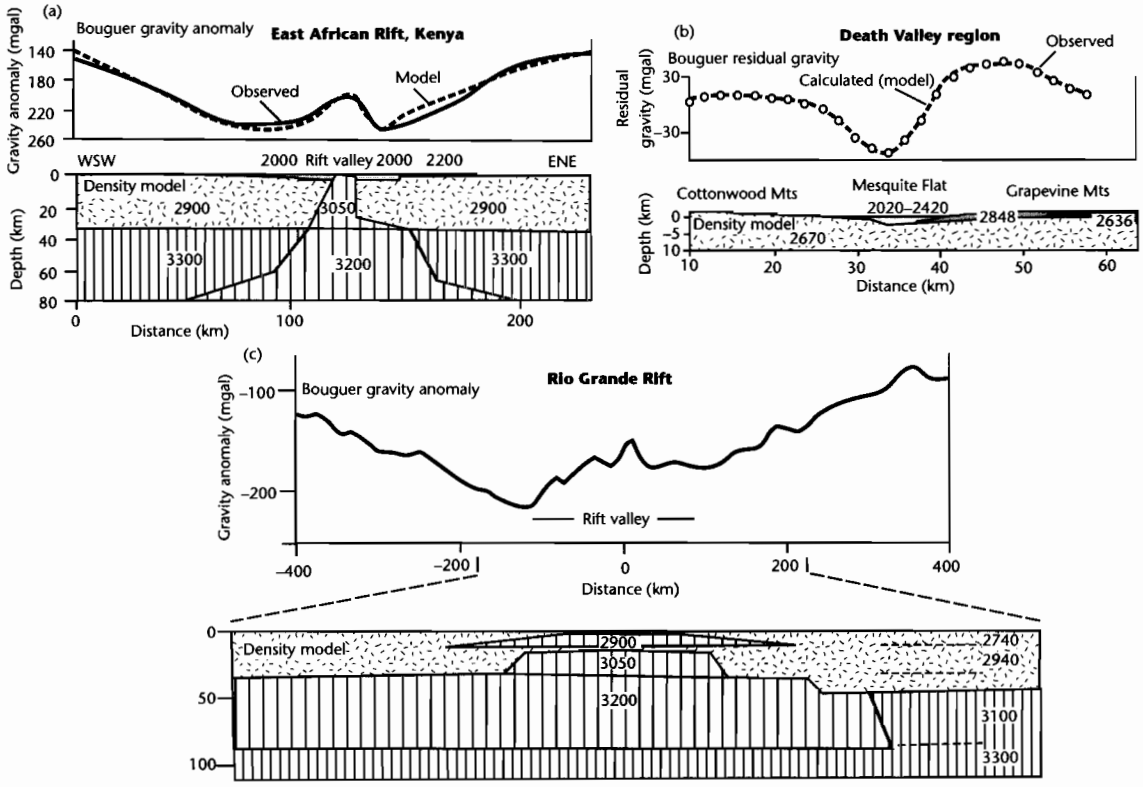

Fig. 3.5 Gravity profiles across rift zones. (a) Gravity profile and density model across the Gregory Rift, Kenya. The secondary gravity high is modeled as due to the intrusion of dense magma bodies beneath the rift valley (after Baker and Wohlenberg 1971); (b) Gravity profile and density model for a profile across Mesquite Flat, northern Death Valley, California (after Blakeley et al. 1999); (c) Gravity profile (*c.* 33 °N) and density model for the Rio Grande Rift of New Mexico (after Ramberg 1978). The secondary gravity high is thought to be due to the presence of dense igneous bodies beneath the rift. Densities shown in $kg\,m^{-3}$.

active extension and overlies crust as much as 70 km thick.

Gravity: It has been recognized for some time that rift zones have characteristic gravity signatures – typically a long wavelength Bouguer gravity low (Fig. 3.5) with sometimes a secondary high located in the centre of the rift zone (Fig. 3.5a, c). The conventional explanation is that rift zones have anomalously hot material in the mantle beneath the rift, producing a mass deficit and therefore a negative gravity anomaly. The subsidiary gravity high is thought to be due to the intrusion of dense magma bodies within the continental crust. Regions of widespread, diffuse extension such as the Basin and Range province of SW USA show a series of gravity highs corresponding to basement blocks, and *c.* 20 km-wide gravity lows corresponding to sedimentary basins (Fig. 2b). The gravity lows most likely reflect the mass deficit of light basin sediments.

Faults: Rift zones are typified by normal dip–slip faults with a variable number of strike–slip faults depending on the orientation of the rift axis in relation to the bulk extension direction. Consequently, the central Death Valley Basin is close to orthogonal to the extension direction and is typified by dip–slip normal faults, whereas the northern Death Valley Basin is more oblique and has faults with important strike–slip motion (Burchfiel and Stewart 1966). Faults in rifts are not infinite in extent: instead there is a displacement–length relationship, with most of the

slip being taken up on a small number of interacting major fault segments. Fault displacement dies out towards the tips of fault segments. The Jurassic Brent–Strathspey–Statfjord fault array system in the North Sea Basin (McLeod et al. 2000), the Neogene fault array of the Gulf of Suez in eastern Sinai (Sharp et al. 2000) and the modern fault array of the Lake Tanganyika Basin (Rosendahl et al. 1986) are all excellent examples. Most major border faults dip steeply inwards towards the basin centre and are planar as far as they can be imaged. However, some rift bounding faults are low-angle and listric, taking up very large amounts of horizontal extension, as in the supradetachment basins of SW USA. Metamorphic rocks may be unroofed from <25 km depth in these "core complexes" (Wernicke 1985).

Topography: Currently or recently active rift zones typically have elevated rift flank topography bordering a depositional basin. There may be two length scales of surface uplift. The best examples of the large length scale (several hundred km) are the >3 km-high topographic swells of Ethiopia and East Africa (Baker et al. 1972; King and Williams 1976) (Fig. 3.6). Other domal uplifts are found in northern Africa such as those in the Tibesti and Hoggar regions. These swells are commonly associated with widespread volcanic activity. Whereas the large

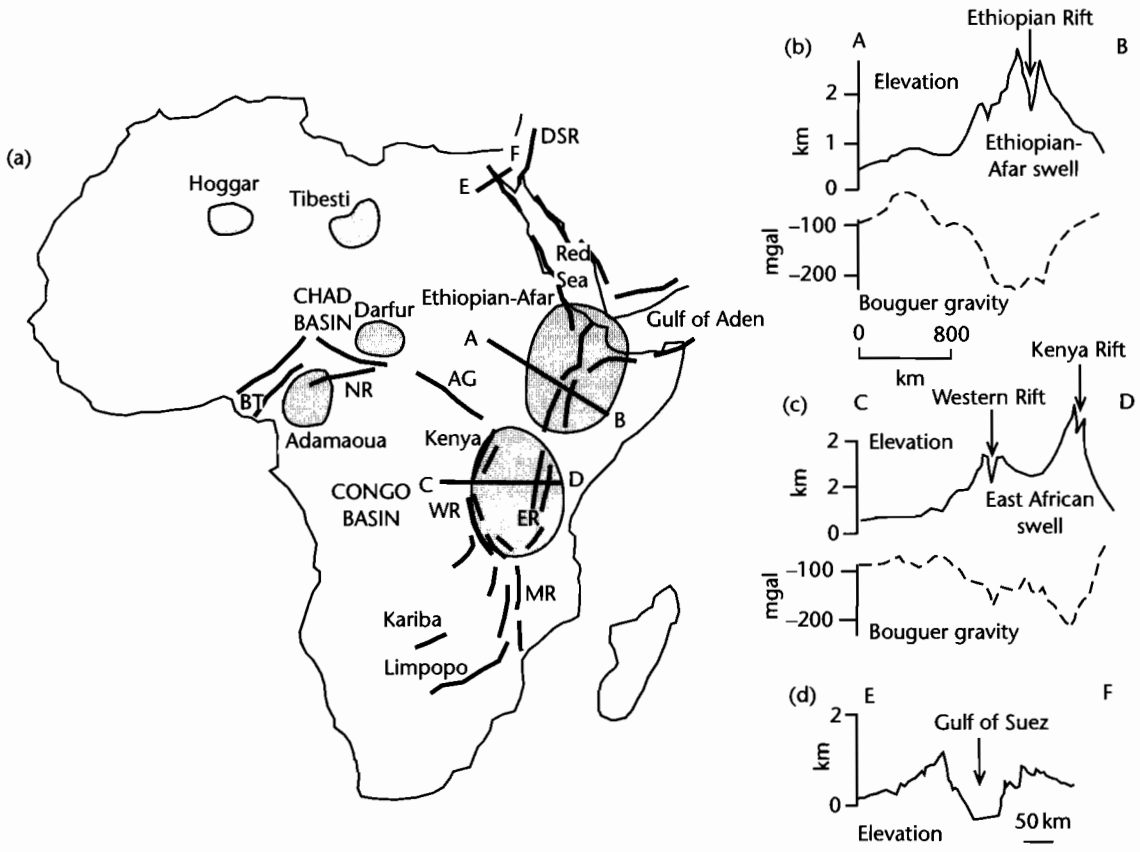

Fig. 3.6 (a) The major domal uplifts of Africa (Afar and East African domes) are due to uplift over hotspots in the mantle. Also shown are the smaller topographic uplifts of central Africa, and the main rift systems: AG, Abu Gabra Rift; BT, Benue Trough; DSR, Dead Sea Rift; MR, Malawi Rift; ER and WR, Eastern and Western Rifts; NR, Ngaoundere Rift. Topographic and Bouguer gravity profiles across the Afar (A–B) and East African (C–D) swells are shown in (b) and (c). (d) Topographic profile along E–F showing rift flank uplift along the Red Sea and Gulf of Suez. After Ebinger et al. (1989).

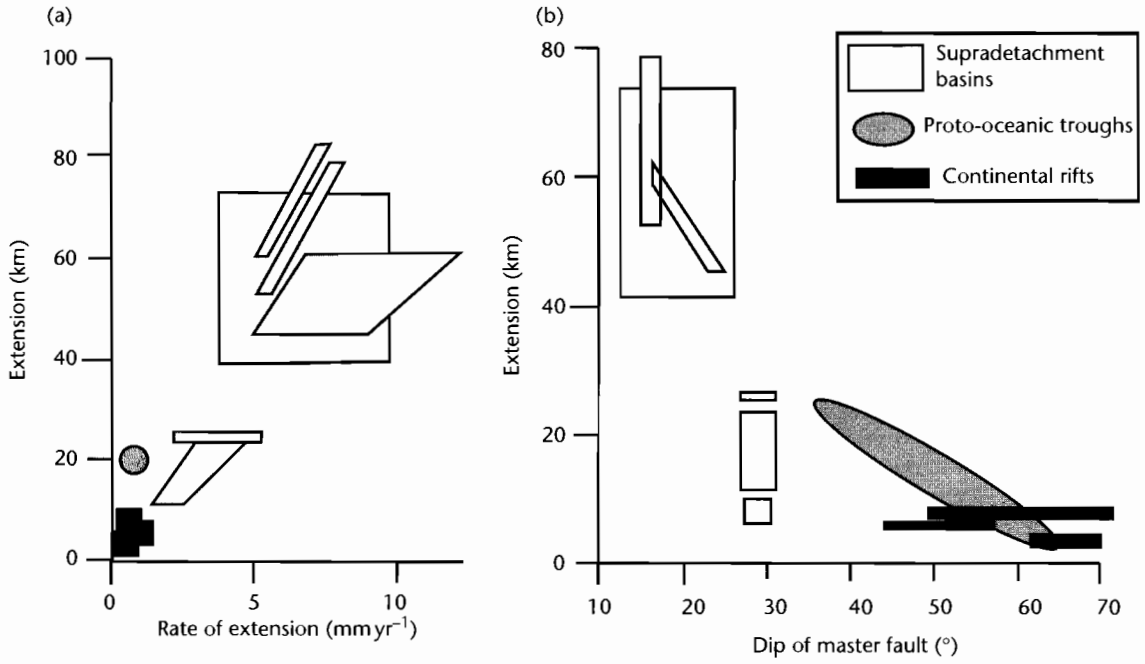

Fig. 3.7 Rifts, supradetachment basins, and proto-oceanic troughs in terms of their strain rate, total extensional strain, and dip of master faults, based on Friedmann and Burbank (1995). Reproduced courtesy of Blackwell Publishing Ltd.

domes of eastern and northeastern Africa are currently undergoing rifting, the smaller domes of north-central Africa are not. At a smaller length scale (<100 km) are the linear rift flank uplifts associated with border fault arrays. The <1 km-high highlands bordering the Gulf of Suez are a good example. Border fault footwalls involve upward tectonic fluxes, leading to enhanced denudation. In the southern Rhine Graben, tectonically driven exhumation of the rift flank has resulted in 2–3 km of erosion, exposing Hercynian crystalline basement in the Vosges of Alsace (France) and the Black Forest of Germany. Regions of extensive, diffuse extension are associated with plateau-type topography, such as the Basin and Range, USA and especially Tibet. In the first case, shallow subduction of relatively buoyant oceanic lithosphere beneath the North American Plate, and in the second case, thickening of continental lithosphere during India Asia collision, are the driving forces for extensive topographic uplift and extension.

Time scale and amount of extension: Extensional basins vary greatly in their duration of subsidence, total extensional strain, and therefore in their strain rate. Friedmann and Burbank (1995) believed there were two distinct families of basins, which could be recognized according to their strain rate, total extensional strain (or stretch factor β), and the dip of master faults (Fig. 3.7):

- Discrete continental rifts located on normal thickness crust (such as the Rhine Graben, Baikal Rift, Rio Grande Rift) extend slowly (<1 mm yr^{-1}) over long periods of time (10–>30 Myr), with low total extensional strain (generally <10 km). Master fault angles are steep (45–70°). Seismicity suggests that crustal extension takes place down to mid-crustal levels. At higher strain rates, narrow rifts may evolve through increased stretching into passive margins;
- supradetachment basins occur within wide extended domains with thickened crust. They typically extend quickly (<20 mm yr^{-1}) over short periods of time (5 12 Myr) with a high amount of total extensional strain (10–80 km). Master faults (detachments) are shallow in dip (10–30°), but may have originated at higher angles. Local anomalies in the ductile lower crust are amplified to produce core complexes (Wernicke 1985).

Table 3.1 Conjugate margins of the Atlantic.

Western margin	Eastern margin	Start of main rifting and duration
Southern Grand Banks	Iberia/Galicia	Valanginian (137 Ma) 15–25 Myr
Flemish Cap	Goban Spur	Barremian (127 Ma) 15–20 Myr
Labrador	SW Greenland	Barremian (127 Ma) 40–65 Myr

3.2.2 Passive continental margins

Passive continental margins involve strongly attenuated continental crust stretched over a region of 50–150 km, and exceptionally as much as 400–500 km (Keen et al. 1987), overlain by thin or thick sediment prisms. They are in general seismically inactive, and in mature examples heat flows are near-normal. Passive continental margins (also known as Atlantic-type margins) are characterized by seaward thickening prisms of marine sediments overlying a faulted basement with synrift sedimentary sequences, often of continental origin. The postrift seaward-thickening sediment prisms consist predominantly of shallow marine deposits. Seismic reflection sections show some passive margins to be underlain by linked listric extensional fault systems which merge into low-angle sole faults. The postrift or drifting phase in contrast is typically dominated by gravity-controlled deformation (salt tectonics, mud diapirism, slumps, slides, listric growth faults in soft sediments).

Passive margins overlie earlier rift systems that are generally subparallel to the ocean margins, or less commonly at high angles to the ocean margin (as in the case of failed arms of triple junctions such as the Benue Trough, Nigeria), or along transform fault zones (e.g., Grand Banks and Gulf of Guinea). The early synrift phase of sedimentation is commonly separated from a later drifting phase by an unconformity (the "break-up" unconformity of Falvey 1974). Some passive margins exhibited considerable subaerial relief at the end of rifting (leading to major unconformities), as in the case of the Rockall Bank, northeastern Atlantic, whereas in others the end of rifting may have occurred when the sediment surface was in deep water, as in the Bay of Biscay and Galicia margin of Iberia (Montadert et al. 1979).

Two end-members of passive margin can be identified based on the thickness of sediments (Fig. 3.8): (i) starved margins (2–4 km thick), and (ii) nourished margins (generally 5–12 km thick). In the central Atlantic, the American margin is nourished whilst the European margin is starved. In addition, some passive margins are associated with strong volcanic activity (Fig. 3.8), generally tholeiitic, at the time of break-up (White and McKenzie 1989). This volcanicity is commonly associated with subaerial emergence, as in the northern North Atlantic in the Early Tertiary (e.g., Skogseid et al. 2000).

Since passive margins represent the rifted edges of a piece of continental lithosphere, now separated by an ocean basin, it is possible to identify the original matching margins on either side of the ocean. These are known as *conjugate margins*. They are particularly well developed on either side of the northern Atlantic (Table 3.1).

Comparison of conjugate margins is informative regarding the geometry of extension prior to ocean basin development. For example, deep seismic reflection profiles show some conjugate pairs of passive margin to be symmetric, with seaward dipping, rotated fault blocks, whereas other deep profiles suggest the presence of a flat-lying or landward-dipping detachment or shear zone, producing a markedly asymmetrical pattern (Fig. 3.9). The profiles across the Labrador and SW Greenland margins show that although the brittle upper crust has been extended symmetrically, the lower crustal extension is particularly asymmetrical. Some margins show thin sediment covering wide regions of highly faulted, upper crust, commonly separated from underlying serpentinized upper mantle by a horizontal detachment (e.g., Iberia, Galicia, and SW Greenland margins). Other margins with thick sediment prisms consist of one or two major tilted crustal blocks and lack a horizontal detachment (e.g., Labrador margin).

In summary, these observations collectively suggest that there are a number of different archetypes of passive margin (Fig. 3.8):

- *Volcanically-active margins* are characterized by extrusive basalts, lower crustal igneous accretions, and significant uplift at the time of break-up. Continental extension and ocean spreading are thought to be intimately related to mantle plume activity;
- *nonvolcanic margins* lack evidence of high thermal activity at the time of break-up. Margins may be: (i) sediment-starved, with thin sediment veneers of 2–4 km draping large arrays of rotated synrift fault blocks above a subhorizontal detachment, as in the Bay

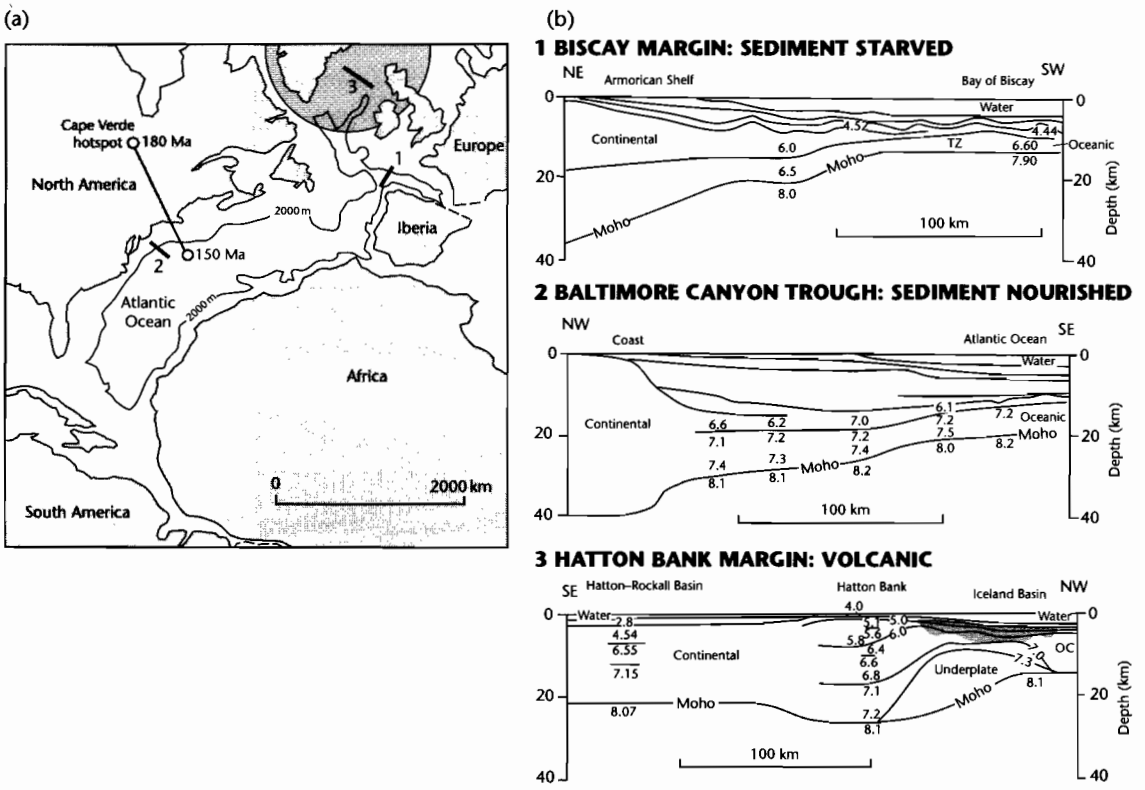

Fig. 3.8 Volcanic, sediment-nourished, and sediment-starved margins (after White and McKenzie 1989). (a) Location of margins in the central-north Atlantic region on a Middle Jurassic reconstruction (170 Ma), shortly after the onset of seafloor spreading; (b) Biscay margin, which is sediment starved; (c) Baltimore Canyon Trough margin, which is thickly sedimented; (d) Hatton Bank margin, which is characterized by important magmatic activity. Shaded area shows extent of extrusive basalts. Moho is overdeepened due to presence of igneous underplate. TZ, ocean–continent transition zone; OC, ocean crust. Reproduced courtesy of American Geophysical Union.

of Biscay, or (ii) sediment-nourished, with very thick (<15 km) postrift sedimentary prisms overlying a small number of tilted upper crustal fault blocks and a wide region of mid–lower crustal extension, as in the Baltimore Canyon region of the Eastern Seaboard of North America and the Labrador margin.

3.3 INTRODUCTION TO MODELS OF CONTINENTAL EXTENSION

3.3.1 Active and passive rifting idealizations

Early investigations of lithospheric extension suggested that rifting fell into two classes (Sengör and Burke 1978; Morgan and Baker 1983; Turcotte 1983; Keen 1985; Bott 1992), active and passive (Fig. 3.10). In *active rifting* deformation is associated with the impingement on the base of the lithosphere of a thermal plume or sheet. Conductive heating from the mantle plume, heat transfer from magma generation, or convective heating may cause the lithosphere to thin. If heat fluxes out of the asthenosphere are large enough, relatively rapid thinning of the continental lithosphere causes isostatic uplift. Tensional stresses generated by the uplift may then promote rifting. In *passive rifting* tensional stresses in the continental lithosphere cause it to fail, allowing hot mantle rocks to penetrate the lithosphere. Crustal doming and volcanic activity are only secondary processes. McKenzie's (1978a) widely accepted model for the origin of sedimentary basins belongs to this class of passive rifting. If

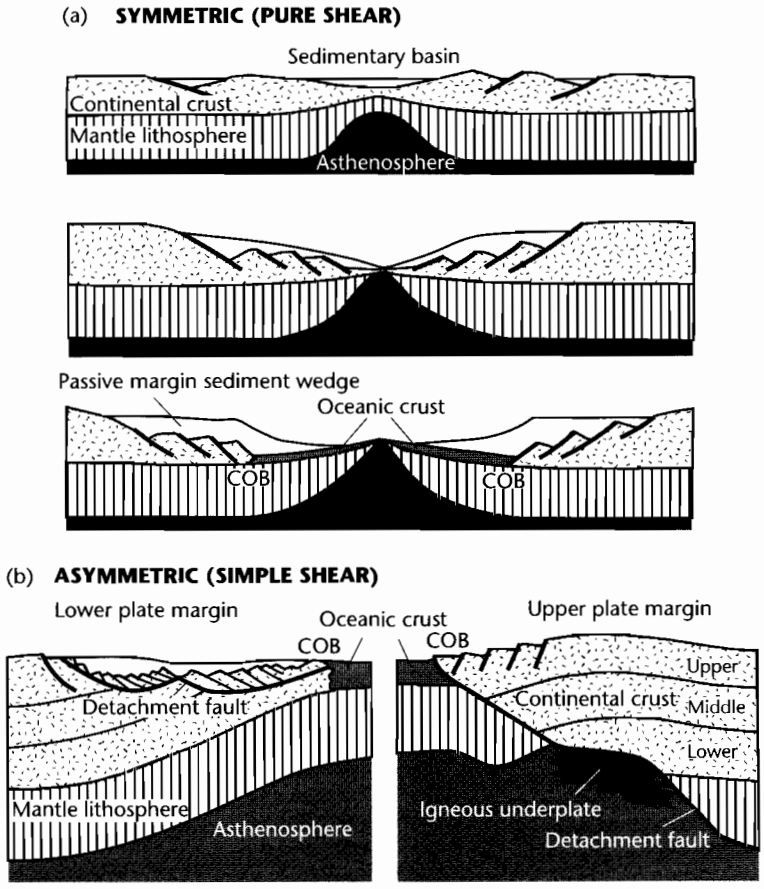

Fig. 3.9 Conjugate margins based on deep seismic information (after Lister et al. 1986; Louden and Chian 1999). (a) Symmetric margin (pure shear), and (b) asymmetric (simple shear) with a lithospheric detachment fault. COB is ocean–continent boundary. Reproduced courtesy of Royal Society London.

passive rifting is occurring, rifting takes place first and doming may follow but not precede it. Rifting is therefore a passive response to a regional stress field. It is not easy to determine whether a given rift is either active or passive, since for small mantle heat flows the amount of uplift may be minimal. In addition, it should be understood that active and passive models are idealized abstractions that represent "end-members." Real world cases may exhibit aspects of each (Khain 1992). The East African Rift appears to be a good candidate for active rifting whereas it has been suggested that the Rio Grande Rift may be due to passive rifting.

Some rifts are at high angles to associated plate boundaries, such as orogenic belts (Burke 1976, 1977). Some of these rifts appear to be linked to arms of triple junctions associated with the early stages of ocean opening – these failed rifts are termed *aulacogens*. Others are aligned at high angles to associated collision zones and are termed *impactogens* (Sengör et al. 1978) or *collision grabens* (Fig. 3.11). Whereas aulacogens are formed contemporaneously with the ocean opening phase, impactogens clearly postdate this period, being related temporally with collision. The Upper Rhine Graben has been cited as an example of an impactogen (Sengör et al. 1978) and collision in the Grenville orogeny has also been invoked as a cause of the Keweenawan Rift in North America (Gordon and Hempton 1986). The effects of compressional in-plane stresses on extensional basin development is discussed in §3.6.3.

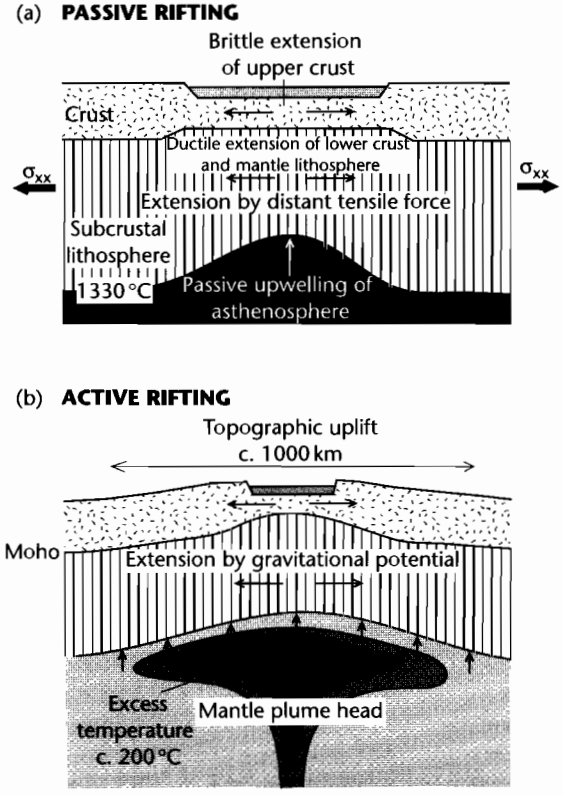

Fig. 3.10 Active and passive rifting end-member idealizations. (a) Passive rifting caused by a distant tensile deviatoric force σ_{xx} causes thinning of the lithosphere and passive upwelling of hot asthenosphere; (b) Impingement on the base of the lithosphere of a mantle plume causes long wavelength topographic doming and gravitationally driven extension of the lithosphere.

3.3.2 Postrift subsidence at passive continental margins

The synrift subsidence during stretching of the lithosphere is caused by brittle extension of the crust. Several mechanisms have been postulated as influences on the subsidence characterizing the postrift (or syn–drift) phase of passive margin development (§ 3.2.2).

It is universally agreed that the main mechanism for subsidence is cooling following lithospheric thinning: the upwelling of asthenosphere (McKenzie 1978a) is followed by thermal contraction (for detailed treatment see §3.4). Lithospheric stretching, however, may be accompanied by important magmatism, producing dyke swarms, plutons and extensive basaltic sheets (Royden et al. 1980; White and McKenzie 1989). Emplacement of large volumes of basaltic melt into the crust (or along its base) should produce transient uplift, followed by subsidence as the extruded, intruded, and underplated material cools. The result, long after emplacement, is determined by the density and thickness of the igneous additions to the lithosphere. Commonly, these igneous additions have a higher density than the crust but lower density than the mantle. Assuming that the bulk of the igneous accretion replaces lithospheric mantle, passive margins with large amounts of magmatic activity should remain relatively elevated compared to nonmagmatic margins (Fig. 3.12) (§3.7.2).

It has been postulated that subsidence may also result from phase changes (gabbro to eclogite) in lower crustal or mantle–lithosphere rocks. It is not known whether this process can be widespread enough to be responsible for significant amounts of subsidence at passive margins.

The growing sediment prism acts as a load on the lithospheric substrate and is supported isostatically. This may be by lithospheric flexure (Beaumont et al. 1982; Watts et al. 1982), as long as the wavelength of the load is sufficiently short. Historically, there was much debate as to whether flexural support involved an elastic plate or a viscoelastic (Maxwell) plate overlying a weak substratum (Watts et al. 1982). Since active faulting and high heat flows accompany the early stages of rifting, it has been assumed that an Airy isostatic model is most applicable during this period. However, postrift sediments are gently dipping and of wide extent, suggesting that flexure takes over at some stage after the end of rifting. Watts (1982) believed that the characteristic pattern of stratigraphic onlap on the eastern Atlantic and other margins suggested an increasing rigidity of the lithosphere with time – the expected result of an elastic lithosphere heated during the rifting stage and subsequently cooling.

3.3.3 Dynamical models involving lithospheric strength and rheology

In the last decade, emphasis has shifted away from active and passive rifting models and towards an understanding of the dynamics of stretching a piece of continental lithosphere with a particular strength and viscosity structure (Houseman and England 1986; Sonder and England 1989; Newman and White 1999). Increasingly, sophisticated numerical model predictions are examined alongside high-resolution 3-D seismic reflection data sets. The

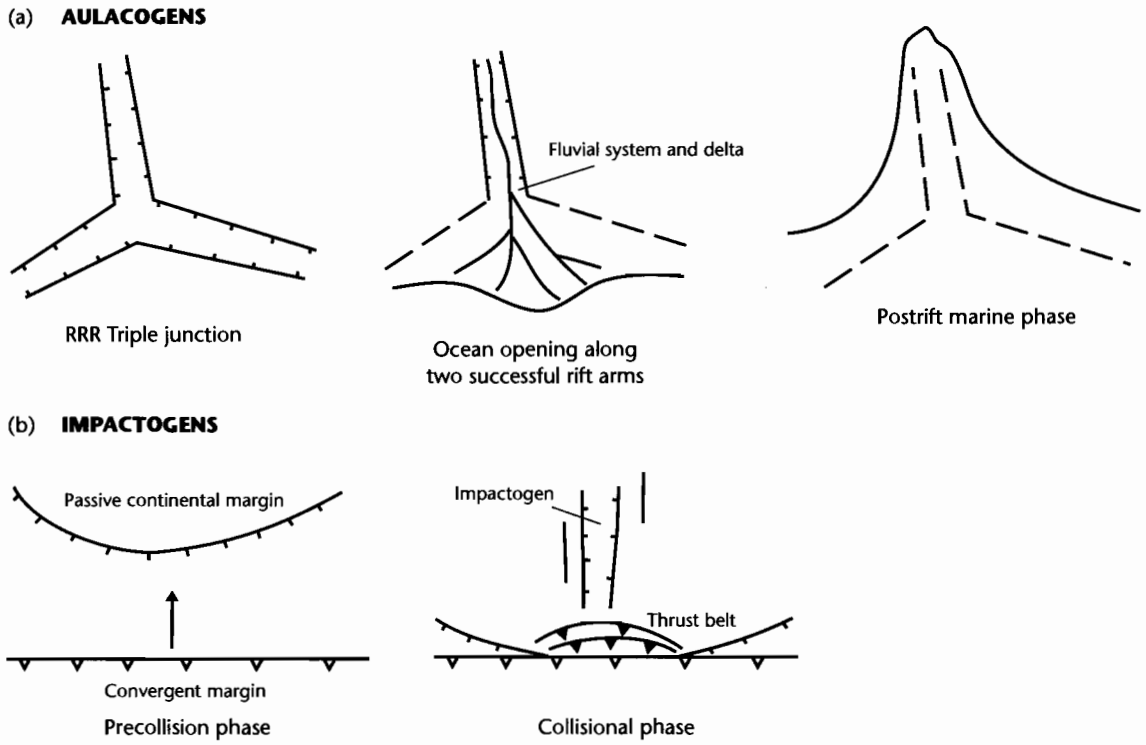

Fig. 3.11 Schematic diagrams to illustrate the development of (a) aulacogens and (b) impactogens, based on Sengör et al. (1978). In (a), successful opening of an ocean basin along two rift arms at a triple junction causes the development of a rift–sag basin along the third, failed rift arm. In (b), collision with a passive continental margin causes an extensional graben at high angles to the orogenic front.

fundamental infrastructure of these numerical models is the description of the rheology of the continental lithosphere (Fernandez and Ranalli 1997).

The *strength of the lithosphere* can be judged from laboratory experiments (e.g., Kohlstedt et al. 1995), though there is the problem of "scaling-up" laboratory experiments to the strain rates experienced by rocks in the lithosphere. The concept of the *strength envelope* (Goetze and Evans 1979; Ranalli 1995), which is the profile of lithospheric strength as a function of depth, underpins the rheological modeling of lithospheric extension and is discussed in greater detail in §2.4.6.

The *rheology of the lithosphere* and its response to extensional deformation is most strongly controlled by its temperature and its mineralogy. A material can only maintain stresses over geological time if the ratio of actual temperature to its melting temperature (known as the *homologous temperature*) is less than about 0.4. This implies that only the upper parts of the crust and upper mantle are capable of supporting elastic stresses over long periods of time. Most dynamic models of lithospheric extension use laboratory data for the dominant mineral comprising crust and mantle – that is, quartz + felspar for the crust, and olivine for the mantle. On a graph of stress at which failure takes place (σ_1–σ_3) versus depth in the continental lithosphere, two brittle–ductile transitions and two stress-supporting regions are predicted, one in the upper–midcrust, and the other in the upper mantle lithosphere (Figs. 1.3, 3.13). Since the quartz + felspar rheology of the continental lithosphere is weak at high temperatures, zones of orogenic thickening are prone to collapse by extension – an idea originally proposed by Tapponnier and Molnar (1976).

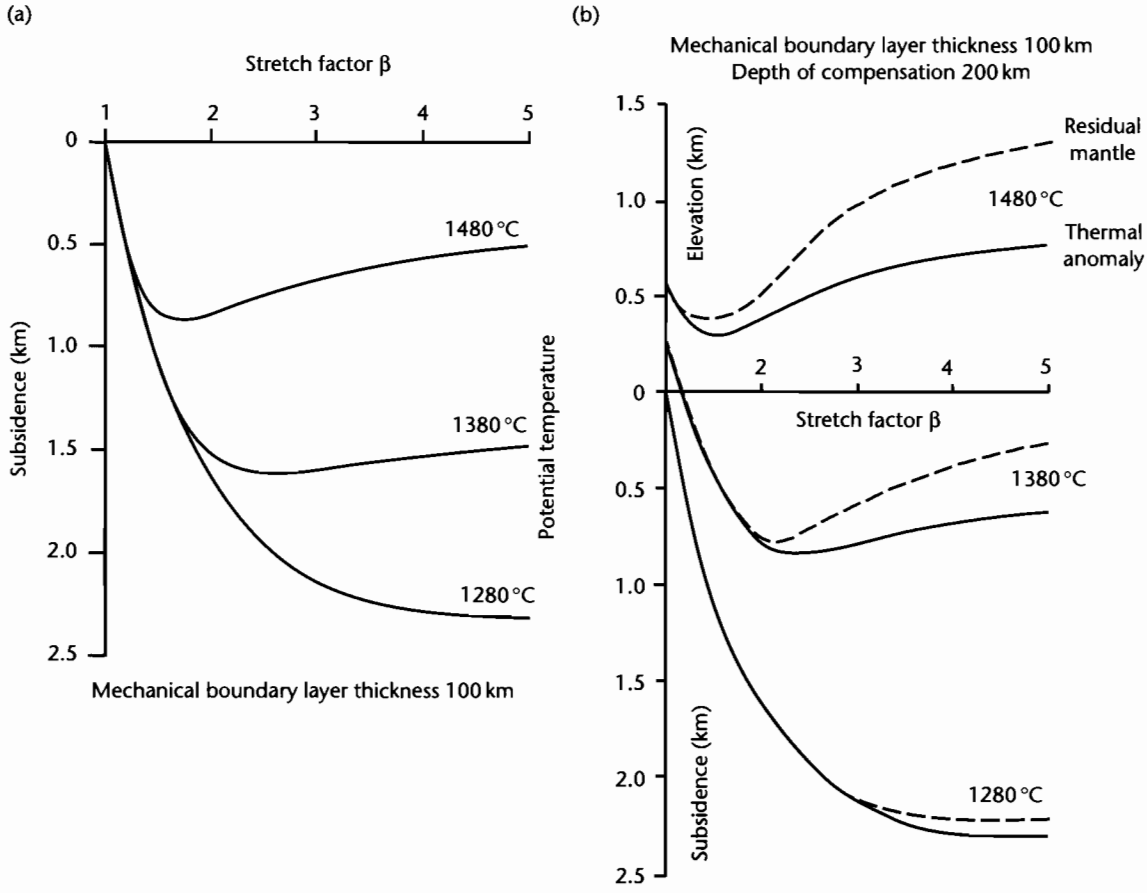

Fig. 3.12 Uplift and subsidence associated with plume activity at a spreading margin (after White and McKenzie 1989). (a) Subsidence at the time of rifting as a function of the stretch factor for potential temperatures of 1280 °C (normal), 1380 °C, and 1480 °C. Each curve incorporates the effects of lithospheric thinning, and crustal additions of melts caused by decompression of the mantle; (b) The effects of the reduced density of the abnormally hot asthenosphere (thermal anomaly) and the reduced density of the depleted mantle from which melt has been extracted (residual mantle) for three potential temperatures, as in (a). Plume activity causes the lithosphere to be elevated well above the level expected for an asthenosphere of normal temperature. The depth of compensation of 200 km is typical of the depth over which anomalously hot mantle is likely to extend. Reproduced courtesy of American Geophysical Union.

We will examine the results of numerical models of lithospheric extension in §3.6. One of the major results of numerical modeling is that the changing temperature field of lithospheric particles during extension results in a changing viscosity of the mantle lithosphere over time. Consequently, dependent on the initial strain rate, the extending lithosphere may extend rapidly into a runaway state, or may stop extending. This may explain dynamically the strain rate and bulk strain history of narrow rifts, wide rifts, and passive margins.

3.4 UNIFORM STRETCHING OF THE CONTINENTAL LITHOSPHERE

3.4.1 McKenzie's (1978a) uniform stretching model

Falvey (1974) proposed that the subsidence histories of various continental rift basins and margins could be explained qualitatively by extension in both crust and subcrustal lithosphere. The crust was assumed to fail by

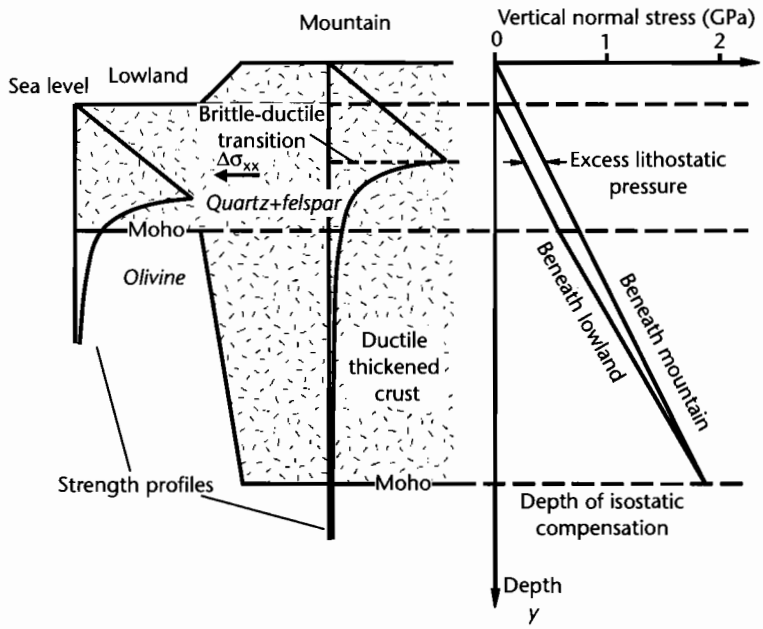

Fig. 3.13 Strength of the continental lithosphere and extensional collapse of thickened continental lithosphere. Thickened crust collapses for two reasons: (i) the quartz-felspar crust is rheologically weak, and (ii) the lithostatic stress is higher under the mountain than under the lowland region, causing it to spread laterally under a horizontal deviatoric stress (130 MPa at 10 km beneath the lowland). If the brittle yield strength of granite is 400 MPa, the brittle–ductile transition should be at a depth of *c.* 15 km beneath the mountain (density of granite 2750 kg m^{-3}).

brittle fracture and the subcrustal lithosphere to flow plastically. The isostatic disequilibrium caused by the crustal extension leads to a compensating rise of the asthenosphere, and consequent regional uplift. Partial melting of upwelled asthenosphere leads to volcanism and further upward heat transfer. Eventually, after the continental lithosphere has been extended and thinned to crustal levels, new oceanic crust is generated as the rift evolves into a continental margin.

McKenzie (1978a) considered the quantitative implications of a passive rifting or mechanical stretching model, assuming the amount of crustal and lithospheric extension to be the same (*uniform stretching*). The stretching is symmetrical, no solid body rotation occurs, so this is the condition of *pure shear*. He considered the instantaneous and uniform extension of the lithosphere and crust with passive upwelling of hot asthenosphere to maintain isostatic equilibrium (Fig. 3.14). The initial surface of the continental lithosphere is taken to be at sea-level and since the lithosphere is isostatically compensated throughout (Airy model), the subsidence or uplift consequent upon mechanical stretching can be obtained.

The results of McKenzie's (1978a) quantitative model of uniform stretching can be summarized as follows:

- The total subsidence in an extensional basin is made of two components: an initial *fault controlled subsidence* which is dependent on the initial thickness of the crust and the amount of stretching β; and a subsequent *thermal subsidence* caused by relaxation of lithospheric isotherms to their prestretching position, and which is dependent on the amount of stretching alone;
- whereas the fault-controlled subsidence is modeled as instantaneous, the rate of thermal subsidence decreases exponentially with time. This is the result of a decrease in heat flow with time. The heat flow reaches 1/e of its original value after about 50 Myr for a "standard" lithosphere, so at this point after the cessation of rifting, the dependency of the heat flow on β is insignificant.

The assumptions, boundary conditions, and development of the model are elaborated in the boxed text.

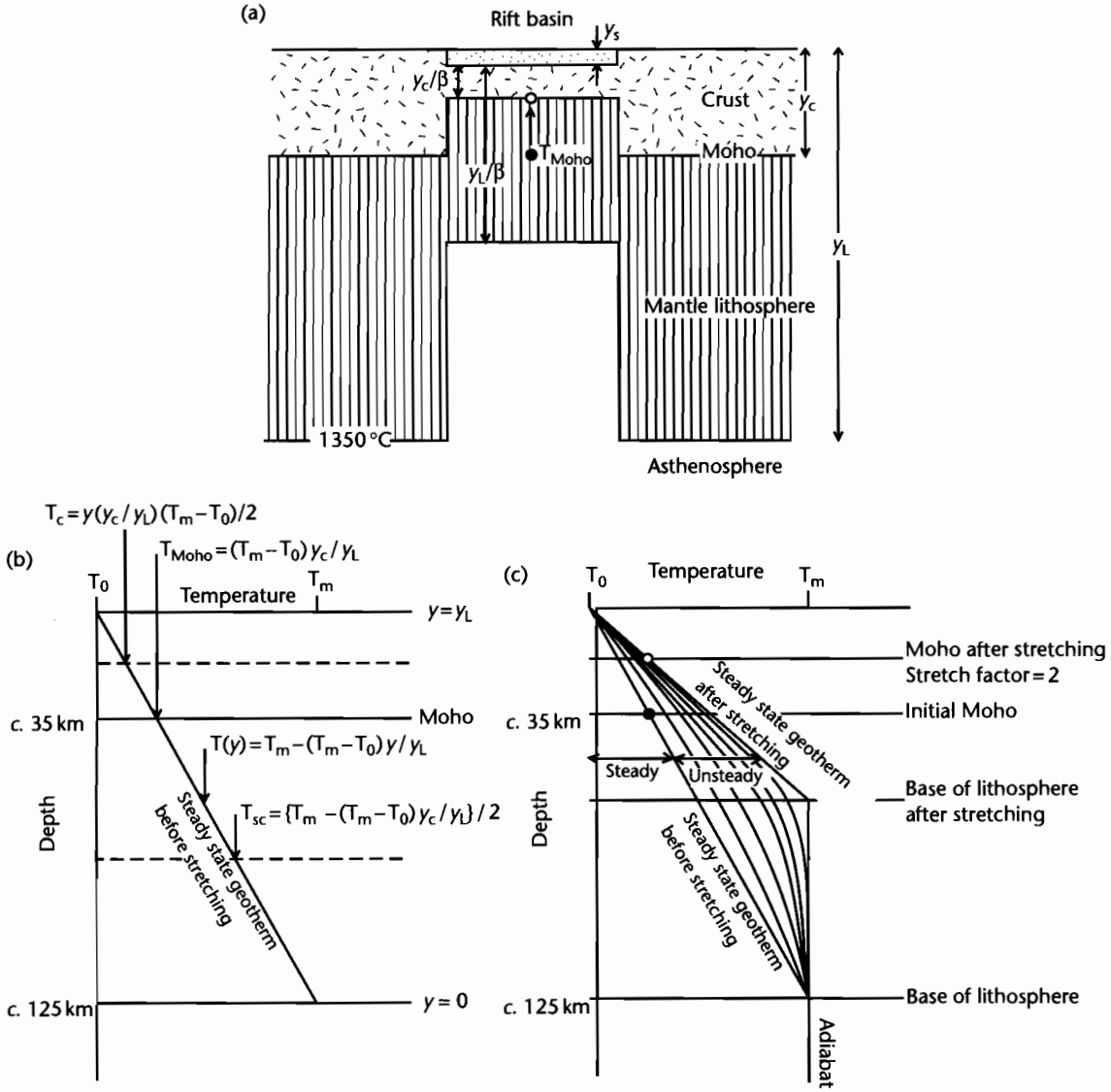

Fig. 3.14 Set-up for McKenzie's (1978a) uniform stretching model. (a) The crust and subcrustal lithosphere stretch horizontally and thin vertically uniformly with depth; (b) Derivation of average crustal and subcrustal temperatures from the steady state geotherm; (c) Geotherm following instantaneous stretching. The total temperature is made of steady and unsteady (transient) components. The transient temperature is shown as curves as a function of time.

BOXED TEXT 3.1: McKenzie's (1978a) Uniform Extension Model

The lithostatic column before rifting is made up of two components (see §2.1)

$$y_c\rho_c g + (y_L - y_c)\rho_{sc} g \tag{3.1}$$

where y_c and y_L are the thicknesses of the crust and lithosphere respectively, ρ_c and ρ_{sc} are the average densities of the crust and subcrustal lithosphere and g is the gravitational acceleration, which, because it is common to all lithospheric columns, can be ignored in the following analysis. These densities are assumed to have a linear relationship to temperature, and the geotherm is also assumed to be linear from T_m at the base of the lithosphere to T_0 at the surface (Fig. 3.14). As a result the average densities are given by

$$\rho_c = \rho_c^*(1 - \alpha_v T_c) \tag{3.2}$$

and

$$\rho_{sc} = \rho_m^*(1 - \alpha_v T_{sc}) \tag{3.3}$$

where ρ_c^* and ρ_m^* are crustal and mantle densities at 0 °C, α_v is the volumetric coefficient of thermal expansion and T_c and T_{sc} are the average crustal and subcrustal temperatures. Since the geotherms are linear, T_c and T_{sc} can be easily obtained as

$$T_c = \frac{(T_m - T_0)}{2}\frac{y_c}{y_L} \tag{3.4}$$

and

$$T_{sc} = \frac{1}{2}\left\{T_m - \frac{y_c}{y_L}(T_m - T_0)\right\} \tag{3.5}$$

By assuming that the surface temperature is 0 °C, these expressions simplify to

$$T_c = \frac{T_m}{2}\frac{y_c}{y_L} \tag{3.6}$$

and

$$T_{sc} = \frac{T_m}{2}\left(1 - \frac{y_c}{y_L}\right) \tag{3.7}$$

After rifting there are four components to the lithostatic stress at the depth of the original lithospheric thickness:

$$y_s\rho_s + (y_c/\beta_c)\rho_c + \{(y_L/\beta_L) - (y_c/\beta_c)\}\rho_{sc} + \{y_L - (y_L/\beta_L) - y_s\}\rho_m \tag{3.8}$$

where the new terms introduced are y_s, the thickness of sediment, water or air filling the rift axis; β_c and β_L, the stretch factors for the crust and lithosphere (for uniform stretching $\beta_c = \beta_L$); ρ_s, the average sediment, water, or air bulk density; ρ_{sc}, the subcrustal, lithospheric mantle density, equal to $\rho_m^*(1 - \alpha T_m)$ where ρ_m^* is the mantle density at 0 °C.

Balancing the columns before and after uniform stretching ($\beta_L = \beta_c = \beta$)

$$y_c\rho_c + (y_L - y_c)\,\rho_{sc} = y_s\rho_s + (y_c/\beta)\,\rho_c + (y_L - y_c)\,(1/\beta)\,\rho_{sc} + (y_L - y_s - y_L/\beta)\,\rho_m$$

Regrouping the terms

$$y_s = \frac{(1 - 1/\beta)}{(\rho_m - \rho_s)}\{\rho_m y_L - y_c\rho_c - (y_L - y_c)\rho_{sc}\} \tag{3.9}$$

Substituting the correct terms for ρ_c, ρ_{sc}, ρ_s, and ρ_m into (3.9) we have after rearrangement

$$y_s = \frac{y_L\left\{\left(\rho_m^* - \rho_c^*\right)\frac{y_c}{y_L}\left(1 - \alpha_v\frac{T_m}{2}\frac{y_c}{y_L}\right) - \frac{\alpha_v T_m \rho_m^*}{2}\right\}(1 - 1/\beta)}{\rho_m^*(1 - \alpha_v T_m) - \rho_s} \tag{3.10}$$

where β is the stretch factor, y_L is the initial thickness of the lithosphere, y_c is the initial thickness of the crust, ρ_m^* is the density of the mantle (at 0 °C), ρ_c^* is the density of the crust (at 0 °C), ρ_s is the average bulk density of sediment or water filling the rift, α_v is the thermal expansion coefficient of both crust and mantle, T_m is the temperature of the asthenosphere, and y_s is positive for subsidence, negative for uplift. Typical values for the above parameters, mostly derived from oceanic lithosphere studies (Parsons and Sclater 1977), are $y_L = 125$ km, $\rho_m^* = 3330\,\text{kg m}^{-3}$, $\rho_c^* = 2800\,\text{kg m}^{-3}$, $\alpha_v = 3.28 \times 10^{-5}\,°\text{C}^{-1}$, and $T_m = 1333$ °C.

For all values of the stretch factor, the initial subsidence S_i is positive for values of crust/lithosphere thickness ratio of greater than 0.12, corresponding to a crustal thickness y_c greater than about 15 km within a lithosphere of 125 km (parameter values as above, and sediment density of $2000\,\text{kg m}^{-3}$). McKenzie's model therefore predicts an initial subsidence with no uplift where continental crusts are "normal" in thickness (Fig. 3.15). The initial subsidence caused by isostatic

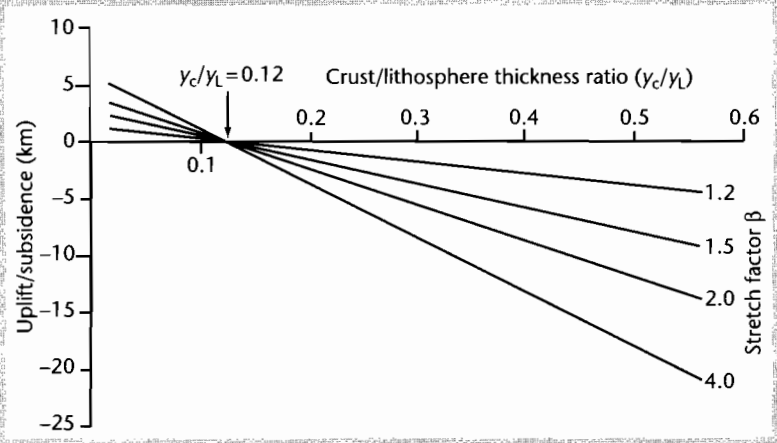

Fig. 3.15 Synrift subsidence as a function of the crustal/lithosphere thickness ratio y_c/y_L for stretch factors β between 1.2 and 4, using the uniform stretching model. Crustal, mantle and sediment densities are 2700 kg m^{-3}, 3300 kg m^{-3} and 2000 kg m^{-3} respectively. At a crust/lithosphere thickness ratio of 0.12 (corresponding to a crust of 15 km in a lithosphere 125 km thick), there is neither uplift nor subsidence during rifting. For thinner crusts, uplift occurs, and for thicker crusts, subsidence occurs. Since crustal thicknesses are typically 30–35 km, the synrift phase should be characterized by subsidence.

adjustment to mechanical stretching is followed by a long-term gradual subsidence caused by cooling and thermal contraction of the lithosphere following extension. This *thermal subsidence* is dependent on β alone.

The stretching of the lithosphere causes two responses: (i) the thinning of the crust and the fault-controlled subsidence is *permanent*, i.e., the brittle crust cannot regain its original thickness, and (ii) the thinning of the mantle lithosphere and any elevation changes caused by the presence of hot asthenosphere are *transient*.

In order to predict the cooling of the lithosphere following rifting that causes the thermal subsidence, we must know the heat flow through time. Following the *instantaneous* increase in heat flow accompanying rifting in the McKenzie (1978a) model, the heat flow decreases exponentially with time. We know two boundary conditions and we make two assumptions:

Boundary conditions:
(1) $T = 0$ at $y = y_L$
(2) $T = T_m$ at $y = 0$

Assumptions:
(1) lateral temperature gradients are much smaller than vertical gradients;

$$\left(\frac{\partial T}{\partial x} \approx 0 \approx \frac{\partial T}{\partial z}\right)$$

(2) internal heat production from radioisotopes is ignored.

The 1-D unsteady (that is, time-dependent) heat flow equation is

$$\frac{\partial T}{\partial t} = K\frac{\partial^2 T}{\partial y^2} \tag{3.11}$$

where the second derivative gives the curvature of the geotherm as it relaxes to its prestretching gradient. The temperature at any depth and time ($T(y, t)$) is made up of a steady-state solution $s(y) = T_m(1 - y/y_L)$ which applies to a linear geotherm in the lithosphere, and an unsteady-state component $u(y, t)$. The general solution for the unsteady term is

$$u(y,t) = \sum_{n=0}^{\infty} An \sin\left(\frac{n\pi y}{y_L}\right) \exp\left(\frac{-n^2\pi^2\kappa t}{y_L^2}\right) \tag{3.12}$$

where A is a constant and n is an integer that expresses the order of the harmonic of the Fourier transform, and κ is the thermal diffusivity. Therefore, as n increases, the negative exponential becomes very small and ceases to contribute to the unsteady temperature field. As a gross approximation it is frequently satisfactory to consider only $n = 1$. The constant A depends on the asthenospheric temperature (T_m) and the amount of stretching.

Continued

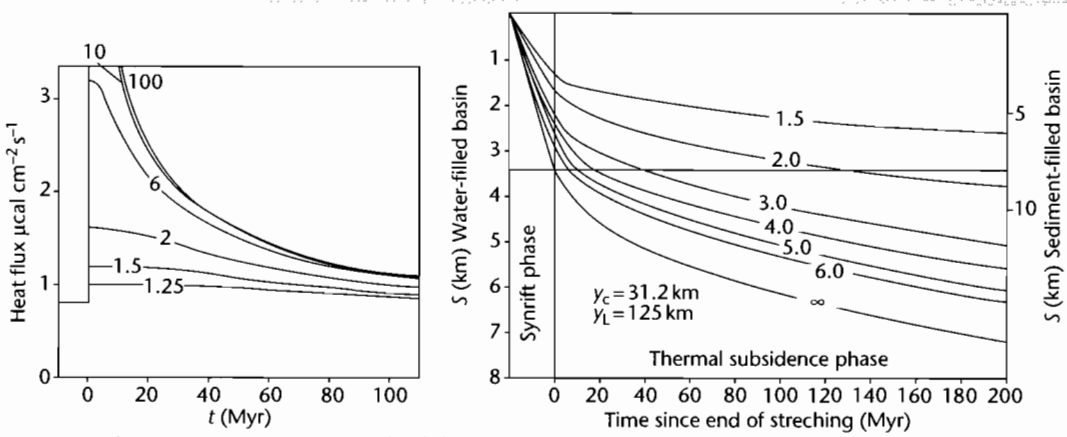

Fig. 3.16 Heat flow and subsidence as a function of the stretch factor using the uniform stretching model. (a) Heat flux against time (after McKenzie 1978a, p.28). After *c.* 50 Myr, the heat fluxes are similar for all values of stretch factor; (b) Elevation change (subsidence) against time for water-filled and sediment-filled basins, showing the negative exponential form of the subsidence history during the postrift, thermal contraction phase (after Sclater et al. 1980a).

At $t = 0$,

$$An = \left\{\frac{2}{n}(-1)^{n+1}\frac{\beta}{n\pi}\sin\left(\frac{n\pi}{\beta}\right)T_m\right\}$$

so if $n = 1$, An simplifies to $\frac{2}{\pi}\frac{\beta}{\pi}\sin\left(\frac{\pi}{\beta}\right)T_m$

The full solution for $T(y, t)$ is therefore the sum of the steady and unsteady components,

$$T(y,t) = T_m\left(1-\frac{y}{y_L}\right)+\left\{\frac{2}{\pi}\frac{\beta}{\pi}\sin\left(\frac{\pi}{\beta}\right)T_m\right\} \exp\left(-\frac{\pi^2\kappa t}{y_L^2}\right)\sin\left(\frac{\pi y}{y_L}\right) \quad (3.13)$$

or regrouping and simplifying

$$\frac{T(y,t)}{T_m} = \left(1-\frac{y}{y_L}\right)+\frac{2}{\pi}\frac{\beta}{\pi}\sin\left(\frac{\pi}{\beta}\right)\exp\left(-\frac{t}{\tau}\right)\sin\left(\frac{\pi y}{y_L}\right) \quad (3.14)$$

where $\tau = y_L^2/\pi^2\kappa$, and is known as the *thermal time constant* of the lithosphere.

The surface heat flux is given by Fourier's law (§2.2.1) which states that the flux is the temperature gradient times the thermal conductivity ($q_{y=L} = K\delta T/\delta y$). For $n = 1$, this is

$$q = \frac{KT_m}{y_L}\left\{1+\frac{2\beta}{\pi}\sin\left(\frac{\pi}{\beta}\right)e^{-t/\tau}\right\} \quad (3.15)$$

The subsidence caused by the thermal contraction is then given by

$$S(t) = E_0\frac{\beta}{\pi}\sin\left(\frac{\pi}{\beta}\right)(1-e^{-t/\tau}) \quad (3.16)$$

where

$$E_0 = 4y_L\rho_m^*\alpha_v T_m/\pi^2\left(\rho_m^*-\rho_s\right) \quad (3.17)$$

and ρ_s is the average density of the water or sediment filling the basin, ρ_m^* is the mantle density at 0 °C, α_v is the volumetric coefficient of thermal expansion, and the remaining terms are defined above.

The result of equation (3.15) is that heat flux is strongly dependent on the amount of stretching, the dependency becoming insignificant after about one thermal time constant (τ), or 50 Myr. At times younger than ~20 Myr, higher harmonics ($n = 2, 3 \ldots$) should be used in equation (3.12). Heat flux is sketched in Fig. 3.16a. Subsidence due to thermal relaxation is shown in Fig. 3.16b for comparison. If the subsidence history of a basin is known, it is therefore possible to estimate β from the thermal subsidence curve (§3.8.1).

Heat flux and subsidence calculated from the above uniform stretching model is provided in a Matlab exercise at www.erdw.ethz.ch/Allen.

3.4.2 Uniform stretching at passive continental margins

The uniform stretching model has been applied to the formation of passive margins (e.g., Le Pichon and Sibuet 1981). For the situation where stretching of the whole lithosphere occurs instantaneously at time $t = 0$ (or within a period of 20 Myr according to Jarvis and McKenzie 1980), heat production from radioactivity is ignored, local (Airy) isostatic compensation is maintained throughout, and the continental surface is initially at sea-level, the initial subsidence is given by equation (3.10). But since we are now dealing with passive margins, it is important to investigate the subsidence S_∞ at time $t = \infty$. The initial subsidence S_i (eqn 3.10) is a linear function of $(1 - 1/\beta)$ and S_∞ can also be expressed as a linear function of $(1 - 1/\beta)$. By introducing new parameters ρ'_{sc} and ρ'_c as the average densities of the subcrustal mantle part of the lithosphere and crust at time t_∞, the final subsidence S_∞ can be expressed

$$S_\infty = \frac{y_L(\rho'_{sc} - \rho_{sc}) + y_c\{\rho_{sc} - (\rho'_{sc}/\beta) + (\rho'_c/\beta) - \rho_c\}}{(\rho_m - \rho_w)} \quad (3.18)$$

The average densities of the subcrustal, mantle part of the lithosphere and the crust at time t_∞ are

$$\rho'_{sc} = \rho^*_m\left(1 - \frac{\alpha_v}{2}T_m - \frac{\alpha_v}{2}T_m\frac{y_c}{\beta y_L}\right) \quad (3.19)$$

and

$$\rho'_c = \rho^*_c\left(1 - \frac{\alpha_v}{2}T_m\frac{y_c}{\beta y_L}\right) \quad (3.20)$$

where, as a reminder y_L is the initial lithospheric thickness, y_c the initial thickness of the continental crust (at $t = 0$), the temperature at the base of the lithosphere is equal to the temperature of the asthenosphere T_m, ρ^*_m, and ρ^*_c are the densities of the mantle material and continental crust at 0 °C, ρ_w is the density of the seawater, α_v is the coefficient of thermal expansion. The average densities of the mantle part of the lithosphere, the crust before stretching and the asthenosphere are ρ_{sc}, ρ_c, and ρ_m.

From (3.18) to (3.20),

$$S_\infty = y_c(1 - 1/\beta)\left\{\frac{\rho_{sc} - \rho_c + \rho^*_m(\alpha_v/2)T_m + \varepsilon}{\rho_m - \rho_w}\right\} \quad (3.21)$$

where

$$\varepsilon = \left(\frac{\rho^*_m - \rho^*_c}{\beta}\right)\left(\frac{\alpha_v}{2}T_m\frac{y_c}{y_L}\right) \quad (3.22)$$

or by slight rearrangement,

$$S_\infty = y_c(1 - 1/\beta)\left\{\frac{(\rho^*_m - \rho^*_c)[1 - (\alpha_v/2)T_m(y_c/y_L)]\varepsilon}{(\rho_m - \rho_w)}\right\} \quad (3.23)$$

In fact, neglect of the additional term ε introduces an error of less than 0.5%.

The difference between the initial subsidence S_i and the final subsidence S_∞ is the subsidence caused by the progressive return to thermal equilibrium, i.e., that due to thermal contraction on cooling. The latter is termed thermal subsidence S_t and of course $S_t = S_\infty - S_i$.

3.4.2.1 Application to the sediment-starved Bay of Biscay and Galicia margins

As an example of this kind of analysis, it is possible to examine seismic reflection profiles across the northern Bay of Biscay and Galicia continental margins (Montadert et al. 1979) (Fig. 3.8a) and to test whether the uniform stretching model accurately predicts the observed subsidence. Active extensional tectonics started in the Late Jurassic–Early Cretaceous (*c.* 140 Ma). Extension extended outwards from a central region, creating new fault blocks which were progressively tilted. By the time oceanic crust was emplaced (120 Ma) the subsiding trough had reached a depth of about 2.4 km, and simultaneously active tectonics ceased, giving way to thermal subsidence. The Bay of Biscay is relatively starved of sediment, minimizing the effects of sediment loading compared to, say, the US Atlantic continental margin.

The following constants were chosen to fit the Biscay and Galicia data (Le Pichon and Sibuet 1981): $y_L = 125$ km (from Parsons and Sclater 1977); $y_c = 30$ km (from refraction data); $\rho^*_m = 3350\,\mathrm{kg\,m^{-3}}$; $\rho^*_c = 2780\,\mathrm{kg\,m^{-3}}$; $\rho_w = 1030\,\mathrm{kg\,m^{-3}}$; $\alpha_v = 3.28 \times 10^{-5}\,^\circ\mathrm{C}^{-1}$ (from Parsons and Sclater 1977); $T_m = 1333\,^\circ\mathrm{C}$ (from Parsons and Sclater 1977). Using these constants, the initial fault controlled subsidence simplifies to

$$S_i = 3.61(1 - 1/\beta)\,\mathrm{km} \quad (3.24)$$

and the final subsidence becomes

$$S_\infty \sim 7.83(1-1/\beta)\,\text{km} \tag{3.25}$$

so the thermal subsidence is the difference between S_i and S_∞,

$$S_t \sim 4.21(1-1/\beta)\,\text{km} \tag{3.26}$$

However, since the Bay of Biscay margin is 120 Myr old rather than being infinitely old, S_{120} is somewhat smaller than S_∞. As a result, the total subsidence at 120 Myr is

$$S_{120} \sim 7.23(1-1/\beta) \tag{3.27}$$

and the thermal subsidence at 120 Myr is

$$S_{t120} \sim 3.64(1-1/\beta) \tag{3.28}$$

Mid-ocean ridge crests are generally at about 2.5 km water depth, suggesting that zero-age oceanic lithosphere under 2.5 km of water is in equilibrium with a "standard" continental lithospheric column. Therefore during rifting, the asthenosphere should theoretically not be able to break through the thinned continental lithosphere as long as S_i is less than 2.5 km. Using equation (3.24) for the initial subsidence, the stretch factor required to produce 2.5 km of subsidence is 3.24; the crust by this time will be reduced in thickness to 9.25 km and will most likely be highly fractured – it is likely therefore that the asthenosphere would break through when this depth was reached. This represents the continent–ocean transition.

In the Bay of Biscay the estimated total subsidence at 120 Myr since rifting (S_{120}) for $\beta = 3.24$ is 5.2 km (eqn 3.27) and the final subsidence (S_∞) for an infinitely large β is 7.8 km (eqn 3.25). One should therefore expect to find continental crust in the Bay of Biscay at water depths of 5.2 km or shallower in the absence of sedimentation. [With the addition of a sediment load driving further subsidence, the entire sedimentary column could be as much as 15 to 20 km thick.] Oceanic crust should not be found at shallower water depths.

The extension estimated from fault block geometries in the upper crust is relatively high (*c.* $\beta = 2.6$) based on migrated seismic reflection profiling, indicating that the crust is substantially thinned and close to the value at which the asthenosphere could break through. Along the seismic profile the depth to the surface of the continental block is 5.2 km, which suggests that the model very satisfactorily explains the main features of the Biscay margin.

A regional synthesis suggests that water depth varies linearly with the thinning of the continental crust, following a relation close to

$$S_w = 7.5(1-1/\beta) \tag{3.29}$$

which is almost identical to the model prediction (eqn 3.27).

It is perhaps surprising that the Biscay and Galicia data fit the simple uniform stretching model so well. This is probably because during phases of rapid stretching, and in the absence of large sediment loads, the lithosphere is compensated on a local scale rather than responding by flexure.

3.4.2.2 The sediment-nourished eastern US and Canadian passive margin

It has been known for decades that the US and Canadian Atlantic margin is very thickly sedimented, with over 10 km along most of the margin, and considerably more in areas such as the Baltimore Canyon where a deep offshore well (COST B-2) was drilled in March 1976 (Poag 1980). The subsidence history of thickly sedimented margins such as this is profoundly affected by the *sediment load*. The sediment load is supported by the rigidity of the plate, and the borehole records (and seismic reflection profile data) need to be *backstripped* to obtain the tectonic subsidence (§8.3.3).

The main structural regimes of the US continental margin are shown in Fig. 3.8b. From landward to seaward, the *coastal plain* contains a seaward-thickening wedge of sediments. Basement depth increases rapidly in the *hinge zone*, thought to represent the transition between relatively undeformed continental crust and the highly attenuated and heated crust that has been modified by rifting. Seaward of the hinge zone lies the locus of the thickest sediment accumulations and still further seaward lies the true *oceanic crust*.

The backstripped COST B-2 well can be compared with theoretical curves to estimate the amount of extension. Using a simple uniform extension model, β varies from 3–3.5 for Airy isostasy, to 5 (up to mid-ocean ridge values) using a flexural isostatic model. The Airy results and the flexural results probably bracket a realistic estimate of about $\beta = 4$, which would suggest that the continental crust has been thinned to almost the oceanic

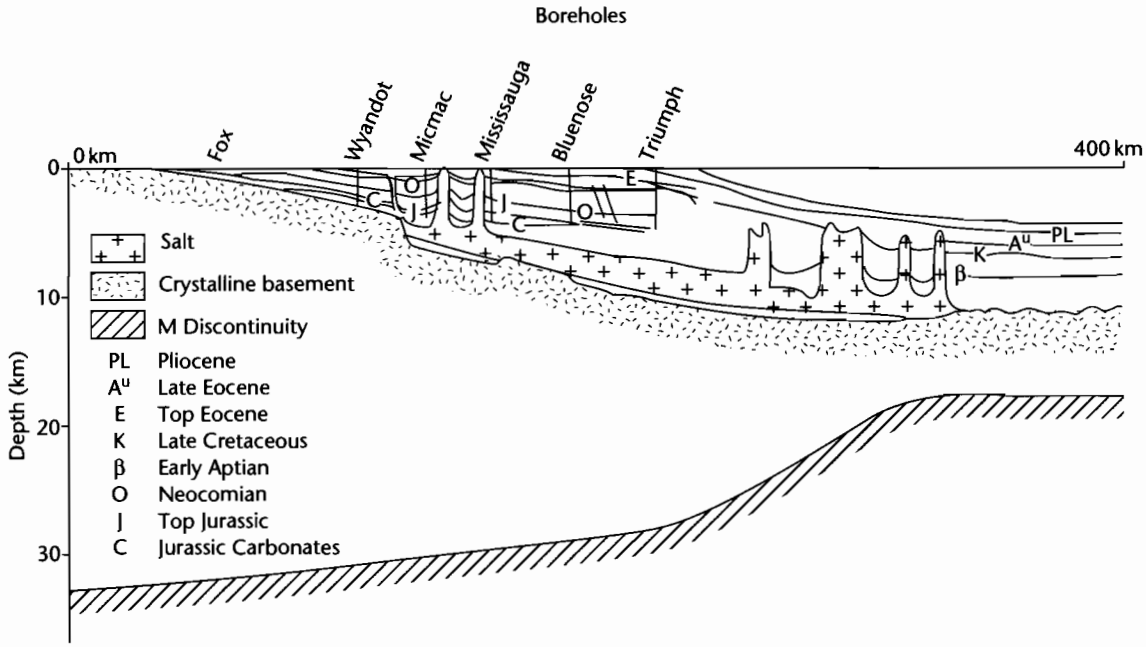

Fig. 3.17 Composite cross-section of the Scotian basin and crust. The sediment–basement interface is based on wells that penetrate it in addition to seismic reflection and refraction observations (Jansa and Wade 1975). After Beaumont et al. (1982).

thickness. This is supported by gravity modeling of crustal thickness (Grow et al. 1979).

The magnitude of the tectonic subsidence (and extension) varies systematically across the margin. Extension seaward of the hinge zone reaches values as great as $\beta = 4$, whereas the hinge zone has suffered much less extension ($\beta = 1.5$–2.0), and there is no synrift extension landward of the hinge zone, postrift subsidence being accomplished by thermal contraction and flexure.

The passive margin off Nova Scotia is one of the best studied mature examples available. The margin underwent rifting between 200 and 180 Ma. Its thick stratigraphy is well known from deep exploratory boreholes and seismic reflection data, and the deepest parts of the basin together with the variation in crustal thickness in the ocean–continental transition are known from seismic refraction. The composite cross-section is shown in Fig. 3.17.

In general, passive margins such as the US Atlantic and Scotian margins are adequately explained by a uniform stretching model coupled with melt segregation from the asthenosphere and migration into the crust (see §3.5.5), with postrift subsidence influenced by flexural support for thick sediment loads (§3.5.8). The importance of nonuniform, depth-dependent stretching is assessed in §3.5.1.

3.5 MODIFICATIONS TO THE UNIFORM STRETCHING MODEL

It is clear that there are a number of observations in regions of continental extension that suggest that the assumptions in the uniform stretching model should be re-examined. As a summary, these assumptions (some are implicit rather than stated) are as follows:

1. Stretching is uniform with depth;
2. stretching is instantaneous;
3. stretching is by pure shear;
4. the necking depth is zero;
5. Airy isostasy is assumed to operate throughout;
6. there is no radiogenic heat production;
7. heat flow is in one dimension (vertically) by conduction;

8 there is no magmatic activity;
9 the asthenosphere has a uniform temperature at the base of the lithosphere.

Modifications to the uniform stretching model invariably result in departures from the expressions for synrift and postrift subsidence given in equations 3.10 and 3.16. We briefly consider modifications to the uniform stretching model under the following headings:

- *Nonuniform (depth-dependent) stretching*: the mantle lithosphere may stretch by a different amount to the crust;
- *pure versus simple shear*: the lithosphere may extend along trans-crustal or trans-lithospheric detachments by simple shear;
- *protracted rifting*: continental rifts typically have synrift phases lasting 20–30 Myr;
- *elevated asthenospheric temperatures*: the base of the lithosphere may be strongly variable in its temperature structure due to the presence of convection systems such as hot plumes;
- *magmatic activity*: the intrusion of melts at high values of stretching modifies the heat flow history and thermal subsidence at passive margins;
- *induced mantle convection*: the stretching of the lithosphere may induce secondary mantle convection in the region of upwelled asthenosphere;
- *radiogenic heat production*: the granitic crust provides an additional important source of heat;
- *depth of necking*: necking may be centred on strong layers deeper in the midcrust or upper mantle lithosphere;
- *flexural compensation*: the continental lithosphere has a finite elastic strength and flexural rigidity, particularly in the postrift thermal subsidence phase.

3.5.1 Nonuniform (depth-dependent) stretching

Two families of models have been proposed to deal with the possibility of nonuniform stretching (Fig. 3.18):

- *Discontinuous* models, in which there is a discontinuity or decoupling between two layers with different values of the stretch factor β;

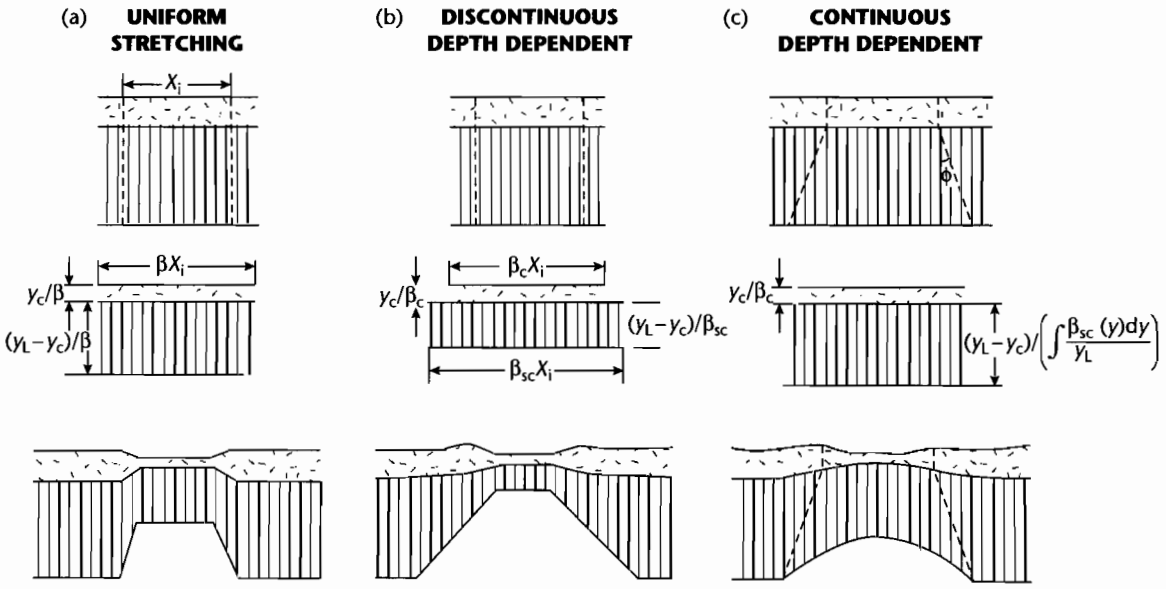

Fig. 3.18 Schematic diagrams to illustrate differences between (a) uniform, (b) discontinuous, and (c) continuous depth-dependent stretching. (a) Uniform extension in which the crust and subcrustal lithosphere extend by identical amounts; (b) Discontinuous depth-dependent extension in which the crust extends by a different amount to the subcrustal lithosphere, necessitating a decoupling between the two layers. The crustal and subcrustal extensions are independent but are uniform throughout the crust and subcrustal lithosphere (Royden and Keen 1980; Beaumont et al. 1982; Hellinger and Sclater 1983); (c) Continuous depth-dependent extension in which the stretching is a continuous function of depth in the subcrustal lithosphere and the crustal stretching is the same as in (a) and (b) (Rowley and Sahagian 1986).

- *continuous* models, where there is a smooth transition in the stretching through the lithosphere.

Critically, both sets of models make a first-order prediction – that zones of continental stretching should be characterized by elevated rift margin topography.

3.5.1.1 Discontinuous stretching with depth

Extension may not be uniform with depth because of the changing rheologic properties of the lithosphere. If the lithosphere extends inhomogeneously and discontinuously, there must be a depth d at which the upper and lower parts of the lithosphere are decoupled. This zone of detachment or shear is where listric faults in the overlying brittle zone sole out (Montadert et al. 1979; Kusznir et al. 1987). Structural evidence (e.g., seismic studies of the Basin and Range Province, Bay of Biscay and northwestern European continental shelf) demonstrates that some steep faults near the surface become listric into near-horizontal detachments where a transition to ductile behavior takes place. The focal depths of earthquakes in old cratons further suggest that while the upper part of the lithosphere has relatively high strength and is seismically active, the lower part is aseismic, probably due to the operation of ductile deformation mechanisms (Sibson 1983; Scholz 1988). In some instances at least, there may therefore be decoupling of the upper and lower zones at about midcrustal levels, allowing the two rheologic layers to extend by different amounts, giving a nonuniform discontinuous stretching.

The initial subsidence and thermal subsidence for the case of depth-dependent extension where the zone above d extends by β_c and the zone below d extends by ductile deformation by a different amount β_{sc}, is given by Royden and Keen (1980). If the lower zone stretches by ductile deformation more than the brittle upper zone, uplift should occur if the depth to decoupling approximates the crustal thickness ($d \approx y_c$). This uplift occurs at the same time as extension, and is an attractive feature of the model in view of the updoming characteristic of many present-day rift systems such as East Africa.

As an example of discontinuous depth-dependent stretching, in the centre of the Pattani Trough, Gulf of Thailand, the stretch factors for crust β_c and lithosphere β_L derived from subsidence plots were 2.35 and 1.90, indicating that crustal thinning was 20% greater than lithospheric thinning in the graben region (Hellinger and Sclater 1983).

The temporal relationship between faulting and rift flank uplift and the wavelength and amplitude of the rift flank uplift provide important constraints on the lithospheric stretching model. For example, if prerift sedimentary rocks are preserved in the graben but eroded from the flanks, it is a good indication that crustal uplift did not precede rifting. Footwall uplift may be due to coseismic strain along border faults, in which case the wavelength of the uplift (*c.* 10 km) will be smaller than the fault spacing. However, if the rift flank uplift has a much larger wavelength, it might imply that the subcrustal lithosphere was extended over a larger region than the more confined crustal extension. At first the crustal thinning, causing subsidence, outstrips the uplift from subcrustal thinning in the graben area, but the reverse is true beyond the graben edge. Later, after extensional tectonics has ceased, both flanks and graben should subside due to cooling and thermal contraction of the upwelled asthenosphere.

Regions initially at sea-level that are uplifted, such as graben flanks, are subject to erosion and theoretically should subside to a position below sea-level after complete cooling. But a second effect is the added crustal uplift caused by isostatic adjustment to the removed load. These two processes govern how much erosion will take place before the rift flanks subside below sea-level and erosion effectively stops. In the southern Rhine Graben, the present day surface uplift of the rift flanks is about 1 km. The erosional exhumation of footwall rocks is, however, of the order of 2.5 km (Illies and Greiner 1978). A further implication of rift flank erosion is an increase in the area of subsidence, so nonuniform extension models incorporating erosional effects predict larger subsiding basins than uniform extensional models. Regions that are not initially at sea-level prior to rifting, such as the Tibet Plateau and the Basin and Range province, have a different, lower base level for erosion.

A comparison of the stratigraphies generated by the uniform (one-layer) stretching model and the two-layer (depth-dependent) stretching model from the passive margin off New Jersey, USA is shown in Fig. 3.19. Both models show a well-developed coastal plain, hinge zone and inner shelf region underlain by a thick sequence of seaward dipping strata. The main difference is in the stratigraphy of the coastal plain, the one-layer model over-predicting synrift sediment thickness. The two-layer model, however, explains the lack of synrift (Jurassic) stratigraphy by the lateral loss of heat to the flanks of the rift, causing uplift and subaerial emergence.

3.5.1.2 Continuous stretching with depth

The implication of different amounts of stretching in the crust and mantle lithosphere is that there must be a

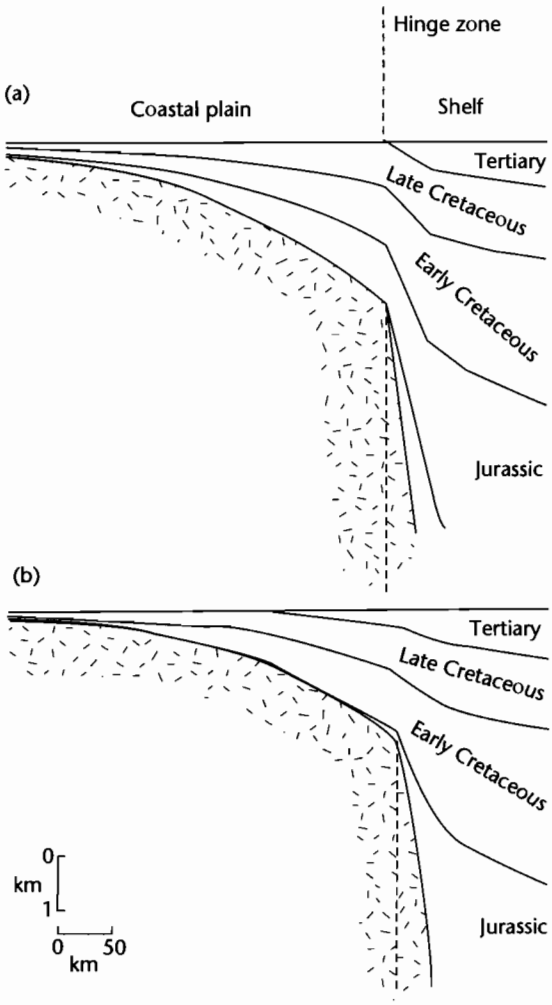

Fig. 3.19 Synthetic stratigraphy along profiles crossing the coastal plain and shelf off New Jersey constructed using the flexural loading model of Watts and Thorne (1984). (a) One-layer uniform stretching model; (b) two-layer model in which the lithosphere and crust are thinned by equal amounts seaward of the hinge zone, but only the mantle lithosphere is thinned landward of the hinge zone. The lithospheric thinning promotes early uplift of the zone landward of the hinge line, and helps to explain the absence of Jurassic strata from this region (after Steckler et al. 1988).

surface or zone of discontinuity separating the regions with the different values of β. Although such models are successful in explaining the common rift flank uplift that accompanies extension (e.g., Nova Scotian and Labrador continental margin, East African Rift, Red Sea, Rhine Graben), they have a number of requirements:

- The existence of an intralithospheric discontinuity, which although evident in some settings (e.g., Biscay Margin), is by no means universally "proven";
- a mechanism by which the mantle is detached and stretched by a different amount to the overlying crust, and a means of solving the attendant space problem in the mantle.

If the stretching is nonuniform but *continuous* with depth, these objections are removed (Rowley and Sahagian 1986). It is possible that the mantle may respond to extension as a function of depth, the strain rate decreasing as the extension is diffused over a wider region. This can be modeled by considering a geometry of an upward tapering region of stretching (Fig. 3.20). If ϕ is the angle between the vertical and the boundary of the stretched region in the mantle lithosphere, the amount of stretching depends on the depth beneath the crust and angle ϕ. The variation of β_{sc} with depth can then be integrated from the base of the crust to the base of the lithosphere to obtain estimates of initial and total subsidence in a similar fashion to the uniform stretching case. For large values of ϕ, the initial subsidence is increased but the amount of postextension thermal subsidence is decreased. The wider zone of mantle stretching results in uplift of the rift shoulders, and the horizontal length scale of the uplift is an indication of the value of ϕ. In the Gulf of Suez region, the horizontal width over which the topographic uplift occurs is about 250 km. Since the thickness of the subcrustal lithosphere is likely to be approximately 90 km, the taper angle ϕ is given by $\phi = \tan^{-1}(250/90) = 70°$. In the Rhine Graben, ϕ is approximately $\tan^{-1}(80/90) = 40°$.

A point in the rift shoulder region should therefore initially experience rock uplift, followed by a comparable amount of subsidence; if erosion has occurred, the final elevation of the point will be below its initial height. The same general pattern is observed where the crustal stretching varies from a minimum at the rift margin to a maximum at the rift centre (Fig. 3.20) (White and McKenzie 1988). The implications of stretching the mantle over a wider region than the crust (but with equal total amounts of extension) is that stratigraphic onlap should occur over previous rift shoulders during the

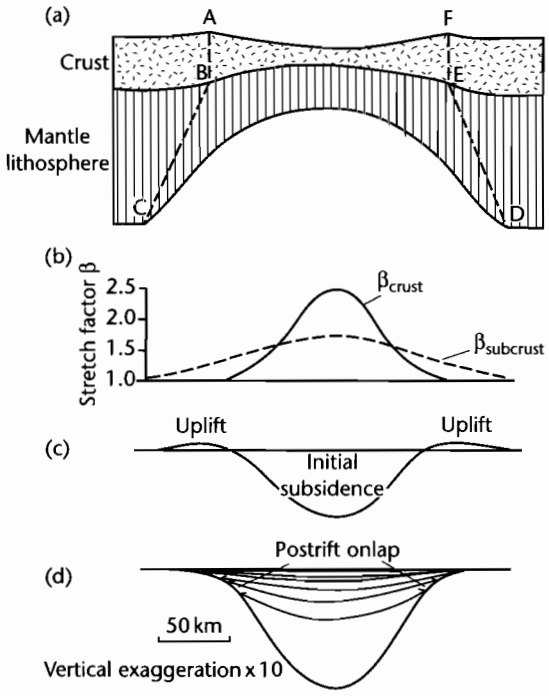

Fig. 3.20 Basin filling pattern resulting from continuous depth-dependent stretching (Rowley and Sahagian 1986; White and McKenzie 1988). (a) Geometry of a tapering region of extension in the subcrustal lithosphere; (b) Stretch factors in the crust and subcrustal lithosphere as a function of horizontal distance; (c) Initial subsidence and uplift immediately after stretching, showing prominent rift flank uplift; (d) Total subsidence 150 Myr after rifting, showing progressive onlap of the basin margin during the thermal subsidence phase, giving a "steer's head" geometry.

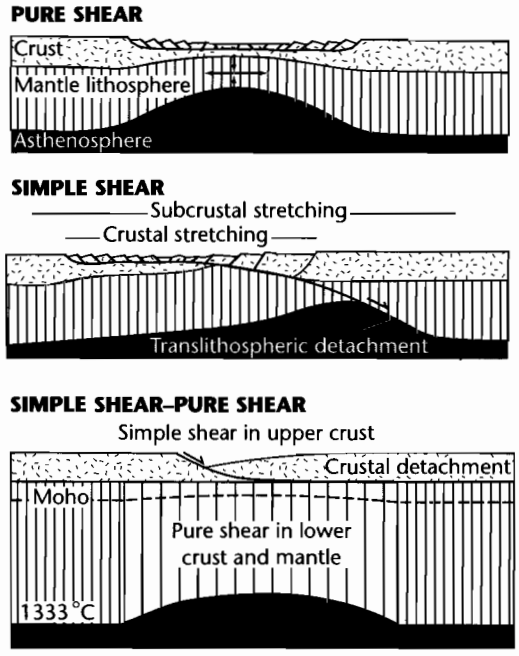

Fig. 3.21 Models of strain geometry in rifts (Coward 1986; Buck et al. 1988). (a) Pure shear geometry with an upper brittle layer overlying a lower ductile layer, producing a symmetrical lithospheric cross-section with the initial fault-controlled subsidence spatially superimposed on the thermal subsidence. The ductile stretching may be accompanied by dilation due to the intrusion of melts (Royden et al. 1980); (b) Simple shear geometry with a through-going low-angle detachment dividing the lithosphere into an upper plate or hangingwall, and a lower plate or footwall. Thinning of the lower lithosphere is relayed along the detachment plane, producing a highly asymmetrical lithospheric cross-section (after Wernicke 1981, 1985). Initial fault-controlled (synrift) subsidence is spatially separated from the thermal subsidence; (c) Hybrid model of simple shear in the upper crust on listric (shown) or planar faults, and pure shear in the ductile lower crust and mantle lithosphere (Kusznir et al. 1991).

postrift phase, a feature commonly found in "rift-sag" or "steer's-head" type basins.

3.5.2 Pure versus simple shear

The lithosphere may extend asymmetrically where the zone of ductile subcrustal stretching is relayed laterally from the zone of brittle crustal stretching (Buck et al. 1988 and Kusznir and Egan 1990 for quantitative analyses) (Fig. 3.21). This is the situation of *simple shear*. Wernicke (1981) proposed such a model, based on studies of Basin and Range tectonics, envisaging that lithospheric extension is accomplished by displacement on a large scale, gently dipping shear zone that traverses the entire lithosphere. Such a shear zone transfers or relays extension from the upper crust in one region to the lower crust and mantle lithosphere in another region. It necessarily results in a physical separation of the zone of fault-controlled extension from the zone of upwelled asthenosphere.

Wernicke (1981, 1985) suggested that there are three main zones associated with crustal shear zones (Fig. 3.22):

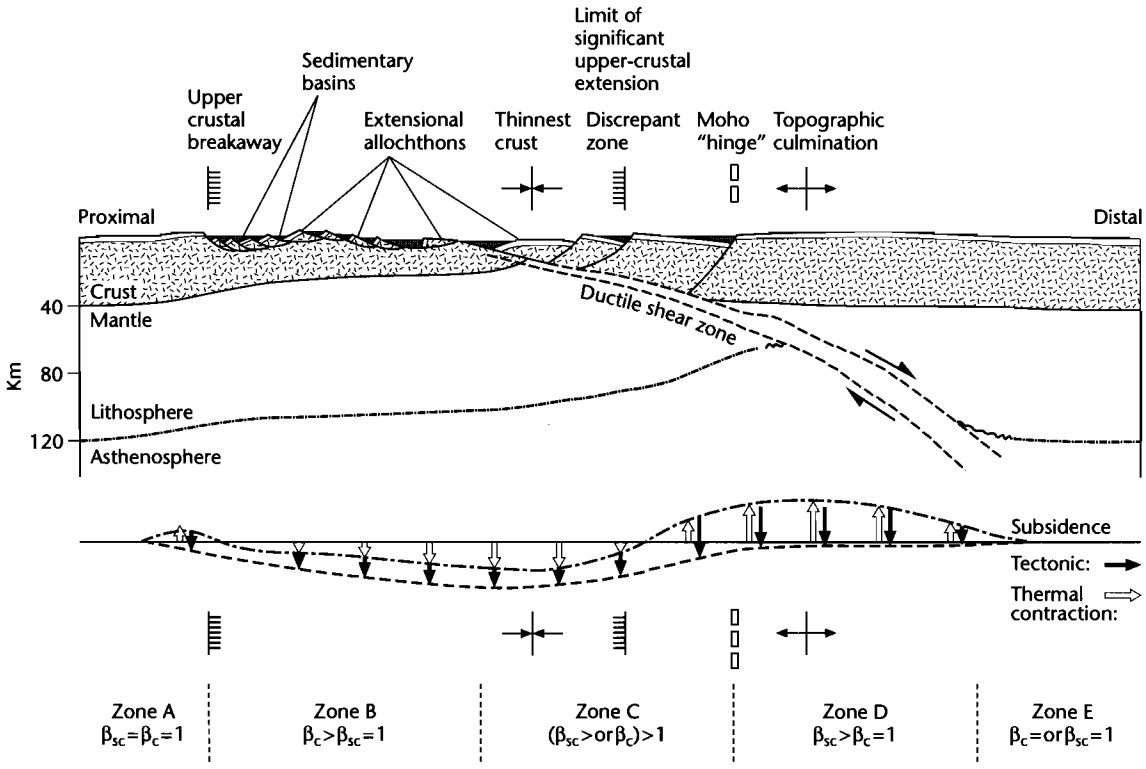

Fig. 3.22 Normal simple shear of the entire lithosphere, developed from the Basin and Range province of SW USA (Wernicke 1985). This geometry takes of the order of 10–15 Myr to develop. Midcrustal rocks in the hangingwall may initially pass through greenschist or amphibolite metamorphic conditions in the ductile shear zone, followed by uplift, cooling, and deformation in the brittle field.

(i) a zone where upper crust has thinned and there are abundant faults above the detachment zone, (ii) a "discrepant" zone where the lower crust has thinned but there is negligible thinning in the upper crust, and (iii) a zone where the shear zone extends through the subcrustal (mantle) lithosphere.

Since crustal thinning by fault-controlled extension causes subsidence but subcrustal thinning produces uplift, we should expect subsidence in the region of thin-skinned extensional tectonics but tectonic *uplift* in the region overlying the lower crust and mantle thinning (the discrepant zone of Wernicke). Subsequent asthenospheric cooling may result in one of two things. Thermal subsidence of the region above the discrepant zone may simply restore the crust to its initial level. However, if subaerial erosion has taken place in the meantime, thermal subsidence will lead to the formation of a shallow basin above the discrepant zone. The basement of the basin should be unfaulted. However, beneath the zone of thin-skinned extensional tectonics there should be minimal thermal subsidence.

Stretching of the lithosphere combined with unloading along major detachment faults can result in the unroofing of mantle rocks in their footwalls. These are called *core complexes* and *gneissic domes*. The turtlebacks of the Death Valley region and the Whipple Mountains of Nevada are examples (Wright and Coleman, 1974; Lister and Davis 1989).

Tectonic unloading may also result in flexural uplift of adjacent footwall areas along major detachment faults (Fig. 3.23). Kusznir et al. (1991) refer to this as the *flexural cantilever effect*. They use a model of simple shear in the

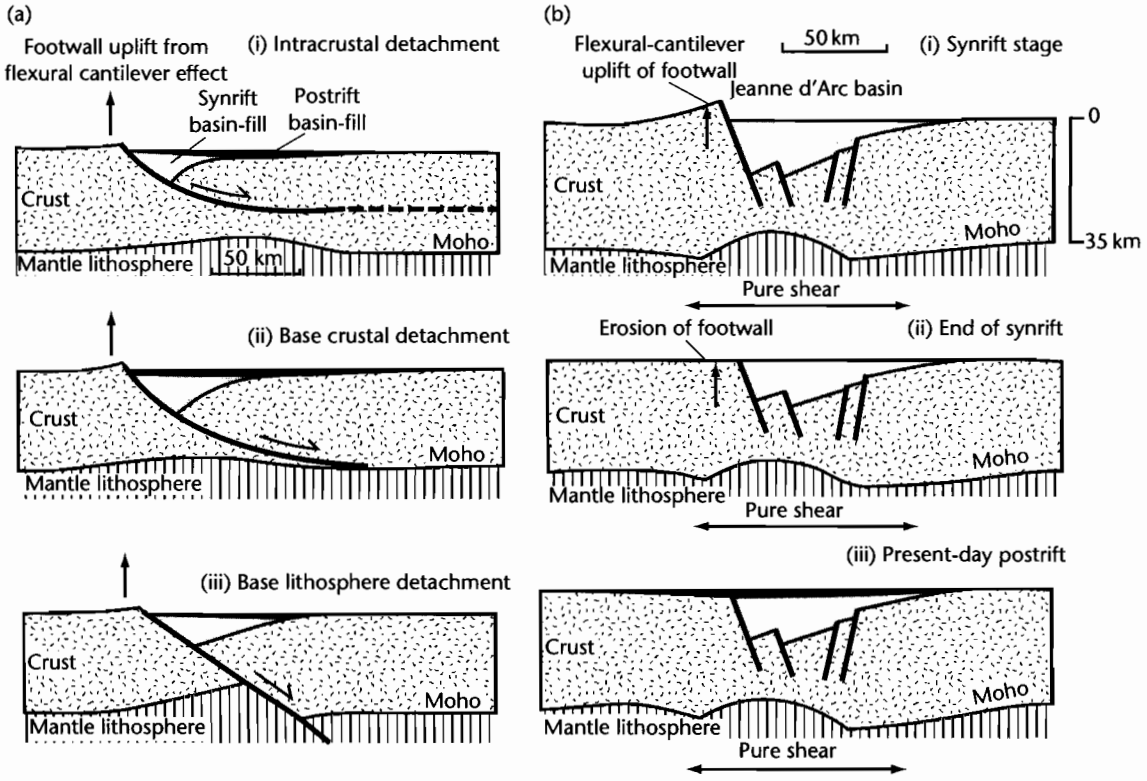

Fig. 3.23 Sedimentary basin geometry and crustal structure predicted by a simple shear–pure shear model including the flexural cantilever effect (Kusznir and Egan 1990; Kusznir et al. 1991). (a) Crustal structures after 100 Myr and 30 km extension with an equivalent elastic thickness of 5 km, for an intracrustal detachment (i), a base-crustal detachment (ii), and a base-lithosphere detachment (iii); (b) Sequential development of the Hibernia-Ben Nevis profile of the Jeanne d'Arc basin, showing flexural uplift and erosion of the unloaded footwall of the main detachment fault. The total amount of extension is 18 km, initial fault dip = 60°, initial crustal thickness is 35 km, and Te = 10 km. Reproduced courtesy of Geological Society of London.

crust and pure shear in the lithospheric mantle. The scale of the flexural cantilever effect depends on the depth at which the detachment soles out. The model has been successfully used to explain footwall uplift and erosion in the Jeanne d'Arc Basin, Grand Banks of Newfoundland, and Viking Graben, North Sea (Marsden et al. 1990; Kusznir et al. 1991), and Tanganyika Rift of East Africa (Kusznir and Morley 1990).

Models involving large-scale simple shear do not explain basins that have a thermal subsidence spatially superimposed on a fault-controlled subsidence, as in the North Sea (Klemperer 1988). Such examples are more suggestive of pure shear.

3.5.3 Protracted rifting and lateral heat conduction

The quantitative model of McKenzie (1978a) assumed instantaneous rifting of the lithosphere followed by thermal subsidence as the lithosphere re-equilibrates to its pre-extension thickness. This is an attractive assumption since it gives a simple, well-defined initial condition for the thermal calculations. Jarvis and McKenzie (1980) revised this 1-D model by allowing for protracted periods of stretching. If the duration of stretching is large compared with the diffusive time scale of the lithosphere ($\tau = y_L^2/\pi^2\kappa$), which is 50–60 Myr for a standard litho-

sphere, some of the heat diffuses away before the stretching is completed. In the general case, if the time taken to extend the continental lithosphere by a factor β is less than $60/\beta^2$ Myr, the results are similar to those of the uniform stretching model with instantaneous stretching. However, the sensitivity of the results depends on the value of the stretch factor and whether total subsidence or heat flow is being considered.

Considering total subsidence, if $\beta < 2$, the duration of extension must be less than $60/\beta^2$ Myr for the instantaneous stretching model to be a reasonable representation. If $\beta > 2$, the duration of extension must be less than $60(1 - 1/\beta)^2$.

Considering heat flow, if $\beta < 2$, the duration of extension must be less than 60 Myr for the instantaneous stretching model to be a reasonable representation. If $\beta > 2$, the duration of extension must be less than $60(2/\beta)^2$.

Stretching in the Pannonian Basin is thought to have lasted for up to 10 Myr (Sclater et al. 1980b), and stretch factors are <3. Consequently, the instantaneous model is a reasonable representation of the subsidence in the Pannonian Basin since the critical duration of extension is $60(1 - 1/3)^2 = 27$ Myr. It is also a reasonable representation of the heat flow history since the critical duration of extension is also 27 Myr. However, many sedimentary basins appear to have undergone protracted periods of rifting, considerably in excess of $60/\beta^2$ Myr (about 20 Myr for a stretch factor of 1.75). The Paris Basin, for instance, rifted in the Mid-Permian and sedimentation was restricted to elongate rift troughs until close to the end of the Triassic. The rift phase was therefore close to 60 Myr in duration. The Triassic (Carnian–Norian, 212–200 Ma) continental red beds and evaporites of the Atlantic margin of northeastern USA and Canada were deposited in fault-bounded rifts, but seafloor spreading did not commence until the Bajocian at about 170 Ma. The stretching in the Red Sea (Cochran 1983) appears to have occurred diffusely through a combination of extensional block faulting and dyke injection over an area of the order of 100 km wide. This phase of diffuse extension has lasted for 20–25 Myr in the northern Red Sea and is still occurring. A phase of rifting took place in the North Sea in the Permo-Triassic. There was another phase in the Jurassic which lasted until the Early Cretaceous. The duration of this major phase of extension was of the order of 50 Myr.

Taking the North Sea as an example, the stretch factor for the Jurassic extensional phase rarely exceeds 1.5, except along the axis of the Viking Graben (§3.8.2). Using $\Delta t = 50$ Myr and $\beta = 1.5$, the critical duration of rifting from Jarvis and McKenzie (1980) is about 27 Myr. Consequently, on this basis, we should expect the protracted duration of extension during the Jurassic phase in the North Sea to have had significant effects on the heat flow and subsidence history. Despite this, the North Sea appears to be satisfactorily explained by the uniform stretching model (Sclater and Christie 1980; Wood and Barton 1983).

The effect of a finite time of rifting is to cause a loss of heat and thus additional subsidence prior to the end of rifting or the onset of seafloor spreading. It effectively transfers a portion of the cooling from the postrift phase to the synrift phase.

Lateral heat loss during prolonged periods of rifting is caused by the large lateral temperature gradients set up by lithospheric thinning (Steckler 1981). The longer the rifting event, the more important lateral heat loss and uplift of basin margins are likely to be. Lateral heat conduction is also important in narrow basins such as pull-aparts in strike–slip zones. Effects of lateral heat flow are greatest near the basin edge ("hinge-zone" between strongly extended lithosphere and little-extended lithosphere) where horizontal temperature gradients are largest (Cochran 1983). The effects decrease towards the centre of the basin (Fig. 3.24).

In Cochran's (1983) models, the postrift subsidence near the centre of the basin is decreased (relative to the instantaneous case) by a minimum of 10–15% for a 10 Myr rifting event and by about 25% for a 20 Myr rifting event. Since the synrift subsidence is increased at the expense of the postrift subsidence, the effect is to flatten the postrift subsidence curves relative to those predicted by the instantaneous 1-D model. This should lead to underestimates of the stretch factor β. The model subsidence curves cross-cut the lines of equal β because of the lateral transport of heat out of the basin. The basin may be filled with sediment rather than water and the effects of the load of the sediments distributed by flexure. For a 20 Myr rifting time, about 70% of the sedimentary column is represented by synrift sediments in the finite rifting time model. In the North Sea Grabens, however, the synrift subsidence is only *c.* 40% of the total subsidence, which is more typical of the prototype uniform stretching model.

3.5.4 Elevated asthenospheric temperatures

The prototype uniform stretching model of McKenzie (1978a) envisages an asthenosphere with a laterally uniform temperature (1330 °C), which rises passively to

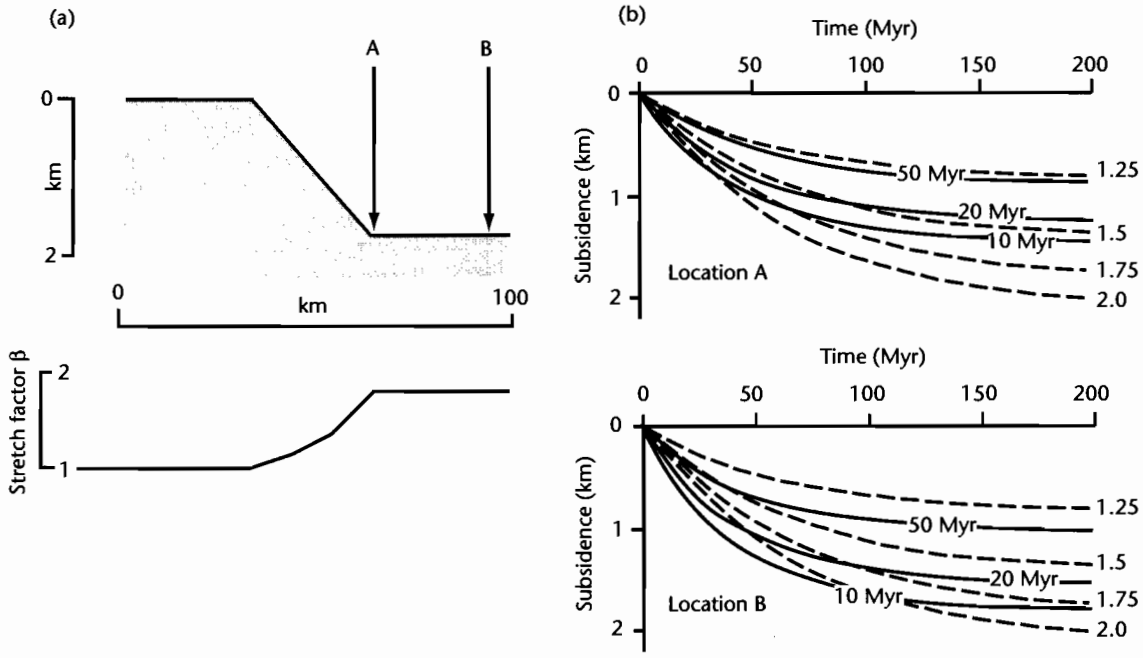

Fig. 3.24 Thermal subsidence for locations A and B in a water-filled basin as a function of time since the end of rifting, for stretch factors of 1.25–2.0, for finite rifting times of 10, 20, and 50 Myr (after Cochran 1983). Dashed lines are subsidence curves for the instantaneous uniform stretching model with $\beta = 2$ in the basin centre. Note that the two sets of curves cross-cut, making estimates of the amount of stretching from postrift thermal subsidence problematical unless the duration of stretching is known.

fill the region of lithospheric stretching. Some workers have suggested that continental stretching is in some cases associated with mantle plume activity (Spohn and Schubert 1983; Houseman and England 1986). Such activity may raise the local asthenospheric temperatures by *c.* 200 °C. Plume heads typically have diameters in the region of 1000 km (Griffiths and Campbell 1990) (§3.7). Laboratory experiments indicate that starting plumes may generate *c.* 600 m of surface uplift (R.I. Hill 1991) – insufficient to solely explain the 3 km-high swells of eastern Africa. However, mantle plume activity may drive continental extension by elevating the lithosphere, including its surface, thereby giving it excess potential energy compared to its surroundings (Houseman and England 1986).

The driving stress caused by the uplift may exceed a threshold value, causing *run-away or accelerating extension*, eventually leading to ocean crust production. Alternatively, the driving stress may be considerably lower than (about half of) the threshold value, causing *negligible extension*, as in many low-strain continental rifts. If the driving stress is intermediate in value, the extension is thought to be *self-limited* by the cooling of the ductile portion of the lithosphere. This produces aborted rift provinces such as the North Sea. These ideas are further developed in §3.7.

One of the complexities of this type of model is the *time scale of the plume*. Removal of the plume head at early, intermediate, or late stages has major effects on basin development. Another aspect is the *volcanicity* generated by the anomalously high asthenospheric temperatures. Mantle plumes are therefore commonly associated with very high volume basaltic igneous provinces such as the Karoo, Deccan, and Parana examples.

Plume activity has been invoked as a particularly effective mechanism of generating new ocean basins, such as the Atlantic. The opening of the northern Atlantic in the Paleocene has been related to the impingement of the Icelandic plume on the base of the lithosphere (White and McKenzie 1989). Mantle plume effects may have been common during supercontinental break-up of

Rodinia (*c.* 750 Ma), Gondwana (*c.* 550 Ma), and Pangea (*c.* 250 Ma).

3.5.5 Magmatic activity at passive margins

The simple uniform extension model does not address the problems of the formation of oceanic crust at passive margins and the nature of the continental to oceanic crustal transition, since as $\beta \rightarrow \infty$ continental lithosphere is thinned to zero and replaced by asthenosphere at the solidus temperature. This would imply enormously large initial subsidence for the oceanic region. This cannot be the case, since newly formed oceanic crust occurs at about 2.5 km depth at mid-ocean ridges. Large amounts of stretching are likely to promote the segregation of melts and their migration into the overlying crust. Melt segregation models involve greater heating (Royden and Keen 1980) than the conduction-based uniform model of McKenzie (1978a).

The melt segregation model assumes that a basaltic melt segregates from asthenosphere that has upwelled to replace stretched lithosphere. The segregated melt can be considered to either constitute new oceanic crust, or to be intruded into or to underplate the stretched lithosphere. The stretching β controls the amount of segregated melt available so that in the case of a laterally varying stretching (with β increasing towards the rift centre), the thickness of segregated melt increases towards the site of ocean floor creation, compensating to some extent for the rapidly thinning continental crust.

Figure 3.25 compares the uniform extension model with $\beta = 4$, the effects of a finite rifting period of 25 Myr (Cochran 1983), and the effects of greater heating by melt segregation (Royden and Keen 1980) on the eastern USA margin. All three curves fit the tectonic subsidence of the postrift phase of the COST B-2 well, although synrift subsidences differ by a factor of 2 between the finite case and the maximum (mid-ocean ridge) heating case.

3.5.6 Induced mantle convection

Models involving an active asthenospheric heat source should predict *uplift before rifting*. At present there is no consensus on the temporal relationships between uplift and extension. However, Steckler (1985) suggested that

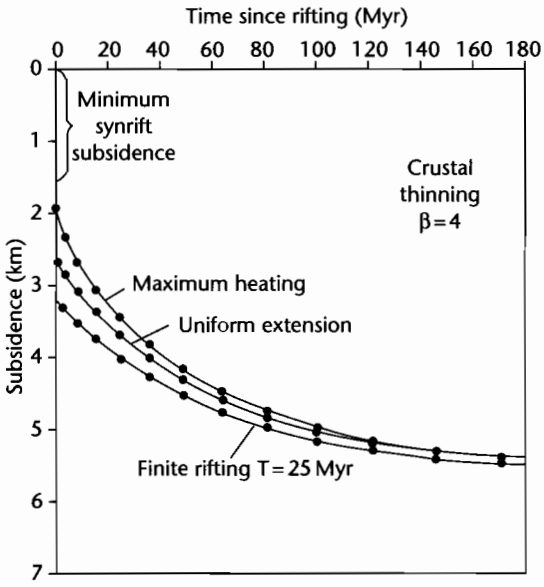

Fig. 3.25 Plot of tectonic subsidence versus time for uniform extension, rifting over a finite period of 25 Myr, and uniform extension with additional heating caused by melt segregation. In all cases the crust is thinned by a factor of 4, as suggested by the COST B-2 borehole. Note that there is minimal difference between the three curves at long time periods following rifting, suggesting that the "memory" of the initial rifting event fades with time (after Steckler et al. 1988).

in the Gulf of Suez, the rift flank uplifts were *not* formed as a precursor doming event prior to rifting, but rather formed *during* the main phase of extension (Fig. 3.26). The rift appears to have initiated (by Miocene times) at near sea-level, since the tilted fault blocks associated with early rifting experienced both subaerial erosion and marine deposition. The Early Miocene topography of the Gulf of Suez region was subdued and stratigraphic thicknesses are uniform over the area (Garfunkel and Bartov 1977). However, at the end of the Early Miocene, 8–10 Myr after the onset of rifting, a dramatic change took place – there is a widespread unconformity, and conglomerates appear at the rift margins suggesting major uplift and unroofing at this time.

The two main causes of vertical movements during rifting are: (i) uplift caused by heating of the lithosphere, and (ii) subsidence caused by thinning (or densification) of the crust. The lithospheric and crustal extensions needed to produce the observed uplift and rift subsidence

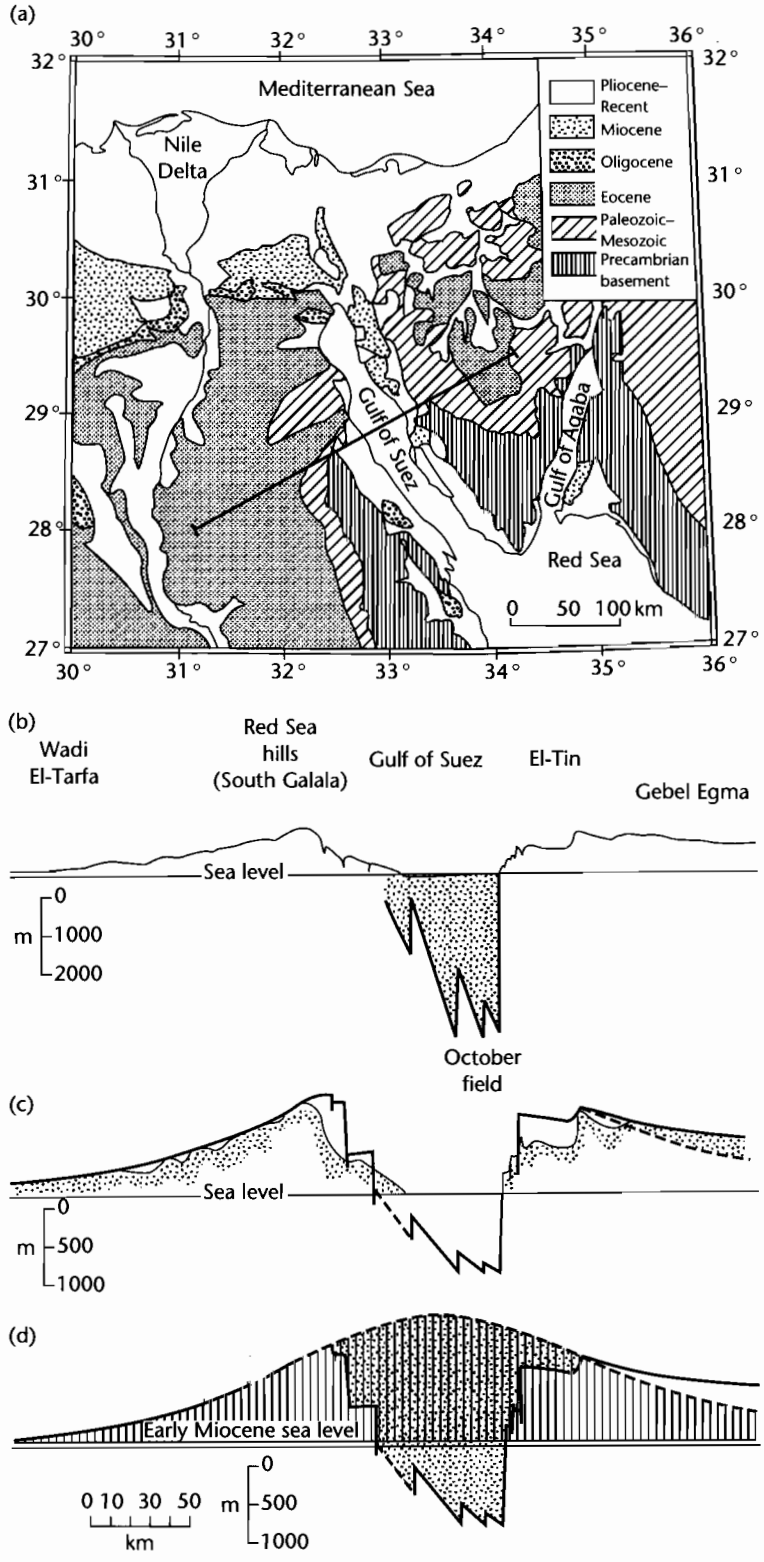

Fig. 3.26 (a) Geological map of the Gulf of Suez region, showing location of topographic profile shown in (b); (b) Topographic profile, vertical exaggeration 20:1. The stippled area represents the sedimentary fill of the Gulf; (c) Reconstructed profile with the effects of erosion and sedimentation removed using Airy isostasy, vertical exaggeration 40:1; (d) Interpretation of profile in (c) involving tectonic uplift due to thermal expansion of the lithosphere (vertical lines) and downfaulting of the rift axis caused by crustal stretching (stipple). After Steckler (1985).

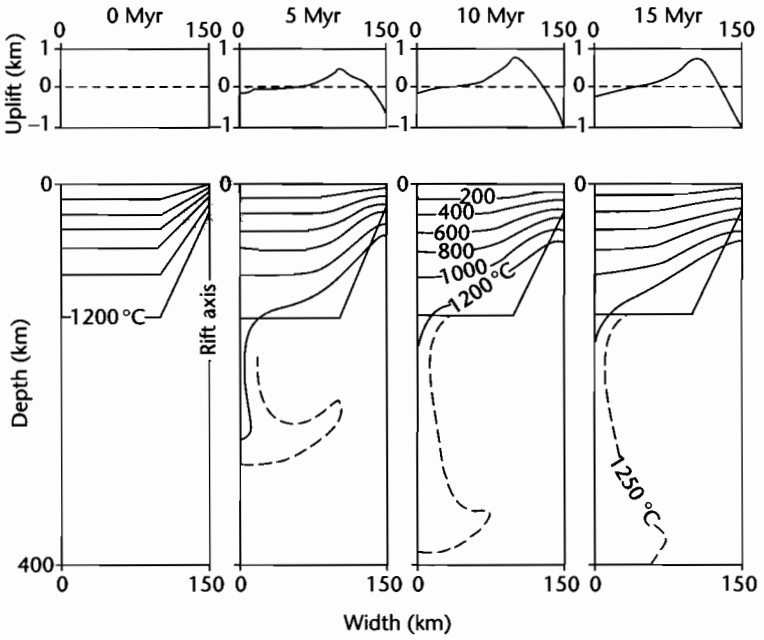

Fig. 3.27 Development of small-scale convection beneath rifts from the numerical experiments of Buck (1984). The rift is assumed to be symmetrical, with an initial half-width of 50 km. The average stretch factor is 1.6 and the internal temperature of the asthenosphere is 1300 °C. Comparison of the 1200 °C isotherm for the four time steps (0 Myr, 5 Myr, 10 Myr, and 15 Myr) shows how the rift flank is progressively heated through time, causing rift shoulder uplift. Top boxes show the topography caused by combined convection and conduction.

can be calculated using Airy isostasy. For the Gulf of Suez, the lithosphere must have extended by 2.5 times as much as the crust to explain the uplift and rift subsidence. This brings the uniform extension model seriously into doubt in terms of its ability to predict the lithospheric heating. How then does one explain the additional amount of heating that the lithosphere under the Gulf of Suez has undergone? This extra heat may have resulted from convective flow induced by the large temperature gradients set up by rifting. Numerical experiments confirm that secondary small-scale convection should take place beneath rifts (Buck 1984). Convective transport should heat the lithosphere bordering the rift, causing uplift of rift shoulders concurrent with extension within the rift itself (Fig. 3.27). If this mechanism is correct, it removes the need for active, sublithospheric heat sources. It also removes the requirement for two-layer extension to explain high heat flows at rift margins.

3.5.7 Radiogenic heat production

Although the very large volume of mantle contributes 80% of the Earth's radiogenic heat, it is the crustal contribution that determines the continental geotherm and which is of importance in basin analysis. The crustal radiogenic heat production can be modeled either as a series of slabs of different internal heat production, or as an exponential that decays with depth (§2.2.3). As a rule of thumb, the radiogenic heat production may be of roughly equal importance to the basal heat flow in determining the continental geotherm.

In practice, this makes little difference to the shape of the subsidence curves predicted by the uniform stretching model of McKenzie (1978a), though it potentially strongly affects paleotemperature estimations. It is therefore very important to include radiogenic contributions to the heat flow in modeling of thermal indicators in sedimentary basins such as vitrinite reflectance (Chapter 9).

3.5.8 Flexural compensation

It is likely that at low to moderate values of stretching the lithosphere maintains a finite strength during basin development (Ebinger et al. 1989), so that it responds to vertical loads by flexure. The degree of compensation (between the end members of Airy isostasy for a plate with no flexural rigidity and zero compensation for an infinitely rigid plate) depends on the flexural rigidity of the plate and the wavelength of the load (§2.3.3). There are two situations where flexure is likely to be important: (i) tectonic unloading by extension along major detachments leading to a regional cantilever-type upward flexure (Kusznir and Ziegler 1992), causing the footwall region to be mechanically uplifted, and (ii) downward flexure under the accumulating sediment loads in the synrift and especially postrift phase. Flexural compensation of sediment loads should be particularly important in passive margin evolution because of the secular increase in flexural rigidity and where sediment loads are narrow, as in pull-apart basins.

On the young (<24 Myr) Gulf of Lion's margin in the western Mediterranean, a local Airy model fitted the subsidence history data well. Thermal subsidence is exponential, of the form $e^{-t/\tau}$ where τ is the thermal time constant of the lithosphere (50–60 Myr), as in the uniform extension model of McKenzie (1978a). At higher values of stretching, the thermal subsidence more closely approximates the oceanic half-space cooling model, with subsidence related to root time. However, thickly sedimented old margins such as that of the Baltimore Canyon region of eastern USA (Steckler and Watts 1978, 1981) show departures from the subsidence history expected of Airy isostasy. In this case, a flexural model with the onset of thermal subsidence at 170 Ma fits the data very well with a $\sqrt{t}$ relationship.

3.5.9 The depth of necking

Necking is the very large scale thinning of the lithosphere caused by its mechanical extension. Necking should take place around one of its strong layers (Braun and Beaumont 1987; Weissel and Karner 1989; Kooi et al. 1992). The *depth of necking* is defined as the depth in the lithosphere that remains horizontal during thinning if the effects of sediment and water loading are removed. For the McKenzie uniform stretching model, the necking depth is implicitly 0 km. That is, all depths below the surface experience an upward advection during thinning (when sediment/water loading is removed). However, the necking depth may be deeper in the shallow mantle lithosphere. In this case, there is advection of material upwards from below the necking depth, but advection of material downward from above the necking depth.

The regional isostatic response to the different necking depths is shown in Fig. 3.28. If the necking depth is in the strong mantle lithosphere, there is a regional flexural uplift, causing a pronounced rift shoulder. We would expect a deep necking depth where the lithosphere is cold and strong, with a strong subcrustal mantle, such as in the Transantarctic Mountains and Red Sea region (Cloetingh et al. 1995). However, if the necking depth is within the upper–midcrust, there is a downward regional flexure, promoting subsidence of the rift margins. This should occur where the lithosphere is weak, or where the crust is thickened, as in the Pannonian Basin of eastern Europe (Horvath and Cloetingh 1996). The level of necking therefore controls the amount of rift shoulder denudation, and consequently, the sediment delivery to the basin during the synrift phase (van Balen et al. 1995; ter Voorde and Cloetingh 1996). There is theoretically an equilibrium depth of necking where there is no net flexural response. For a sediment-filled basin and initial crustal thickness of 33 km within a 100 km-thick lithosphere, this equilibrium depth is *c.* 10 km. Odinsen et al. (2000) used a necking depth of 18 km for their analysis of the northern North Sea, which therefore can be viewed as a relatively deep necking depth, promoting regional flexural uplift.

3.6 A DYNAMIC APPROACH TO LITHOSPHERIC EXTENSION

3.6.1 Generalities

Dynamic approaches to the modeling of continental extension use the constitutive laws of lithospheric materials to describe the 3-D deformation of the continental lithosphere under extension. A number of *plane strain* models making a range of assumptions of lithospheric rheology (Keen 1985, 1987; Buck 1986; Braun and Beaumont 1987; Dunbar and Sawyer 1989; Lynch and Morgan 1990; Bassi 1991) show, in general, that the style of deformation is controlled by strain rate, initial geotherm and rheologic structure. Consequently, any initial heterogeneities causing variability in the mechanical and

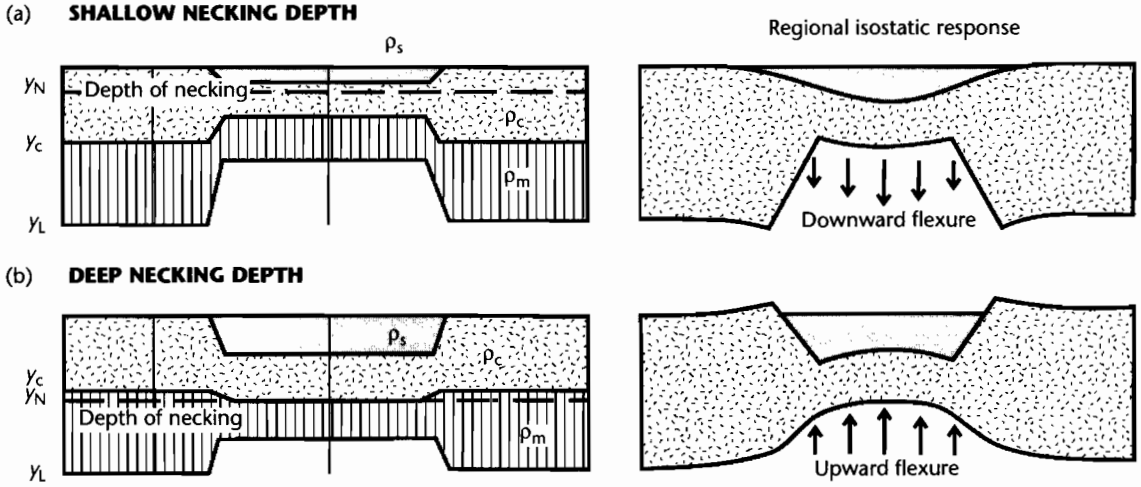

Fig. 3.28 Regional isostatic response to different depths of necking, based on Braun and Beaumont (1989), Kooi et al. (1992), Cloetingh et al. (1997). y_c, y_L and y_N are the initial thicknesses of the crust and lithosphere and the necking depth respectively; ρ_c, ρ_m, and ρ_s are the densities of the crust, mantle, and sediments respectively. In (a) a shallow depth of necking results in a net downward acting force on the lithosphere, causing a regional downward flexure. In (b) the necking depth is deep, resulting in an upward acting force on the lithosphere that causes flexural uplift of the rift flanks.

thermal properties of the lithosphere are likely to be highly influential in determining the resulting deformation. These initial perturbations that cause lateral strength variations might be thickness variations, pre-existing deep faults, thermal anomalies or rheologic inhomogeneities (Fernandez and Ranalli 1997).

Plane stress models approximate the lithosphere to a thin viscous sheet, in which the rheologic properties of the sheet are vertically averaged (examples are England and McKenzie 1982, 1983; Houseman and England 1986; Sonder and England 1989; Newman and White 1999). A single power-law rheology is used in these models to describe lithospheric deformation.

Dynamic models require *boundary conditions* on the margins of the extending lithosphere (Fig. 3.29). The choice of boundary conditions has important implications for the evolution through time of parameters in the model. As examples, the implications of five different boundary conditions are given below:

1 *Constant velocity boundary condition*: if L_0 is the initial width and v_0 is the extension velocity, the width of the extending zone after time t is

$$L = L_0 + v_0 t \tag{3.30}$$

and the extensional strain rate is

$$\dot{\varepsilon}(t) = (1/L)(\mathrm{d}L/\mathrm{d}t) \tag{3.31}$$

The extensional strain rate clearly decreases with time for a constant velocity boundary condition. A constant velocity boundary condition might be applicable to a situation where the extension is driven by relative plate motion, which over the duration of the extension has a constant vector.

2 *Constant strain rate boundary condition*: the width of the extending zone must vary in time as

$$L = L_0 \exp(\dot{\varepsilon} t) \tag{3.32}$$

and the extension velocity $v = (\mathrm{d}L/\mathrm{d}t)$ must increase as a function of time. For a constant strain rate boundary condition the extensional velocity would accelerate unreasonably.

3 *Constant stress boundary condition*: the result of a constant tectonic force boundary condition is to concentrate the

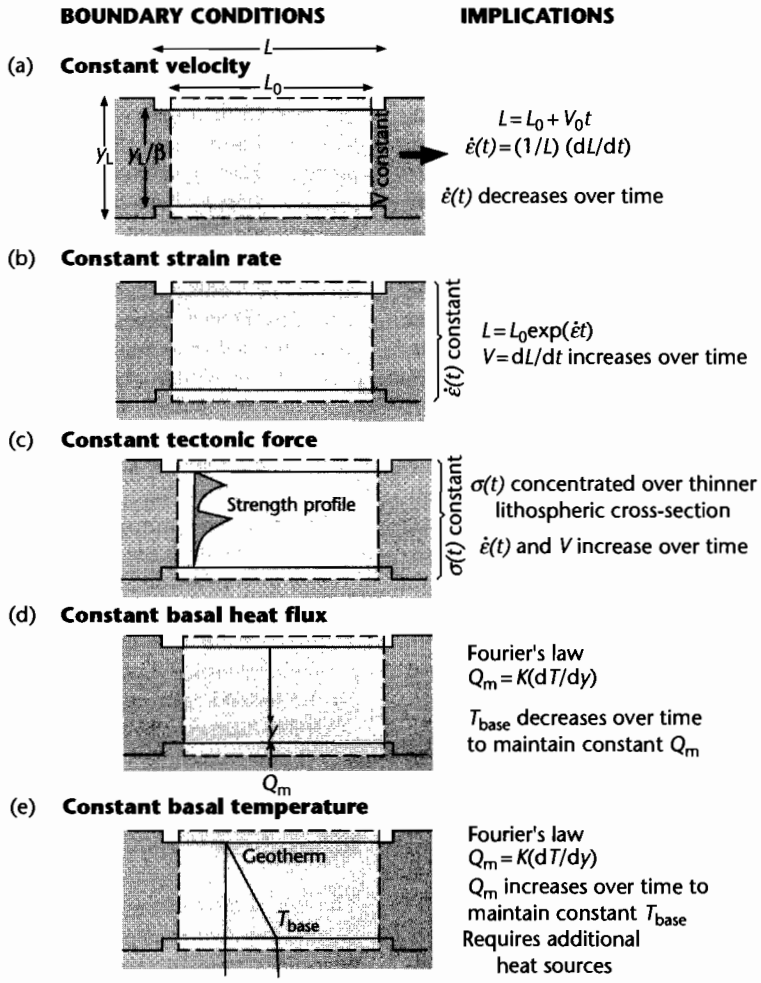

Fig. 3.29 Boundary conditions for dynamic models of lithospheric extension. (a) Constant velocity of extension over time, which implies that the strain rate must decrease over time; (b) Strain rate constant over time, which implies that the extension velocity must increase over time; (c) Constant tectonic force (deviatoric stress) over time, which causes the same force to be concentrated over a thinner lithospheric cross-section over time. This force becomes concentrated in the strong layers in the lithosphere, which undergo large scale necking. The strain rate therefore increases over time; (d) Constant basal heat flux over time, which implies, *via* Fourier's law, that the temperature at the base of the lithosphere must decrease over time; (e) Constant basal temperature over time, which implies that the basal heat flux must increase with time, as in the uniform stretching model of McKenzie (1978a). This requires additional heat sources to increase the basal heat flux.

stress on a progressively thinner lithosphere, especially on those parts of the lithosphere that are most resistant to deformation, such as the strong upper–midcrust or lithospheric mantle (Kusznir 1982). Tensile deviatoric stresses would therefore increase with time at the site of lithospheric necking, leading to accelerating strain rate, unless a "hardening" process prevents it. Such a "hardening" process might be cooling causing an increase in viscosity.

4 *Constant basal heat flux boundary condition*: if it is assumed that there are no additional heat sources in the asthenosphere such as plume heads and secondary convective

cells, the heat flux at the base of the lithosphere can be assumed to be constant as extension proceeds. If so, since $Q = K(dT/dy)$, and the thickness of the lithosphere decreases by extension, the temperature at the base of the lithosphere should decrease by the stretch factor β with time.

5 *Constant basal temperature boundary condition*: in similar fashion, a constant basal temperature implies that the basal heat flow increases (by a factor β) through time. Since the base of the lithosphere is usually taken as the solidus temperature of peridotite (Pollack and Chapman 1977), which is a constant temperature, this is a commonly applied boundary condition, and is implied in the uniform stretching model of McKenzie (1978a). However, it requires additional heat fluxes from the lithosphere, such as those caused by secondary convection, as stretching proceeds.

3.6.2 Modes of continental extension: narrow and wide rifts

There appear to be two different modes of continental extension (Fig. 3.30):

1 *Narrow rifts* with normal thickness crust (e.g., Rhein Graben; Gulf of Suez; Baikal; East Africa) are due to relatively small amounts of extension ($\beta < 2$). Narrow rifts may evolve into passive margins (e.g., Eastern Seaboard USA; Biscay–Armorican margin) alongside oceanic spreading centres. In crust with normal thickness (30–40 km) and geothermal gradient (30 °C km^{-1}), the process of lithospheric stretching is by a very large scale, localized thinning of the lithosphere or *necking* (Kooi et al. 1992). At early stages of lithospheric necking, rifts are 30–40 km wide, with the Moho elevated immediately beneath the rift. Some early rifts, such as those of East Africa, are wider (60–70 km). At late stages of necking, passive margins develop, with widths of 100–400 km and with the Moho shallowing from 30–40 km under the undisturbed lithosphere to 8–10 km at the continent–ocean boundary.

2 *Wide extended domains* where extension follows earlier crustal thickening by *c.* 20 Myr or more, providing time for the thickened brittle crust to spread gravitationally under its own weight over a weak layer in the lower crust (Jones et al. 1996). The width of the extending region can be as wide as the region of previously thickened crust – as much as 1000 km in the Basin and Range, USA. As a result of spreading, crustal thicknesses return to "normal" (*c.* 30 km), at which point extension stops. Local zones of exhumed ductile lower crust are termed *core complexes*. Core complexes are common in the Aegean (Greece) (Lister et al. 1984) and the Basin and Range province (Lister and Davis 1989), and have been interpreted in orogenic belts as diverse as the Alps of Austria–Switzerland (Frisch et al. 2000), the Variscan of west-central Europe (Burg et al. 1994a) and the Pan-African of western Saudi (Blasband et al. 2000). Flat-lying detachments associated with core complexes have been interpreted as initially low-angle faults that traversed the entire lithosphere. More recent studies suggest that they are initially steep and progressively rotated to a very shallow dip during extension, with a flat Moho undisturbed by any translithospheric faults/shear zones.

An important set of questions immediately springs to mind: what controls the duration and total stretching of a piece of continental lithosphere? Do rifts stay narrow because the driving force for extension is removed? Or is it because the mantle lithosphere gains in strength and self-limits extension (England 1983)? The first possibility can be termed "*force-controlled extension*" and the second possibility "*viscosity-controlled extension.*"

3.6.3 Forces on the continental lithosphere

The combination of forces causing stretching of the continental lithosphere may be varied. Extension of the lithosphere must be caused by a set of forces that have a resultant horizontal component that overcomes rock strength. It is known that stresses may be transmitted through the continental lithosphere over large lateral distances. These deviatoric stresses are termed in-plane stresses, since they are in the plane of the plate. For example, the World Stress Map of Zoback (1992) shows that the North Sea, Gulf of Lion, and Pannonian Basin, all of which were extensional tectonic provinces, are in a state of compressional stress at the present day.

Imagine a slab of continental lithosphere acted upon by *distant extensional forces*. Changes in the distant extensional force should cause the region to experience variations in the strain rate at the same time, regardless of location. If the crust varies in thickness across our slab of lithosphere, *buoyancy forces* caused by these thickness variations should interfere with the distant extensional forces.

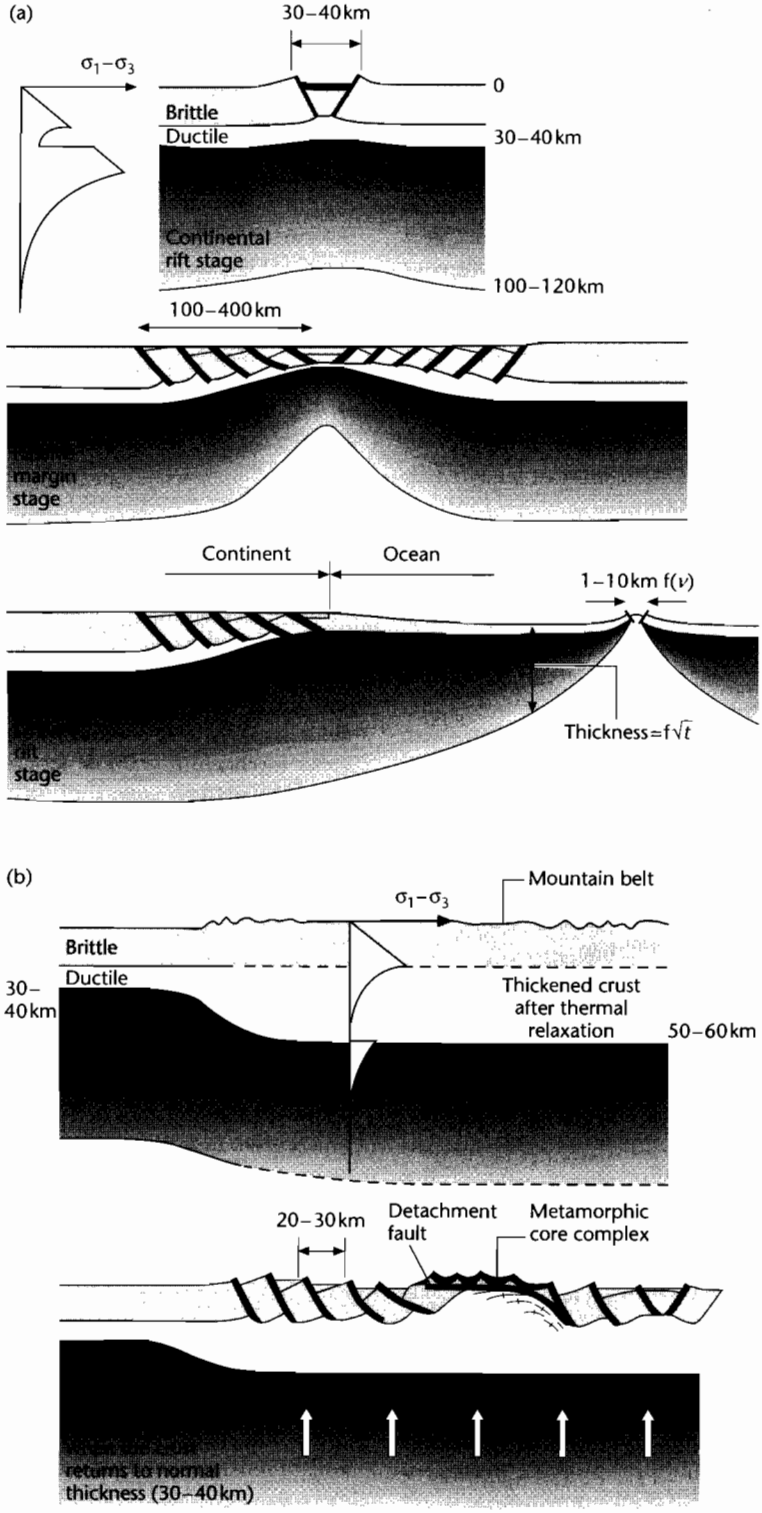

Fig. 3.30 Geological and structural differences between (a) narrow and (b) wide rifts, after Brun (1999). Wide rifts typically develop where the lithosphere has been previously thickened, with a Moho at >50 km. Extension leads to the unroofing of metamorphic core complexes. Reproduced courtesy of Royal Society, London.

Where the crust is thick, buoyancy forces assist the distant force to promote extension. But where the crust is thin, buoyancy forces oppose the distant extensional forces and resist extension. Could extension therefore be stopped by thinning the crust to a critical point? It is also possible that buoyancy forces may operate in the absence of a strong distant extensional force. For example, if the crust is thick, or if the lithosphere is elevated above a mantle plume, the buoyancy forces alone may drive extension. A further source of extensional stresses is the application of shear stresses to the base of the lithosphere, for example from the convectional motion in the mantle, with extension occurring above the divergent flow of a convection cell. However, these stresses are likely to be relatively minor because the asthenosphere has a very low viscosity.

Lateral transmission of mechanical energy through the lithosphere as a result of plate collision has been proposed as a cause of continental rifting by Molnar and Tapponnier (1975). For example, the Baikal Rift of central Asia may be influenced by plate collision along the Himalayan front in the south, and a further convergent plate boundary exists in the Pacific on the east, both boundaries being roughly 3000 km distant from the rift itself. The Rhine Graben has the collision boundary of the Alps in closer proximity in the south and the opening Atlantic (1000 km distant) and subsiding North Sea (500 km distant) in the west and north. However, the frequency of collision boundaries compared to the large number of modern and ancient rifts is negligible. It therefore seems inconceivable that collision events have a *primary* role to play in providing the deviatoric in-plane forces necessary for the rifting of the continents. A numerical model of a plate of constant thickness loaded horizontally by an indenter (Neugebauer 1983), using limits of lithospheric stress under compression and extension (Brace and Kohlstedt 1980), indicates that the predicted stress regime falls considerably short of that required of a self-sustaining mechanism for rifting in the Baikal and Rhine Rifts.

In addition to the forces applied at the edge of a continental plate by relative plate motion, there is an additional set of buoyancy forces set up by crustal thickness contrasts (England 1983; England and McKenzie 1983). The elevation of the continental lithosphere causes pressure differences to exist between it and neutrally elevated lithosphere. The relative importance of this driving force compared to that caused by applied forces at the plate boundaries can be gauged by an *Argand number* Ar (see §4.6). If the Argand number is small, that is, the effective viscosity is large for the ambient rate of strain, the deformation of the continental lithosphere will be entirely due to boundary forces. If Ar is large, however, the effective viscosity will appear to be small and the medium will not be strong enough to support the elevation contrasts, so the forces due to crustal thickness changes will dominate deformation. Numerical modeling using this approach explained the tectonic styles of major crustal shortening in the Himalaya and extension in Tibet (England and Houseman 1988, 1989) (Fig. 3.31).

3.6.4 Rheology of the continental lithosphere

The linkage between the forces on the lithosphere and its deformation is the rheology of lithospheric materials (§2.4). The rheology of the lithosphere controls its deformation under any set of initial and boundary conditions. Consequently, rheology underpins all dynamical models of basin development. Key to the correct treatment of rheology is the concept of the strength envelope (Goetze and Evans 1979; Ranalli 1995). A strength profile of the lithosphere must account for two different deformational mechanisms – brittle (or frictional) and ductile. The high strength regions of stabilized or "standard" continental lithosphere (with a Moho temperature of about 600 °C) occur in the midcrust and mantle lithosphere immediately beneath the Moho. Two low strength regions also occur – in the lower crust, and at greater depths in the mantle lithosphere. The continental lithosphere is therefore, at its simplest, a four-layer model (Fig. 3.32).

Information on rock rheology necessary for basin modeling essentially comes from laboratory experiments of rock deformation. Ignoring for the moment brittle failure (§2.4.3), the constitutive laws derived from these experiments express strain rate as a function of temperature, pressure, and deviatoric stress. Although laboratory experiments may not be fully representative of conditions in the lithosphere, the strain rate of rocks in the lithosphere is thought to obey a *power law creep* relationship as follows:

$$\dot{\varepsilon} = A\tau^n \exp(-E_a/RT) \tag{3.33}$$

where τ is the deviatoric stress, T is the absolute temperature, R is the universal gas constant (8.3144 J mol^{-1} K^{-1}), and A, E_a, and n are constants dependent on the type of material undergoing deformation (Fernandez and Ranalli 1997). The activation energy E_a ranges from

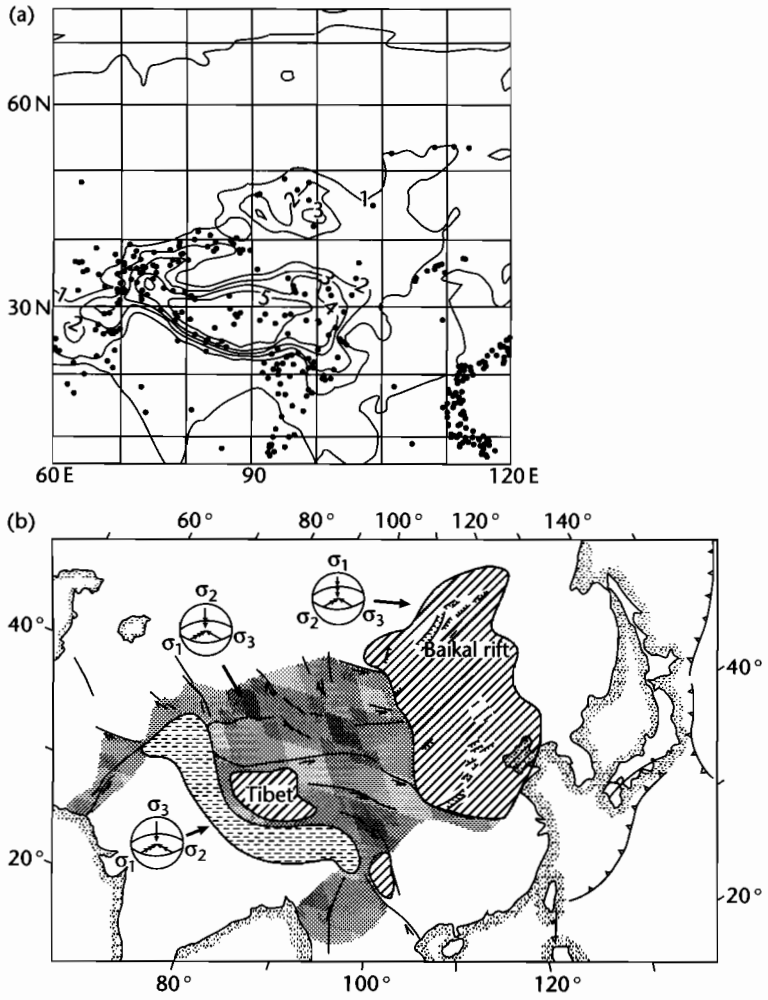

Fig. 3.31 (a) Average topographic elevation of Asia, with locations of earthquakes recorded by at least 50 stations between 1961 and 1977. Note that earthquakes occur diffusely over a very wide region of the Asian continent; (b) The major tectonic regimes for Asia (Tapponnier and Molnar 1976) are explained well by a numerical model of a viscous plate subjected to a collisional force along its southern boundary and gravitational forces arising from its thickness contrasts (England 1983; England and McKenzie 1983). Horizontal ornament, compression; stipple, strike–slip; diagonal hatch, extension.

about $500\,\mathrm{kJ\,mol^{-1}}$ for dry olivine to about $160\,\mathrm{kJ\,mol^{-1}}$ for quartz. The power exponent n is in the range 3–5. Equation (3.33) is in fact the common form of many temperature-activated processes, for example the maturation of organic matter to form petroleum.

It is a simple matter to calculate the difference in strain rate for dry olivine in the uppermost mantle lithosphere for a 20° temperature change from 600 °C to 580 °C (873 K to 853 K). We assume that the driving deviatoric stress τ, exponent n and material coefficient A are constant. A temperature change of just 20 °C causes over an order of magnitude change in the strain rate. This is because *viscosity* is highly dependent on temperature.

Although it is possible to measure strain rates of the surface of the Earth using techniques such as Global Positioning System geodesy (e.g., Bennett et al. 1997; Clarke et al. 1998), it is not known how representative this is of longer time scales and of the lithosphere as a

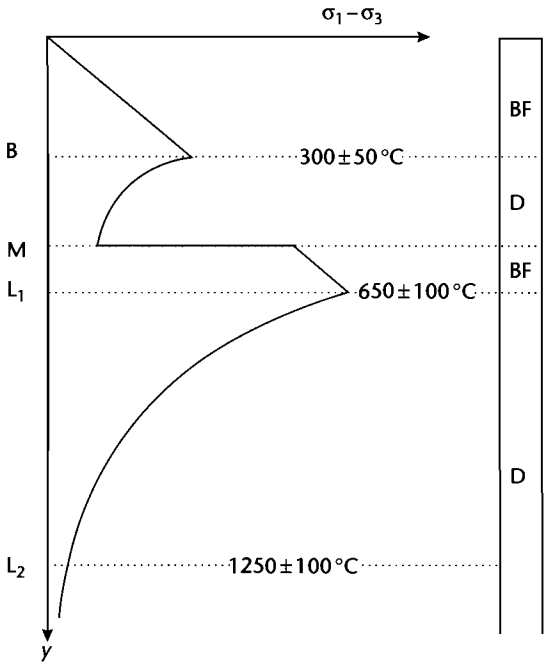

Fig. 3.32 Strength envelope for a four-layer lithosphere, after Fernandez and Ranalli (1997), with critical temperatures and typical rheology for a uniform felsic crust and low geothermal gradient. B, crustal brittle–ductile transition; M, Moho; L_1, mantle brittle–ductile transition; L_2, lithosphere–asthenosphere boundary; BF, brittle frictional; D, ductile power law. Reproduced courtesy of Elsevier.

whole. Whereas deformation of the upper crust is by brittle faulting, it is not known whether this fault-related upper crustal extension follows the same strain rate pattern as the ductile lower crust and lithospheric mantle. In some parts of the world (such as the Basin and Range province of SW USA, and the Aegean region of Greece and Turkey) upper crustal extension is diffuse and widespread, being distributed on very many individual faults. This suggests that extension of the ductile layers of the lithosphere may control the brittle extension of the upper crust. The strain rate of ductile deformation is determined by viscosity. It is open to question whether the amount of extension varies as a function of depth, but in the general case it can be assumed that strain and strain rate are independent of depth, representing the case of *pure shear*. The entire lithosphere is then assumed to extend at a rate determined by the depth-integrated viscosity.

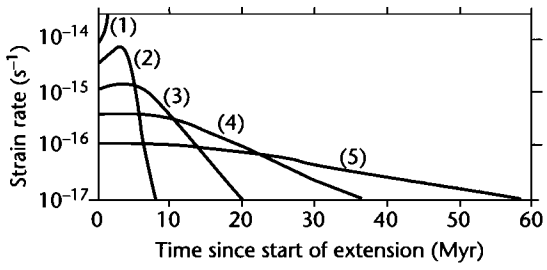

Fig. 3.33 Variation of the strain rate with time based on a set of 1-D numerical experiments (Newman and White 1999). Each experiment uses the same rheology, but the driving force varies, resulting in different initial strain rates. At very high initial strain rates (1), complete, rapid rifting of the lithosphere occurs. In (2) and (3) the strain rate rises at first because the same driving force acts on a progressively thinner lithosphere. Strain rate then falls because of the effect of cooling on viscosity in the mantle lithosphere. In (4) and (5) initial strain rates are low, so the mantle cooling effect dominates. Apart from passive margins, peak strain rates in extensional sedimentary basins rarely exceed $2 \times 10^{-15} s^{-1}$. Reproduced courtesy of Royal Society, London.

3.6.5 Numerical experiments on strain rate during continental extension

Using a relatively simple rheologic model of a low viscosity crust (not temperature-dependent) and a power law creep lithospheric mantle, Newman and White (1999) showed the strain rate history of a piece of extending continental lithosphere assuming pure shear. A number of scenarios are possible, depending on the initial strain rate/magnitude of distant driving force (Fig. 3.33):

- At *high initial strain rate*, complete rifting of the lithosphere takes place before any significant heat loss. The strain rate increases through time because the same distant driving force acts on progressively thinner lithosphere;
- at *lower initial strain rate*, strain rate rises at first because of the same lithospheric thinning effect, but mantle cooling becomes important and reduces the strain rate. The time taken for the strain rate to become negligible (less than about $10^{-17} s^{-1}$) depends on the initial strain rate – it is short for high initial strain rates and long for smaller initial strain rates. In other words, extension continues longer where the strain rate was lower.

How likely is it that the mantle lithosphere will cool sufficiently to significantly increase viscosity and stop

extension? Let us take equation (3.33) and derive an expression for the temperature change at the Moho of a piece of continental lithosphere extending with a stretch factor β required to cause a fall in the strain rate from an initial value $\dot{\varepsilon}_0$ to a new value $\dot{\varepsilon}_1$

$$\log_e \dot{\varepsilon}_0 - \log_e \dot{\varepsilon}_1 = \frac{E_a \Delta T}{R T_{MOHO}^2} - n \log_e \beta \tag{3.34}$$

where T_{MOHO} is the temperature at the Moho and the other parameters are as defined above. The temperature change, ΔT_r, required to lower the strain rate by an order of magnitude is then

$$\Delta T_r = \{2.3 + n \log_e \beta\} \frac{R T_{MOHO}^2}{E_a} \tag{3.35}$$

If the lithospheric stretch factor β is 1.2, $E_a = 500\,\mathrm{kJ\,mol^{-1}}$, $T_{MOHO} = 580\,^{\circ}\mathrm{C}$ (853 K), $n = 3$, $R = 8.314\,\mathrm{J\,mol^{-1}\,K^{-1}}$, the temperature change required to lower the strain rate by an order of magnitude is 34 °C. If the stretch factor β is 2.5, the answer is 61 °C. This is because with the higher stretch factor, the driving force is concentrated on a thinner slab of lithosphere, which causes the deviatoric stress to increase by a factor β as the lithosphere thins. This effect offsets the increase in viscosity caused by cooling.

How long should it take to accomplish the temperature reduction causing an order of magnitude fall in the strain rate? To answer this question requires us to know something about the geothermal gradient in the lithospheric mantle γ_m, the thermal conductivity of crust k_c and mantle lithosphere K_m, the radiogenic heat production of the crust A_c, the thermal time constant of the lithosphere τ, the initial thickness of the crust y_{c0} and initial Moho temperature T_o. The expression for the time period required, t_r, simplifies to

$$t_r = K(\dot{\varepsilon}_0)^{-1/2} \tag{3.36}$$

where the coefficient K is equal to 4×10^{-7} for the following parameter values: initial geotherm $\gamma_m = 25\,^{\circ}\mathrm{C\,km^{-1}}$, lithospheric time constant $\tau = 60\,\mathrm{Myr}$, initial Moho temperature $T_o = 580\,^{\circ}\mathrm{C}$, thermal conductivity of crust $k_c = 2.5\,\mathrm{W\,m^{-2}\,K^{-1}}$, thermal conductivity of mantle $K_m = 3.0\,\mathrm{W\,m^{-2}\,K^{-1}}$, crustal radiogenic heat production $A_c = 1.1\,\mu\mathrm{W\,m^{-3}}$, initial crustal thickness $y_{c0} = 33\,\mathrm{km}$, initial lithospheric thickness $y_{L0} = 120\,\mathrm{km}$.

The striking result is that the time taken to reduce the strain rate by an order of magnitude depends on the inverse square root of the initial strain rate. That is, if the initial strain rate is high, the time taken to reduce it by an order of magnitude is short. If the initial strain rate is low, the time taken to reduce the strain rate by an order of magnitude is long. If the initial strain rate is $3 \times 10^{-15}\,\mathrm{s^{-1}}$, the strain rate reduces to an order of magnitude smaller than this initial value in 7 Myr. When the initial strain rate is $3 \times 10^{-16}\,\mathrm{s^{-1}}$, this time scale becomes 23 Myr. This compares favorably with the observed time scale of rifting known from the geological record.

If the initial strain rate is less than *c.* $10^{-16}\,\mathrm{s^{-1}}$, it may take as much as 60 Myr for the extension to stop. It is likely that during this long period of time the driving force may be removed, for example, by changes in relative plate motion, or by changes in the convectional motion in the mantle (see also §3.7).

The subsidence history of sedimentary basins allows the stretch factor and peak strain rate of the underlying continental lithosphere to be estimated. White (1994) and Newman and White (1999) developed this technique and applied it to literally thousands of borehole subsidence records. They discovered that there was a strong relationship between the peak strain rate and the final stretch factor in all of the sedimentary basins studied (Fig. 3.34).

If continental extension is controlled by a distant driving force, we would expect large variations in this relationship between peak strain rate and stretch factor, since continental lithosphere is heterogeneous. However, if viscosity controls extension, we should expect just the relationship observed. Differences caused by variations in the magnitude of the distant driving forces are much smaller than the effects of viscosity (or values of the activation energy E_a, which may vary significantly).

If our viscosity-controlled extension model is correct, previously stretched lithosphere should be *stronger* than "normal" lithosphere. That is, for a given peak strain rate, we should expect a smaller stretch factor in the case of the previously stretched lithosphere. This appears to be supported by the data of Newman and White (1999). However, there is still an unanswered question: do previously rifted pieces of lithosphere tend to rift again? The geological record suggests "yes." The numerical model suggests perhaps "no."

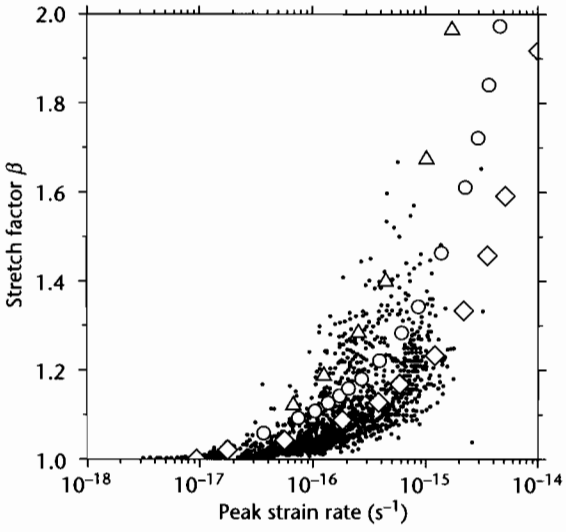

Fig. 3.34 Relation between peak strain rate and stretch factor for 2195 separate rifting episodes (small dots). Model results are for activation energies E_a of $300\,kJ\,mol^{-1}$ (triangles), $500\,kJ\,mol^{-1}$ (circles) and $1200\,kJ\,mol^{-1}$ (diamonds). After White (1994), and Newman and White (1999). Reproduced courtesy of Royal Society, London.

3.6.6 Insights from analogue models

Analogue models are experiments conducted with materials of carefully chosen viscosities, strengths and densities, scaled in such a way as to represent the deformation of a layered lithosphere at the appropriate strain rates. These models are informative about lithospheric stretching under a variety of conditions. Different results are obtained dependent on the strength profile of the lithospheric model and the scaled strain rate of the analogue experiment. The analogue experiments replicate many of the different styles of continental extension, particularly narrow, localized rifts versus extensive tilted fault block terranes (Brun 1999) (Fig. 3.30):

- For a simple two-layer model (brittle upper layer over a ductile lower layer), at low strain rates (and therefore low ductile strengths), deformation remains localized in an asymmetric graben; at high strain rate, the faulted zone is much wider, with highly tilted fault blocks;
- for a simple two-layer model with constant strain rate, small brittle layer thicknesses (therefore low brittle strength) produced extensively faulted models, whereas high brittle strength resulted in localized rifts;
- where the two-layer analogue model is able to extend under its own weight, faulting invades the whole model, producing a wide rift with highly tilted fault blocks rather than horsts and graben.

These results therefore suggest that ductile and brittle strengths and spreading under gravity have major roles in style of deformation. Horsts and graben appear to typify regions of slow strain rate, whereas tilted fault blocks are typical of high strain rate regions.

In four-layer models (two high-strength zones, corresponding to the upper crust and upper mantle lithosphere), low strain rates produce a narrow rift whose delimiting faults sole out into the brittle–ductile interface. Whereas a single zone of necking develops at low strain rates, at higher strain rates multiple necking (that is, *boudinage*) causes a widening of the extending zone, as in the passive margin stage. A local, low viscosity heterogeneity beneath the brittle–ductile interface (such as caused by the thermal effects of a large pluton, or by partial melting) causes an increase in stretching and allows the ductile layer to exhume to form core complexes. Initially steep normal faults are rotated into flat-lying detachments. In wide rifts therefore, local anomalies are prone to amplification to produce strong variations in extension and exhumation.

3.7 MANTLE PLUMES AND IGNEOUS ACTIVITY ASSOCIATED WITH CONTINENTAL EXTENSION

It is beyond doubt that some regions of continental stretching are unrelated to any "active" thermal processes. However, in other instances, continental stretching and break-up is associated with voluminous basaltic volcanism, as in the Deccan of India, the Karoo of southern Africa, and the Parana of South America. Magmatically active rifts and continental margins are commonly associated with anomalously high temperatures in the asthenosphere caused by the presence of mantle plumes (White and McKenzie 1989). We therefore turn our attention to mantle plumes before considering a model for melt generation and emplacement associated with plume activity.

3.7.1 Plumes

Far from their margins, oceanic plates are marked by long chains of volcanic islands (e.g., Emperor–Hawaiian seamount chain) and bathymetric swells elevating the seabed 1–2 km above the adjacent abyssal plains (e.g.,

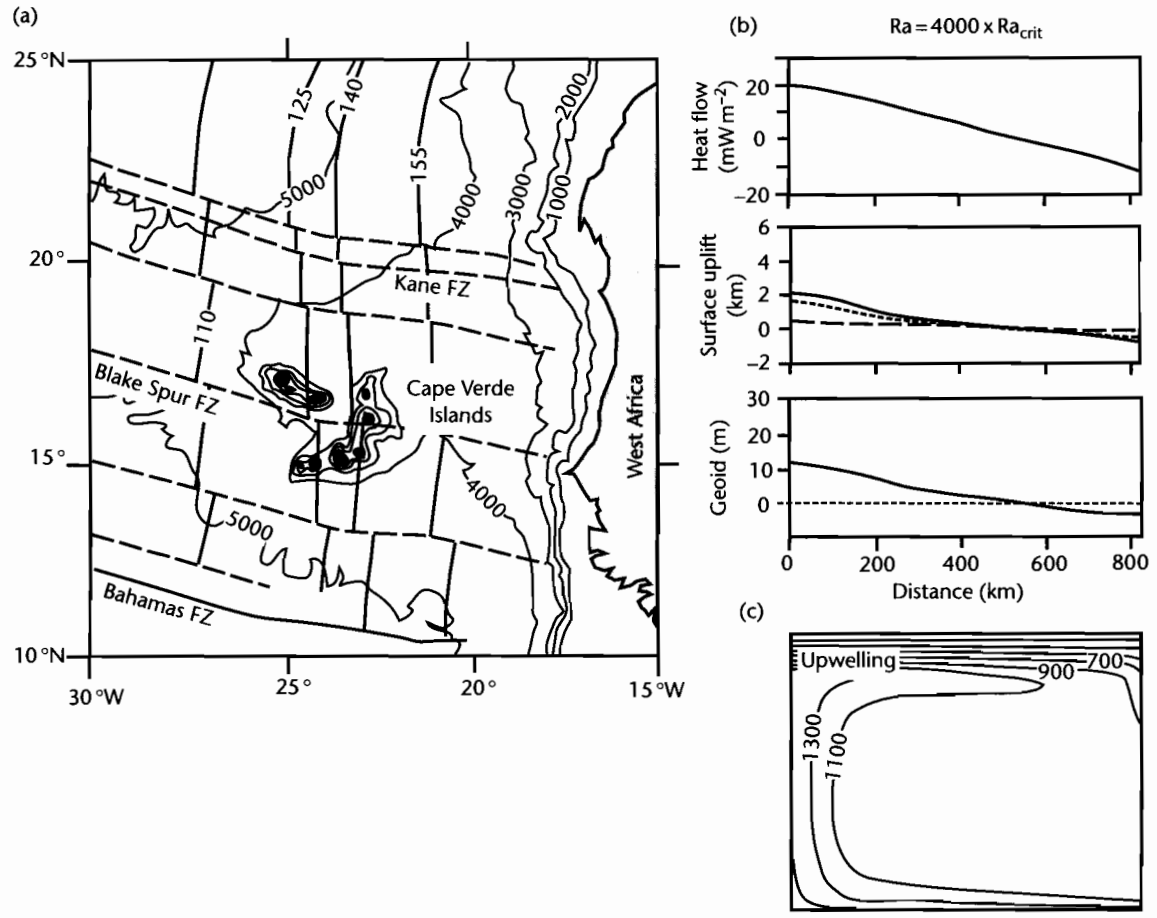

Fig. 3.35 Cape Verde hotspot. (a) Bathymetric map (in m) of the Cape Verde Rise, with isochrons in Ma. Fracture zones are shown in dashed lines; (b) Heat flow, surface uplift, and the geoid for a convection cell at 4000 times the critical Rayleigh number for convection. The total uplift is shown as a conductive component (dashed) and a convective component (dotted); (c) Temperature distribution responsible for the results shown in (b). After Courtney and White (1986). Reproduced courtesy of Blackwell Publishing Ltd. for Royal Astronomical Society.

Cape Verde, Reunion, and Iceland swells) (Wilson 1963; Morgan 1981). The equivalent chains and swells on land are less easy to discern because of the effects of erosion. However, all of these intraplate features are associated with the eruption of extensive basalts, whose geochemistry indicates that they originate by melting of mantle elevated above the normal temperature of the asthenosphere. They can be explained by the rising of hot plumes from the thermal boundary layer at the core–mantle boundary (see also §5.2.4).

The Cape Verde swell typifies plume-related temperature anomalies and bathymetric relief (Courtney and White 1986) (Fig. 3.35). The best fitting convection model to explain the temperature distribution involves a plume neck of 150 km diameter feeding a mushroom-like head of hot mantle material 1500 km across. The temperature anomaly in the plume head at the base of the plate is generally in the region of 100 °C, with the neck of the plume in excess of 300 °C above ambient asthenospheric temperatures. The centre of the Cape Verde swell is elevated by 1900 m relative to the normal oceanic depth: most of this relief can be attributed to dynamic uplift over the convecting plume head.

Geoid anomalies suggest that plume upwellings are spaced at about 2500–4000 km in the upper mantle beneath the oceans (McKenzie et al. 1980), but their distribution beneath the continental lithosphere is more speculative. The highspots associated with alkaline volcanism in north-central Africa, such as the Hoggar and Tibesti domes, may be related to activity in the underlying mantle (Thiessen et al. 1979; Sahagian 1980). Doming over hot plumes has also been interpreted as responsible for particular centrifugal paleodrainage patterns (Cox 1989), as well as for the eruption of vast piles of basalts.

The lithospheric plates move relative to the major mantle upwellings, though the question of whether the upwellings are stationary is unresolved. Two sorts of uplift pattern and igneous activity should result from plume activity depending on whether the lithosphere migrates over a plume head or plume tail. Plume head provinces should be areally extensive and equant (1500 km to 2500 km across), whereas plume tail provinces should be narrow (<300 km wide) and linear, that is, they should be hotspot tracks.

3.7.2 Melt generation during continental extension

Igneous activity in sedimentary basins is diagnostic of basin-forming mechanisms. In the prototype uniform stretching model of McKenzie (1978a), no melts are generated because the geotherm does not intersect the solidus for crustal and mantle materials. However, it is well known that rift provinces are associated with minor (e.g., Western Rift, Africa, North Sea) to major (e.g., Eastern Rift, Africa, Rio Grande) volcanism. Most importantly, continental break-up at high values of stretching is commonly associated with vast outpourings of flood basalts, indicating major melting of the asthenosphere by adiabatic decompression. Melts liberated by decompression are assumed to separate from their residue and to travel upwards to either be erupted at the surface, or to be emplaced as igneous bodies in the crust. McKenzie and Bickle (1988) showed how the amount of melt generated depends on the potential temperature of the asthenosphere – defined as the temperature the asthenosphere would have if brought to the surface adiabatically without melting – and the amount of stretching (Fig. 3.36). For example, if a 100 km-thick lithosphere is stretched by a factor of 2, we would expect a melt thickness of about 2 km for a potential temperature of 1400 °C. At higher values of stretching ($\beta = 5$), we would expect a melt thickness of 10 km for the same potential temperature. The normal potential temperature of the asthenosphere is 1280 ± 30 °C, so the examples above refer to an excess temperature of the order of 100 °C attributable to plume activity.

The conditions at the site of partial melting are reflected in the composition of the erupted basalts. Stretching at infinitely high values at a normal asthenospheric potential temperature of 1280 °C produces melt with the composition of a mid-ocean ridge basalt (MORB). However, increasing the potential temperature to 1480 °C causes an increase in MgO and a decrease in Na_2O. Consequently, we would anticipate the generation of first alkali basalts and then tholeiitic basalts as stretching increases over an asthenosphere with a potential temperature of 1480 °C.

The presence of a hot asthenosphere affects the subsidence experienced at the Earth's surface caused by lithospheric stretching. This is mainly caused by two effects: the addition of igneous bodies beneath the crust, and the dynamic uplift from the mantle plume.

3.7.2.1 Uplift due to igneous underplating

The density of igneous rock generated by adiabatic decompression of the mantle depends on the potential temperature at the site of partial melting, and ranges between 2990 and 3070 kg m^{-3} (at a depth of 10 km) for potential temperatures of 1280 °C and 1480 °C respectively. This range of density is midway between the density of the continental crust and the density of the mantle, so there is a strong likelihood that melts will be trapped and underplated beneath the crust. Since these igneous additions replace lithospheric mantle (density 3300 kg m^{-3}), the net effect is uplift relative to the depth expected from uniform stretching of the lithosphere without magmatic activity (§3.4) (Fig. 3.37).

Assuming Airy isostasy, the amount of underplating X required to generate an amount of surface uplift U can be found by balancing two lithospheric columns. In the undisturbed column, crust of thickness y_c and density ρ_c occurs within a lithosphere of thickness y_L and subcrustal density ρ_m. In the underplated lithospheric column, crust of the same thickness is underlain by a layer of basaltic underplate with thickness X and density ρ_x. The total thickness of this lithospheric column is y_L plus the surface uplift U.

Balancing the pressures at a depth of compensation at the base of the lithosphere yields

$$U = X\left(1 - \frac{\rho_x}{\rho_m}\right) \tag{3.37}$$

The density of the mantle lithosphere can be taken as $3300\,\mathrm{kg\,m^{-3}}$ and density of basaltic underplate as $3000\,\mathrm{kg\,m^{-3}}$. The rock uplift for an underplate thickness of 5 km is therefore 455 m, or approximately one-tenth of the underplate thickness. This is also the surface uplift without any erosion. We can incorporate erosion in the simplest way as follows (Brodie and White 1994). Consider a piece of lithosphere underplated with basalt of thickness X which is eroded so that the surface elevation change is zero. The crust therefore has a thickness of y_c minus the denudation D. We can once again perform an isostatic balance, giving

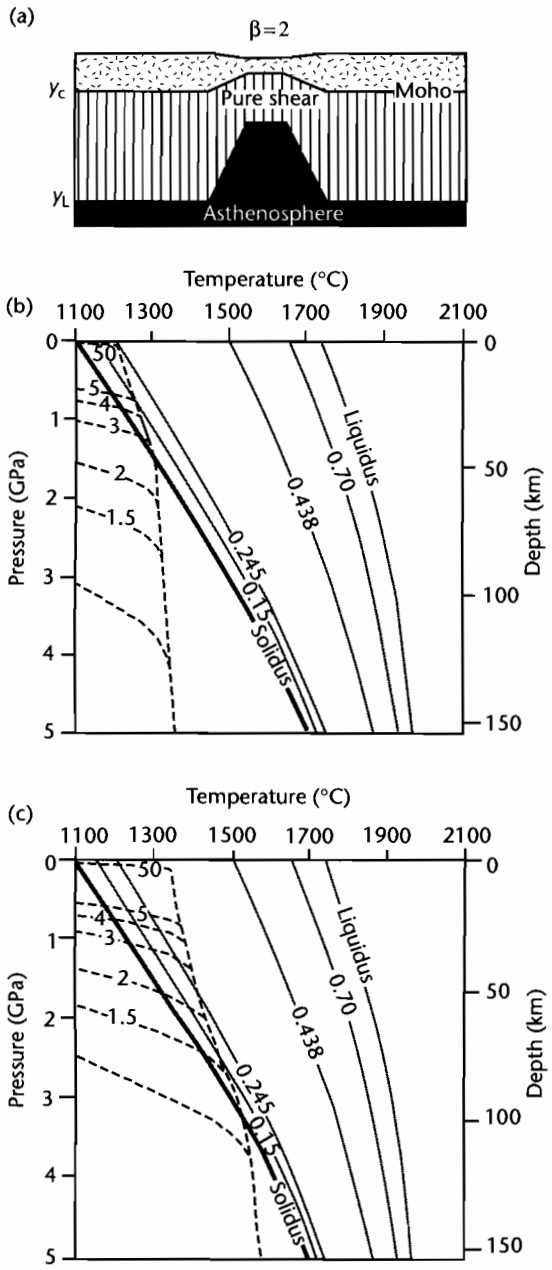

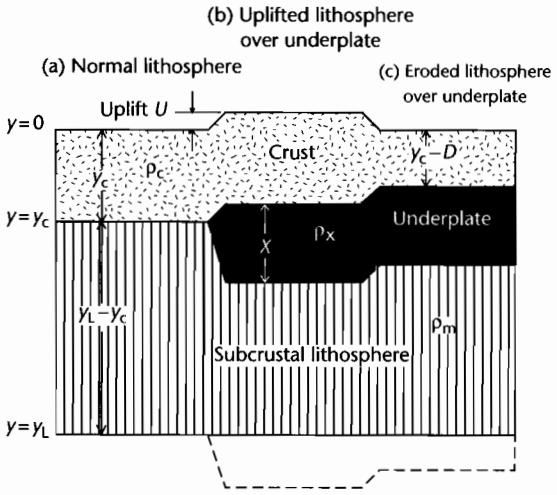

Fig. 3.37 Isostatic effects of igneous underplating as a result of plume activity. Normal lithosphere is shown in (a). An uplifted region results from the emplacement of an igneous underplate in (b). The effects of surface erosion are shown in (c).

Fig. 3.36 Melt generation by adiabatic decompression during pure shear extension, based on McKenzie and Bickle (1988), White and McKenzie (1989), and Latin and White (1990). (a) Uniform stretching of the lithosphere by a stretch factor β of 2; (b) Adiabatic upwelling due to stretching at different values of β from 1.5 to 50. Potential temperature of the asthenosphere 1280 °C, mechanical boundary layer thickness of 100 km, kinematic viscosity $4 \times 10^{15}\,\mathrm{m^2\,s^{-1}}$. Curves between the liquidus and solidus show the melt fraction by weight. Only small amounts of melt can be produced at high values of stretching; (c) As for (b), but with a potential temperature of 1480 °C, showing that large amounts of melt can be liberated at relatively low values of the stretch factor β. Reproduced courtesy of Geological Society of America.

$$D = X\left(\frac{\rho_m - \rho_x}{\rho_m - \rho_c}\right) \quad (3.38)$$

where D is the total denudation of crust caused by the emplacement of a basaltic underplate of thickness X. The total denudation for an underplate thickness of 5 km if there is no change in the surface elevation is 2.5 km, if crustal rocks of density 2700 kg m^{-3} are eroded. We therefore have the maximum erosion case and the no-erosion case. Reality is probably in between. Clearly, magmatic underplating can have significant effects on surface uplift and on the delivery of erosional products to neighboring sedimentary basins (White and Lovell 1997). The uplift caused by magmatic underplating is permanent.

3.7.2.2 Dynamic support produced by mantle plume

The circulation in the mantle plume maintains anomalously high temperatures that cause a dynamic uplift. The amount of dynamic uplift can be approximated by assuming that hot mantle replaces normal mantle down to a depth of compensation. This depth of compensation is most likely 150–200 km. The volumetric coefficient of thermal expansion of mantle rock is about 3.4 $\times 10^{-5}$ °C^{-1}, so there is a 0.34% change in the mantle density for every 100 °C change in its temperature. Dynamic uplift of 500–1000 m is therefore predicted for potential temperatures 100–200 °C hotter than normal. This dynamic uplift is transient, and disappears when the overlying plate migrates away from the anomalously hot asthenosphere, or changes in response to variations in the heat flux into the plume head.

The combined effect of underplating and dynamic support is to elevate the continental plate to sea-level or above during the rifting process for excess asthenospheric temperatures of 100–150 °C. This is entirely supported by the observation that the basalts erupted at rifted continental margins are commonly subaerial rather than submarine, and flow for large distances downslope to produce extensive flood basalt provinces.

3.7.3 The northern North Atlantic and the Iceland plume

The northern Atlantic contains extensive basalts covering *c.* 500 $\times 10^3$ km^2 on both sides of the ocean in Greenland and in northwest Britain, Ireland and the Faeroes. The basalts range from 52 to 63 Ma in age, with a main eruption phase at 59 Ma (Mussett et al. 1988). The thermal anomaly responsible for these igneous provinces is now located beneath Iceland. The Iceland region continues to be dynamically supported by the underlying plume over an area of anomalously shallow seafloor with a radius of 1000 km.

In the subsurface seismic record, extrusive basalt sheets can be recognized as seaward-dipping reflectors along both the east Greenland and Rockall–Faeroes–Norwegian margin (Fig. 3.38). Volumetrically smaller basaltic volcanism can be seen in onshore exposures such as the Tertiary igneous province of northwest Scotland and northeast Ireland. Thick (<8 km) prisms of accreted igneous rocks with seismic velocities >7.2 km s^{-1} have been imaged across the Hatton Bank and Voring Plateau beneath thinned continental crust, most likely representing underplated igneous rocks. White and McKenzie (1989) estimate the combined underplate and extrusive basalt volume as <10^7 km^3.

The Icelandic plume has been identified as the "smoking gun" for the widespread surface uplift of the North Atlantic area in the Early Tertiary (Paleocene). The regional surface uplift caused by underplating and dynamic support is thought to have promoted high rates of denudation and transport of particulate load into the deep sea environments of the North Sea and NW Atlantic margin basins. High rates of denudation in large areas of northwestern Europe during the Early Tertiary can be inferred from apatite fission track analysis (papers in Doré et al. 2002). In the neighboring sedimentary basins, such as the Faroes–Shetland Basin and the Rockall–Porcupine troughs, sandstones were episodically delivered from this exhuming continental landmass. White and Lovell (1997) suggested that the main pulses of submarine fan deposition correspond to the main phases of magmatic activity during the time period 62–54 Ma.

3.7.4 Low-volume melts in the Mesozoic North Sea Rift

We know from the preceding sections that adiabatic decompression is unlikely to be significant for low stretch factors and normal asthenospheric temperatures. Over a "normal" temperature asthenosphere (1280 °C), it is not possible to generate melts until very high amounts of stretching have taken place, by which time the parent material melts at very shallow depths, producing small melt volumes (McKenzie and Bickle 1988). It is therefore interesting to test whether the igneous activity noted in continental rifts with small stretch factors can also be

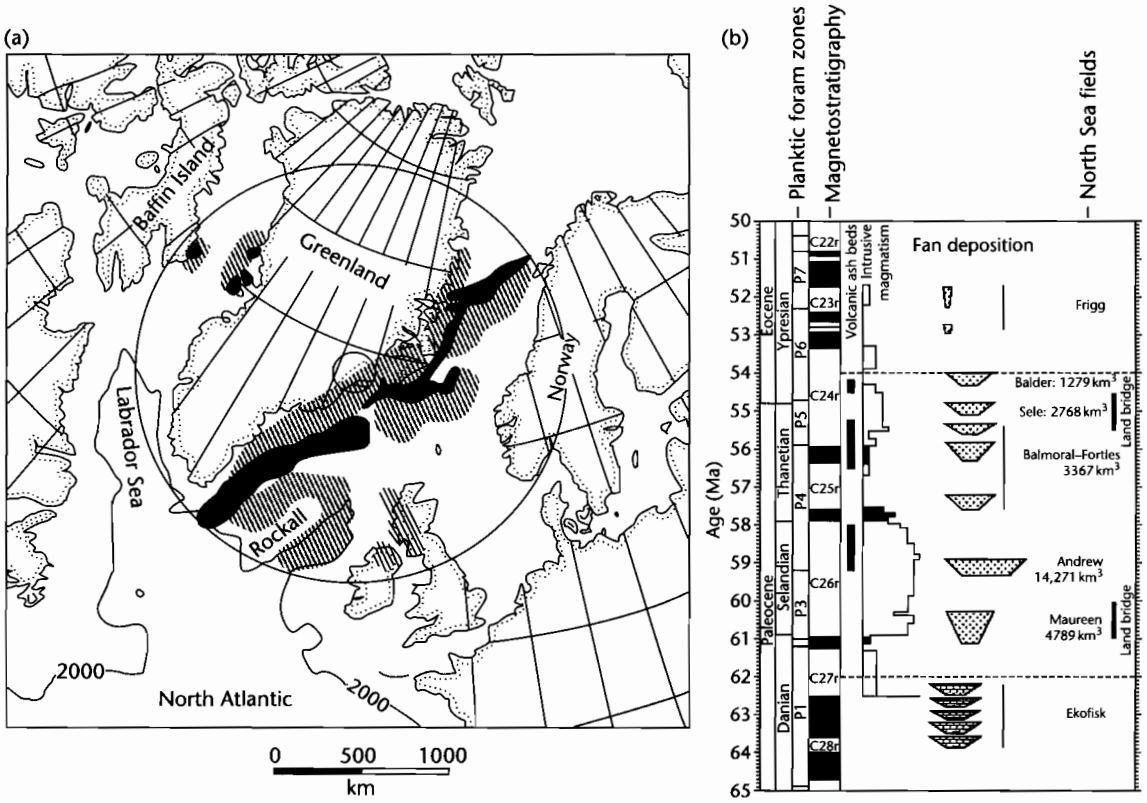

Fig. 3.38 (a) Reconstruction of the northern North Atlantic region just after the onset of ocean spreading (magnetic anomaly 23), showing the extent of the Iceland plume (White and McKenzie 1989). Solid shading shows position of extrusive volcanic rocks, hatching shows extent of Early Cretaceous igneous activity. Uplift over the plume head can be recognized in thermochronologic data such as apatite fission tracks. Reproduced courtesy of American Geophysical Union; (b) Pulsing of the Iceland plume is thought to have caused episodic deposition of sands in the deep sea (White and Lovell 1997). Periods of deep sea fan deposition correspond to times of high levels of intrusive igneous activity. Time scale from Berrgren et al. (1995). Reproduced courtesy of Macmillan Journals.

investigated using the approach outlined in §3.7.2 (Latin and White 1990).

Partial melting can only be achieved by the intersection of the solidus and geotherm. This may be promoted by: (i) high amounts of lithospheric stretching, (ii) presence of volatiles, and (iii) high asthenospheric temperatures, or a combination of factors (Fig. 3.39).

In the North Sea, low volume (*c.* 0.5 km melt thickness) synrift alkali basalts are found in the triple junction area, where the Viking, Central, and Moray Firth Grabens intersect (Fig. 3.4). They postdate the start of rifting by *c.* 30 Myr. The McKenzie and Bickle (1988) model suggests that:

- A combination of a mantle plume (1480 °C) and stretch factor of 1.4–1.6 (estimated from subsidence histories in North Sea Rifts) would give 5 km of tholeiites rather than 0.5 km of alkali basalts. In the triple junction region where β is >2, the model predicts even larger melt thicknesses;
- a combination of stretch factor 1.4–1.6 (observed/calculated), potential temperature of 1280 °C (that is, normal), mechanical boundary layer thickness of 70 km (that is, the lithosphere has been previously thinned/stretched) and a volatile (H_2O) content of 1%, would satisfactorily explain the alkali basalts in the Forties area near the triple junction of the North Sea rifts;
- if the potential temperature was 1380 °C (a "warm plume") and the mechanical boundary layer was 80 km (less previously thinned), the model would explain the

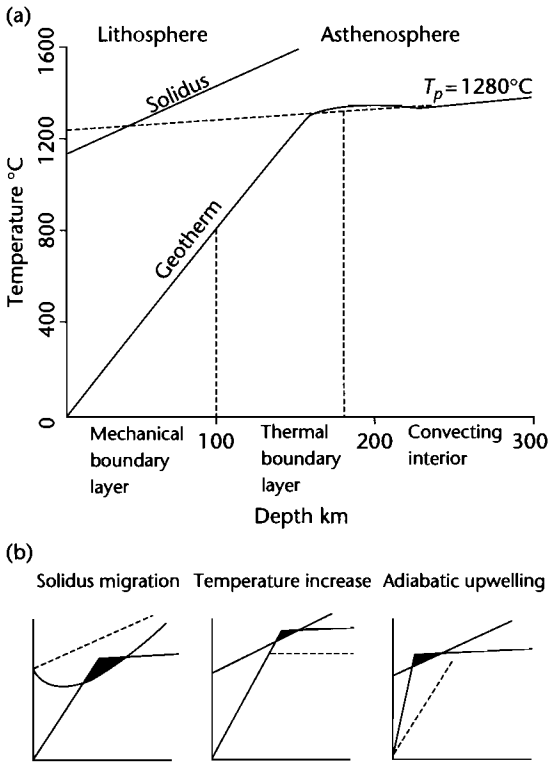

Fig. 3.39 Causes of partial melting related to lithospheric extension (after McKenzie and Bickle 1988, Latin et al. 1990, and Leeder 1995). (a) Geotherm for a potential temperature of 1280 °C and solidus for mantle material. The potential temperature is the temperature on an adiabatic gradient extrapolated to surface pressure; (b) Adiabatic decompression may be facilitated by migration of the solidus caused by the presence of volatiles such as water, by a temperature increase due the presence of a plume in the asthenosphere, or by mechanical thinning of the lithosphere and asthenospheric upwelling.

magmatism *and* the regional uplift over a diameter of *c.* 1000 km.

3.8 ESTIMATION OF THE STRETCH FACTOR AND STRAIN RATE HISTORY

An estimate of the amount of extension that has taken place can be obtained from a number of methods (Fig. 3.40). Knowledge of the strain rate history or total stretch factor is important as a basis for predicting the geothermal gradient and heat flow history of basin sediments, as well as in showing the role of rift structures in accommodating basin sediments.

3.8.1 Estimation of the stretch factor from thermal subsidence history

It has previously been shown (§3.1) that the lithospheric stretching model of the type formulated by McKenzie (1978a) predicts initial uplift or subsidence depending on the ratio of crustal to lithospheric thickness y_c/y_L and the stretch factor β. If y_c/y_L is known for a particular basin, the fault-controlled initial subsidence could in theory be used to estimate the amount of stretching. However, the extreme variations in synrift thicknesses make this a very unreliable technique.

The thermal subsidence in a basin generated by uniform stretching is dependent on the stretch factor alone. The postrift thermal subsidence phase of sedimentary basins also lacks the extreme thickness variations characteristic of synrift deposits. The standard technique is the construction of a set of subsidence curves for different values of the stretch factor β. Curves can be constructed for a water-loaded basin, where the density of the infill is $\rho_w = 1000\,kg\,m^{-3}$. In this case the postrift sediment thicknesses need to be decompacted and backstripped to reveal the water-loaded tectonic subsidence history (Chapter 9). The observed backstripped postrift subsidence can then be compared with the model curves to reveal the best-fitting stretch factor. Alternatively, model curves can be constructed that show the thermal subsidence for different values of the stretch factor β for a sediment-loaded basin. Construction of such curves requires estimation of the bulk density of the sediment column as a function of time. The model sediment-loaded curves can then be compared with the decompacted total subsidence curve derived from borehole data or outcrop sections.

3.8.2 Estimation of the stretch factor from crustal thickness changes

In some circumstances the attenuation of the crust can be estimated from deep seismic (refraction and wide angle reflection) results. For example, the Moho rises by 5 km in the southern part of the Rhine Graben and 3 km of sediment has accumulated. The crust has therefore thinned by 8 km (Emter 1971; Mueller et al. 1973). Simi-

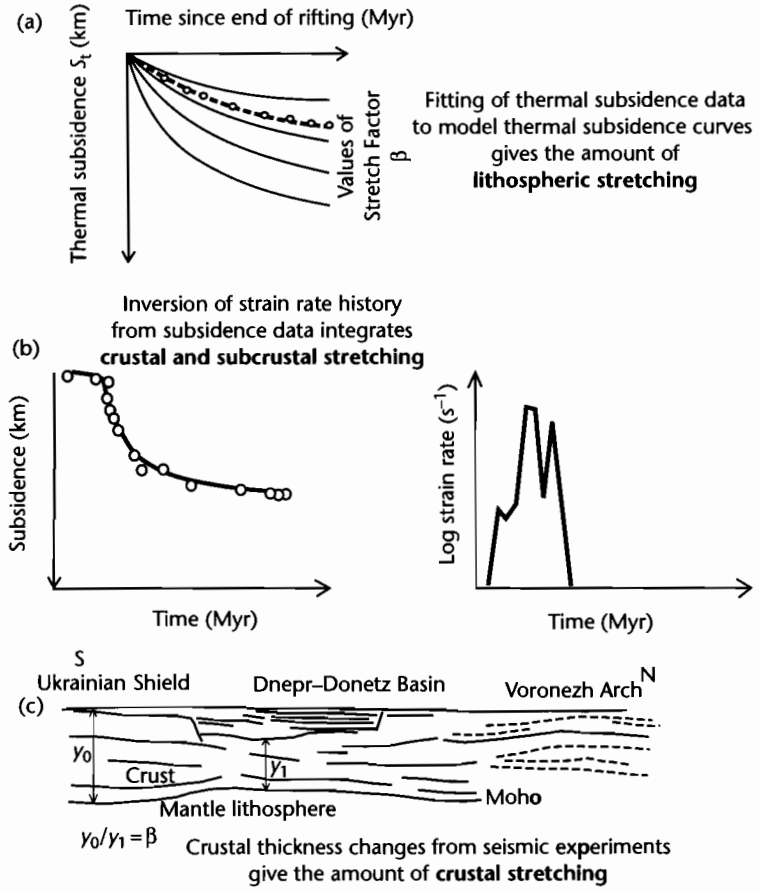

Fig. 3.40 Methods for calculation of the amount of stretching. (a) Calculation of the lithospheric stretch factor from thermal subsidence curves; (b) Inversion of strain rate history of the lithosphere from subsidence curves; (c) Calculation of the crustal stretching from mapping of the Moho.

larly, the nearby Limagne Graben (France) contains 2 km of sediments and the Moho rises to within 24 km of the surface (Hirn and Perrier 1974). Since the crust is about 30 km thick in the Massif Central, which separates the Rhine–Bresse Rift system from the Limagne Graben, the amount of crustal attenuation in these two cases can be estimated to be between 1.2 and 1.3.

The North Sea is a failed rift that underwent rifting in the Jurassic–Early Cretaceous. Regional deep seismic reflection profiles and gravity profiles in the Viking Graben–Shetland platform area have been used to estimate the depth to the Moho (Barton 1986; Klemperer 1988) (Fig. 3.4). More recently, the deep structure of the Viking Graben and adjacent areas of the northern North Sea (60–62 °N) has been investigated based on an integrated study of deep seismic reflection and refraction data, gravity and magnetic data (Christiansson et al. 2000) (Fig. 3.41). Where unaffected by Caledonian crustal roots and by Mesozoic stretching, the Moho lies at a depth of 30–32 km. It shallows to about 20–22 km beneath the Viking Graben. Since the graben is filled with approximately 10 km of Triassic to Cenozoic sedimentary rocks, the thickness of crystalline and Paleozoic crustal rocks in the Viking Graben is only about 10 km. This represents a stretch factor of over 3. In contrast, the East Shetland and Horda Platforms have stretch factors of less than 1.5. These values reflect the cumulative effects of several post-Caledonian stretching events.

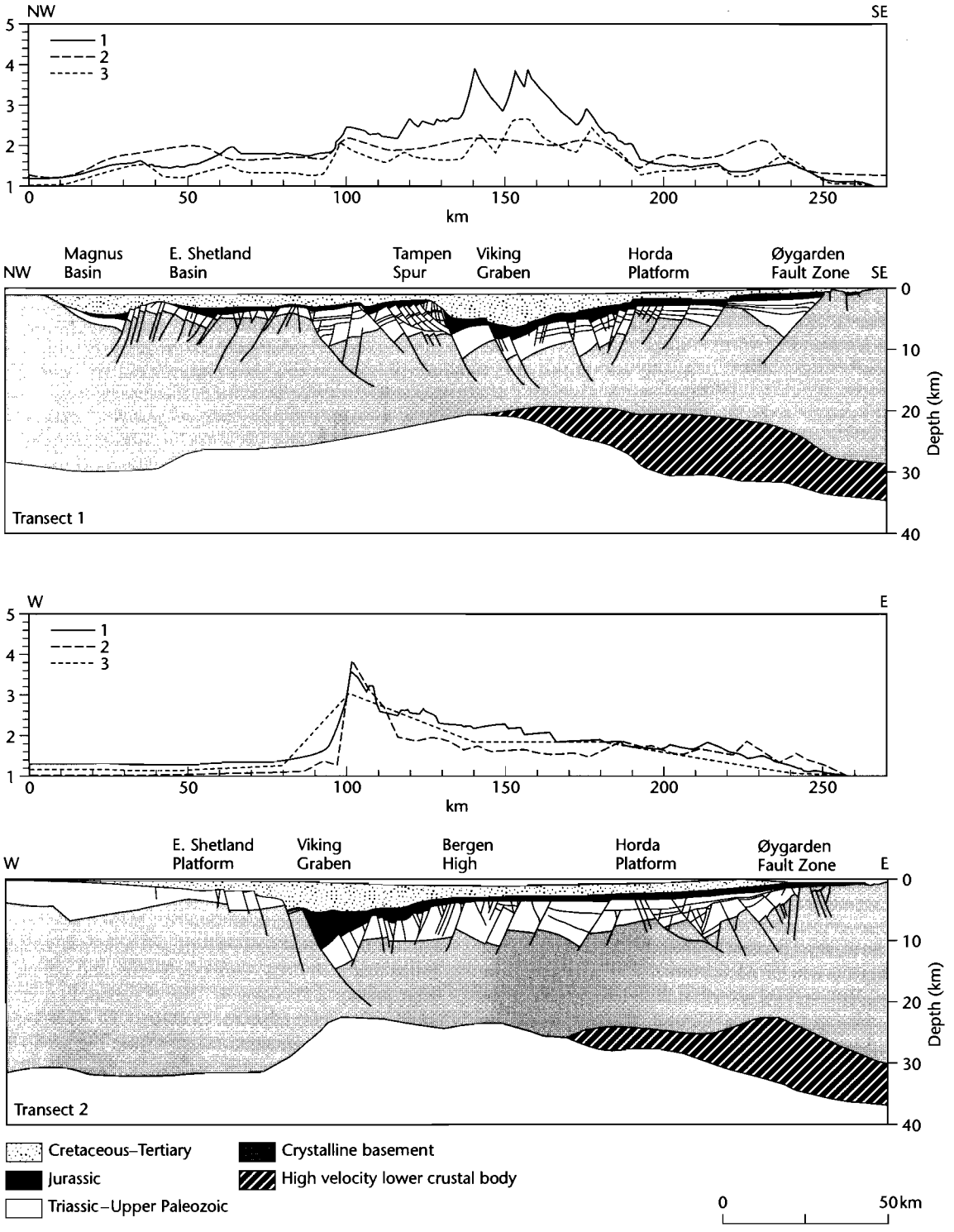

Fig. 3.41 Two crustal transects across the Viking Graben, northern North Sea (from Christiansson et al. 2000; Skogseid et al. 2000), based on the integration of all available geological and geophysical information, with estimates of crustal stretch factor. For each transect, line 1 indicates crustal thinning assuming an initial crustal thickness of 36 km; line 2 is derived from reverse modeling; and line 3 is derived from forward tectonostratigraphic modeling. Reproduced courtesy of Geological Society of London.

The estimates of crustal stretching derived from mapping of the Moho have been compared with estimates from subsidence analysis (Giltner 1987; Badley et al.1988, Christiansson et al. 2000) and forward tectonostratigraphic modeling (Odinsen et al. 2000). The former are somewhat higher than the stretch factors derived from the other two methods, which emphasizes the care that needs to be taken in the interpretation of β estimates. A similar exercise in the Rockall, mid-Norway and SW Barents Sea areas also showed large discrepancies between the crustal stretching estimated from deep seismic imagery and subsidence analysis (Skogseid et al. 2000) (Fig. 3.41).

3.8.3 Estimation of the stretch factor from forward tectonostratigraphic modeling

Stretch factors have been estimated along transects of the northern North Sea where the crustal profile, stratigraphic thicknesses and faults are very well constrained (Odinsen et al. 2000). Forward tectonostratigraphic models simulate crustal structure and basin development through time using a rheologic model of the lithosphere with a finite flexural strength based on Braun and Beaumont (1989) and Kooi et al. (1992) (§3.6). The forward model has the advantage of discriminating the stretching from each rifting event. Odinsen et al. (2000) compared the stretching in the Permo-Triassic (maximum of $\beta = 1.41$ in the Viking Graben) versus Jurassic (maximum of $\beta = 1.53$ in the Viking Graben) rifting events in the northern North Sea. The calculated distribution of stretch factors along two well-constrained crustal transects matches well earlier estimates based on 1-D subsidence analysis (Giltner 1987; Badley et al. 1988) (Fig. 3.41).

3.8.4 Inversion of strain rate history from subsidence data

White (1993, 1994) has taken the novel approach of calculating the strain rate history from the subsidence history of sedimentary basins using inverse methods. The stretch factor β can be viewed as representative of the total strain integrated over the time scale of extension. The stretch factor is therefore related to the vertical strain rate $G(t)$ by

$$\beta = \exp\left(\int_0^{\Delta t} G(t)dt\right) \tag{3.39}$$

where Δt is the duration of stretching. If the strain rate is constant, $\beta = \exp(G\Delta t)$. In the inverse method, the subsidence as a function of time is solved iteratively to give the strain rate as a function of time $G(t)$. Multiple stretching episodes can be resolved by this technique.